ABSTRACT

CAMACHO, MONICA CARIDAD. Agent-Based Modeling of Phytoplankton in Experimental Water Column Reactors. (Under the direction of Dr. Tarek N. Aziz).

Algal blooms in lakes and reservoirs are a serious, worldwide problem, and are especially common in shallow lakes. Algal blooms, also known as harmful algal blooms, pose many challenges for drinking water treatment plants and can be harmful to organism and human health. Some harmful algal blooms consist of phytoplankton that can produce toxins, such as cyanobacteria. Cyanobacteria can regulate their buoyancy in the water column, gaining a light advantage over other phytoplankton that are non-motile. Knowledge of the interplay of environmental factors on algal growth could inform engineering design for better control of harmful algal blooms. The current method to model and predict algal blooms is to combine field or lab studies with lumped-system (population-level) modeling, which are well-established and have been used in studies for many years. However, conventional population-average models tend to overlook heterogeneity in a population (e.g. individual photosynthetic rates), which can result in bloom prediction errors. Agent-based models are increasingly being explored and used as an alternative approach to model microorganisms. Also, water column reactors have been used in recent studies as an alternative to field or lab studies since it merges the two by imitating natural, shallow reservoirs, but in a controlled, lab setting. In this study we ran two water column reactor experiments to explore the impact of low turbidity, high turbidity, intermittent-mixing, and mixing on phytoplankton populations. We then developed and explored the validation of the first agent-based model paired with water column reactor experiment to simulate the behavior of phytoplankton under varying light and mixing conditions in a shallow, eutrophic freshwater environment. The goal was to model two types of phytoplankton: cyanobacteria and non-cyanobacteria. Four different ABMs were developed using NetLogo: a 1-Breed model that

simulates one generic phytoplankton agent type (i.e. breed with similar initial conditions and properties) with property ranges encompassing values found in literature, a 2-Breed-A1 model that simulates 2 generic breeds with the same property range and initialized variables as 1-Breed, a 2-Breed-A model that simulates 2 generic breeds with different initialized variables, and a 2-Breed-B model that simulates 2 breeds—one with strict cyanobacteria and one with strict non-cyanobacteria property ranges. The software optimization tool, BehaviorSearch was used to minimize the root-mean-squared error between simulated and measured chlorophyll-a concentrations. Reactor results showed that high turbidity and mixing suppressed cyanobacteria growth but each had a higher average chlorophyll-a concentration when compared to low turbidity and intermittent-mixing respectively. Simulation results showed that the 1-Breed ABM did well in following the chlorophyll-a measured trends of each treatment, yielding the lowest average total root-mean-squared error of 3.3 μg chl-a/L. The 2-breed-A1, 2-breed-A, and 2-Breed-B models yielded an average error of 3.8, 5.9, and 13.4 μg chl-a/L respectively. It is recommended for future agent-based model versions to consider a variable chl-a/mol C ratio to improve calibrations to chlorophyll-a for all model types in this study. In future research, these models can be used to explore the impacts of nutrients and temperature on phytoplankton communities. With more features added (e.g. variable chlorophyll-a), and more reactor calibrations and validations. Future simulations could also be used to explore the impact of changing climactic conditions on phytoplankton communities and the potential role of engineering water supply systems to mitigate adverse impacts. This research also demonstrates the potential of coupling the experimental water column reactors with agent-based modeling. Future research could further couple these experimental methods to gain further insights into the interplay of nutrients, mixing, and light on phytoplankton communities.

Agent-Based Modeling of Phytoplankton in Experimental Water Column Reactors

by
Monica Caridad Camacho

A thesis submitted to the Graduate Faculty of
North Carolina State University
in partial fulfillment of the
requirements for the degree of
Master of Science

Environmental Engineering

Raleigh, North Carolina
2021

APPROVED BY:

_____	_____
Tarek N. Aziz, Ph.D. Committee Chair	Daniel R. Obenour, Ph.D.
_____	
Emily Zechman Berglund, Ph.D.	

DEDICATION

To my grandfather, Miguel de la Grana, who has sacrificed a lot to give his family opportunities such as this.

BIOGRAPHY

Monica Camacho was born on December 14, 1994, in south Florida, USA. She earned her Bachelor of Science degree in Environmental Engineering in 2017 with a minor in Environmental Science from the University of Florida. After graduating, Monica began a Master of Science degree in Environmental Engineering at North Carolina State University in 2018 where she was funded by the NSF GRFP. During her time as a graduate student, Monica was the president of NC-AWWA-WEA student chapter and participated in the Sube Ritmo Latin Dance group.

ACKNOWLEDGMENTS

I would like to thank my graduate advisor, Dr. Tarek N. Aziz, along with the rest of my committee, Dr. Daniel R. Obenour and Dr. Emily Berglund. I would also like to thank my friends and family for their constant support and advice, as well as Alexandre Mangot, Yini Shangguan, Yue Han, and Darwin Rhoads.

Thank you to Dr. Astrid Schnetzer and her NCSU Plankton Ecology Lab, the North Carolina State Center for Applied Aquatic Ecology (CAAE), the Biological and Agricultural Engineering laboratory (BAE), the National Science Foundation, and the North Carolina Policy Collaboratory.

TABLE OF CONTENTS

LIST OF TABLES

LIST OF FIGURES

1.0 Introduction

Algal blooms in lakes and reservoirs are a serious, worldwide problem. Shallow lakes (less than 3 m deep) make up nearly 85% of lakes globally (Cael et al., 2017; Downing et al., 2006) and are more susceptible to eutrophication via nutrient loading. Therefore, many shallow lakes experience high cases of algal blooms and high turbidity, greatly reducing water quality (Cael et al., 2017). Algal blooms pose many challenges for drinking water treatment plants and are harmful to organism and human health (Huisman et al., 2004; Visser et al., 2016). Blooms can also deplete oxygen levels in the environment, resulting in mass deaths of aquatic organisms. Some harmful algal blooms (HAB) produce toxins and many other chemicals that lead to undesirable properties in source water (Knappe et al., 2004). Of particular challenge are HABs consisting of cyanobacteria, a type of phytoplankton that can regulate their buoyancy in the water column, gaining a light advantage over other phytoplankton that are non-motile (Huisman et al., 2004). Cyanobacteria blooms have resulted in the shutdown of a number of water facilities over the years, and threatens many others (Ke et al., 2007; Paerl et al., 2016). For example, in August 2014, algal blooms caused the city of Toledo, OH to issue a do-not-drink order that affected a half million residents for two days (Rowe et al., 2016).

Temperature, light, and nutrients are all important to the growth of phytoplankton and have been linked to increases in magnitude and frequency of bloom events (Chapra, 2008; Paerl et al., 2011; Visser et al., 2016). To better control and predict HABs, researchers have explored control strategies based on each of these factors (Hellweger, 2017; Hellweger & Kianirad, 2007; Huisman et al., 2004; Paerl et al., 2011; Verhamme et al., 2016). Of particular interest in this research is the interplay of water column mixing and turbidity to better understand the effects of these factors on phytoplankton access to light in the water column. Knowledge of the interplay of these factors

could inform engineering designs for better control of HABs. At present there is limited research as to how exactly these two factors—individually and simultaneously—impact phytoplankton populations and community structures in shallow systems, especially because studies have shown that responses to environmental factors, such as mixing, can differ among different species of phytoplankton (Hawkins & Griffiths, 1993; Huisman et al., 2004; Mangot, 2018; Reynolds et al., 1983; Visser et al., 2016)

The conventional method to model and predict algal blooms is to combine field or lab studies with lumped-system (population-level) modeling (LSM), which are well-established and have been used in studies for many years. These include models such as the DYRESM–CAEDYM (i.e. combined one-dimensional hydrodynamic model called Dynamic Reservoir Simulation Model and Computational Aquatic Ecosystem Dynamics Model) (Trolle et al., 2008), PROTECH (i.e. Numerical model called Phytoplankton RespOnses To Environmental Change) (Lewis et al., 2002), and Environmental Fluid Dynamics Code (EFDC; a finite-difference model that simulates hydrodynamic and thermodynamic behavior in aquatic environments) (Verhamme et al., 2016). However, conventional population-average models can overlook heterogeneity in a population (e.g. individual photosynthetic rates of diverse species within a single population), which can result in bloom prediction errors (Bucci et al., 2012; Hellweger, 2017). LSMs do not consider the life histories of organisms, reducing insight to their individual and therefore collective behavior. For example, differing life histories result in distributed photosynthetic rates, which varies growth rates vertically along the water column (Hellweger & Kianirad, 2007). Photosynthetic rates are impacted by light availability, which depends on vertical positions (impacted by diffusion) along the WCR and are hindered by shading from phytoplankton above. Considering these individual

properties and interactions between phytoplankton can help serve as an alternative to making predictions of the overall population (Hellweger, 2017).

Due to our growing knowledge in microorganism behaviors, advances in molecular biology, and improved computational resources, agent-based models (ABM) are increasingly being explored and used as an alternative approach to model microorganisms (Hellweger & Bucci, 2009; Hellweger & Kianirad, 2007). Instead of modeling population-level properties, ABMs model individuals as "agents", including their states (e.g. biomass) and behavior (e.g. shading) by encoding individual properties and interaction "rules" (Hellweger & Kianirad, 2007). ABMs then observe the emergence of higher-level properties, such as total chlorophyll-a concentration or population counts (Berglund & Asce, 2015).

ABMs have been built in previous studies to model intracellular phosphorus levels within phytoplankton, but many of these models don't consider the complex impact that light variation down the water column (i.e. from the water's extinction coefficient and from algal shading) has on phytoplankton, nor do many consider individual phytoplankton photosynthetic rates (Fredrick et al., 2013; Hellweger & Kianirad, 2007), so the exploration of light and individual photosynthetic rates calculated by ABM is still a new area to explore. Moreover, current ABM data sources come from low-diversity laboratory cultures of selected phytoplankton species in an unnatural laboratory setting, *in silico* (computer simulation) results, or field data from uncontrolled, variable environments (Fredrick et al., 2013; Hellweger et al., 2008; Paerl et al., 2011). In contrast, the source data used to calibrate this study's ABM is from novel water column reactors (WCR). The WCRs contain a naturally diverse phytoplankton assemblage from lake-water, but are located in a laboratory to allow for control of otherwise variable environmental parameters such as diffusion, turbidity, source light intensity, and nutrients—all necessary parameters for phytoplankton growth

(Mangot, 2018). The WCRs allow us to observe phytoplankton population dynamics in response to changes in many environmental conditions, but this particular study focused on diffusion and turbidity.

The purpose of this study is to develop and explore the validation of the first ABM/WCR experiment to simulate the behavior of phytoplankton under varying light and mixing conditions in a shallow, eutrophic freshwater environment. The ABM will track individual photosynthetic rates and biomass as determined by light available at the phytoplankton's vertical position in the water column. This study aims to use WCRs to understand 1) the impacts of turbidity and diffusion on phytoplankton populations (i.e. cyanobacteria and non-cyanobacteria) and on chlorophyll-a (chl-a) concentrations, 2) explore different ABM versions to best replicate WCR results, 3) assess the performance of the ABM in reproducing chl-a concentration results of each WCR, and 4) understand phytoplankton behavior by analyzing the impact of turbidity and diffusion on phytoplankton's individual properties as determined by optimizing the ABM to WCR data.

2.0 Methods

The aim of this study was to develop and calibrate an ABM using controlled experimental water column reactors (WCRs). The objective of these experiments was to explore the effects of turbidity and mixing on phytoplankton communities collected from Jordan Lake, NC, a shallow eutrophic reservoir prone to cyanobacterial blooms and high chlorophyll-a (chl-a) concentrations especially during summers. In this methods section we first describe the experimental approach to study the phytoplankton from Jordan Lake, then detail the agent based model (ABM), the process we used to calibrate that model, and model simulations we performed demonstrating additional uncalibrated model functionality.

2.1 Water Column Reactor (WCR) Experiments

2.1.1 Study Site

Two water column reactor (WCR) experiments were performed: one in spring 2019 (SP19) and one in summer 2019 (SU19). Jordan lake is a reservoir that has a mean depth of 4.3 m (Han, 2020), an average of 29 mg/L of suspended solids, and average light extinction coefficient of 0.2 m^{-1} and 5 m^{-1} year-round, and an average temperature of 28 ˚C (Mangot, 2018; Touchette et al., 2007). The reservoir has a history of eutrophication, and dominating cyanobacteria over the summers cause high concentrations of chl-a (Han, 2020).

Both experiments used natural phytoplankton assemblages that were collected from Jordan Lake, Apex, North Carolina, USA. Water was collected on the mornings of March 14, 2019 (SP19) and May 30, 2019 (SU19) from the location specified in Figure 2.1. Subsurface water was collected at a depth of approximately 0.5 m. Additionally, a phytoplankton tow using a 20 μm mesh was added to the WCRs to make up for the assemblage dilution that would occur when filling the columns to their final volume using deionized water (DIW). This tow was further filtered using a 100 μm Nitex mesh to remove larger copepods/grazers.

Figure 2.1: The location of our water collection for the 2019 WCR experiments.

Initial samples were taken of the source water for both experiments to conduct algal assemblage analysis, which were performed at the North Carolina State University Center for Applied Aquatic Ecology (CAAE, NCSU), and to conduct algal assemblage analysis using a digital flow cytometer (FlowCAM, Fluid Imaging Technologies), which was performed in the Plankton Ecology Lab at NCSU.

2.1.2 Experimental Design

The materials and experimental set-up used in this study were described in detail by Mangot (2018). In contrast to the experiments by Mangot (2018), an additional WCR was included in this experiment for a total of four WCRs. This allowed each treatment to be tested in duplicates. Figure 2.2 details the configuration of the WCR for these experiments. In brief, the acrylic columns are each 2 m tall with a total internal volume of 146 L. Sampling ports are located down the WCRs at 15 cm intervals to allow sampling at different depths. A total of two experiments were conducted – a turbidity experiment (SP19) with high and low turbidity (HT and LT

respectively), and a mixing experiment (SU19) with intermittent mixing and complete mixing (IntMix and Mix respectively).

In SP19, 2 LT and 2 HT WCRs were tested. Light extinction coefficients commonly found in regional shallow reservoirs vary between 0.2 m^{-1} and 5 m^{-1} (Mangot, 2018). To replicate this turbidity artificially, we added bentonite clay to the WCR reactors. Previous experiments with the WCR used 300 mg/L of bentonite to achieve this light attenuation. In the present experiment we defined LT as a 200 mg/L bentonite addition and HT as a 400 mg/L bentonite addition in the WCR.

In SU19, 2 Mix and 2 IntMix WCRs were tested. A turbidity of 300 mg/L of bentonite was used in each WCR to represent the typical light extinction coefficient found in Jordan Lake (2.5 m^{-1}). The Mix WCRs were continuously mixed at 100 RPM, representing vertically well-mixed lake conditions, resembling the conditions of a well-mixed, shallow lake (Mangot, 2018). The IntMix WCRs were mixed from 8PM to 8AM (12 hours). The motor would mix the IntMix WCRs at night at 100 RPM (same intensity as the Mix), simulating the diel destratification that commonly occurs in typical shallow lakes, such as Jordan Lake which vertically mixes (destratifies) at night (Mangot, 2018).

All WCRs for both experiments were filled to a total liquid volume of 134.4 L, which corresponds to a liquid height of 1.9 m. The contents included in all WCRs are shown in Figure 2.2. All WCRs had 40 L of lake water, 10 L of artificial turbidity, approximately 84 L of DIW, and 0.1 L of a nutrient solution. The nutrients added into the WCRs included NO_3^-, NH_4^+, and PO_4^{3-}. The sources and amounts of the added nutrients were 15 µM KNO_3, 5 µM NH_4HCO_3, and 3 µM KH_2PO_4 to make up for the 94.4 L of water added that was not lake water. Therefore, the target starting concentrations of each nutrient for the entire WCR was 0.29 mg/L of PO_4^{3-}, 0.93 mg/L of NO_3, and 0.09 mg/L of NH_4. The first nutrient sample was taken one day after the contents

were placed in the WCR in order to allow the organisms to acclimate. The SP19 and SU19 experiments was run for 20 days (480 hours) and 21 days (504 hours) respectively. More details on the experimental setup procedure can be found in Appendix A: WCR Additional Information.

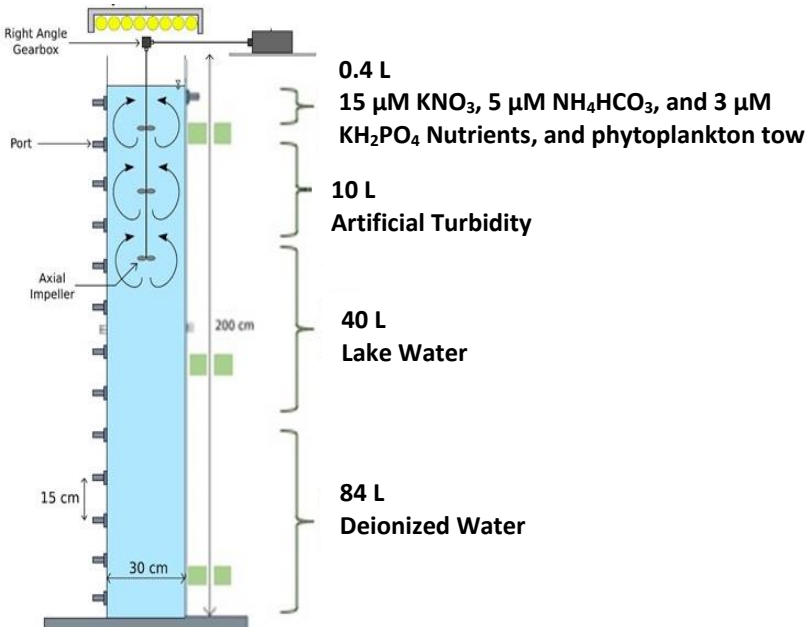

Figure 2.2**:** A schematic of a WCR with the main contents for each experiment, with the exception that a phytoplankton tow was added to experiment SP19.

2.1.3 WCR Sampling

Every 2 days at 10 AM, laboratory temperature was collected. Also at this time, chlorophyll *in vivo* fluorescence (5 mL) samples were taken at depths of 5 cm, 35 cm, and 110 cm and measured immediately using a fluorometer (Turner Designs Trilogy; excitation: 441/82 nm, emission: 660-710 nm; module 7200-043). Since *in vivo* measurements are a proxy to chl-a, and therefore population growth (Huang et al., 2015), these measurements were used to determine the growth phase of the phytoplankton. Growth phases were defined as the lag phase where little to no growth occured (LAG), exponential phase (EXP) where active growth occured, stationary phase (STA) when net growth ceased, or the decline phase (DEC) during which algal biomass decreased

(Mangot, 2018). *In vivo* measurements helped to determine on which days grab samples were taken for more detailed analysis.

One grab sample was taken one day after the phytoplankton were put into the WCR, one in lag phase, two in exponential phase, and one in the stationary/decline phase. Each 200 mL grab samples was taken at 10 AM from a depth of 35 cm. Measurements taken from each grab sample included chl-a, dissolved inorganic nutrients (NH_4^+, PO_4^{3-}, combined NO_2^- + NO_3^-), and phytoplankton community cell counts and composition. Appendix Table A-1 (Appendix A) shows a summary of the volume used for each test and a description of how each sample was tested.

Due to the more frequent sampling of *in vivo* fluorescence, a linear regression was performed between in vivo fluorescence and extracted chl-a in order to interpolate more chl-a values. More chl-a data points provided more data for the ABM to calibrate to. The regression lines for both experiments can be found in Appendix A (Appendix Figure A.3 and Appendix Figure A.4). A day after each grab sample was taken, a radiometer was used to measure light intensity down the entire WCR. Measurements are taken just below the water's surface and at every 15 cm below that down to 155 cm depth (SP19) and 95 cm depth (SU19) in order to construct a light profile of each column.

2.1.4 How WCR data was used with the ABM

The environmental conditions in the WCR and lab were measured and used as inputs for the ABM. The input variables included temperature, turbidity, diffusion (mixing), hours of sunlight and darkness, and light extinction coefficient (k_e). In addition, initial total phytoplankton cell counts and chl-a concentration of the WCR were used to initialize the ABM. Chl-a measurements taken at other time points during the experiment were used to calibrate the ABM.

2.2 Agent-Based Model

The ABM's ODD is found in Appendix D: ABM ODD.

2.2.1 ABM Implementation

This model was created on the NetLogo Framework, version 6.1.0 (Wilensky, 1999). In this framework, 2 elements are modeled: turtles (agents) and patches. Agents are the discrete individuals being modeled, while patches are the background environment. Both agents and patches have their own individual state variables. The model space is a 1 horizontal by 50 vertical patches that represents the WCR with a unit area of 0.071 m^2, height of 1.9 m, and total volume of 134.3 L. The model runs for 600 hours (25 days), where each 1 hour time step is called a "tick".

2.2.2 Light intensity and shading

The available light in each patch was found using Beer-Lambert law (Chapra, 1997):

$$I(z) = I_o e^{-k_e z} \qquad \text{Eq. 1}$$

where I(z) (W/m^2) is the light intensity at depth z, I_0 (W/m^2) is the solar radiation just above the water's surface, k_e (1/m) is the light extinction coefficient, and z (m) is the depth. Since the light setup and its distance from the water's surface was held constant across all experiments, I_0 did not vary and therefore was held constant for each simulation at 81.8 W/m^2. The light extinction coefficient is calculated based on algal and non-algal shading (Riley, 1956):

$$k_e = k_e' + 0.0088a + 0.054a^{\frac{2}{3}} \qquad \text{Eq. 2}$$

where k_e' (1/m) is the non-algal light extinction and a (μg Chl-a/L) is the concentration of chlorophyll-a (Chl-a) above each phytoplankton.

The non-algal extinction coefficient is calculated using (Di Toro, 1978):

$$k_e' = k_{ew} + C_T N \qquad \text{Eq. 3}$$

where k_{ew} (1/m) is the light extinction coefficient of particle-free water and assumed to be negligible, N (mg/L) is the concentration of non-volatile suspended solids (NVSS), and C_T is the NVSS coefficient. C_T is a variable that ultimately relates k_e to the amount of NVSS, and its value changes as it is often re-calculated to find the correct relation for the specific environment being studied (Chapra, 2008; Weiskerger et al., 2018). For the purpose of this study, the NVSS added from the bentonite clay (mg/L) was measured and known, however the NVSS of the added lake water was not known. The data from SU17 Mix WCR experiment was used to calculate C_T. The measurements of k_e (2.6 1/m) and chlorophyll-a (a) concentration (2.4 μg chl-a/L) from day 2 were used to calculate k_e' using Eq. 2. The known added NVSS (N; 300 mg/L) and calculated k_e' were used to calculate C_T using Eq. 3, which resulted in C_T having a value of 0.0081. This results in the final equation of: $k_e' = 0.0081N$.

2.2.3 Phytoplankton Mixing and Motility

The vertical movement of each phytoplankton is determined by their vertical velocity, a random value to account for natural stochasticity, and vertical diffusivity. These are all incorporated into the random-walk equation (Xue et al., 2018) to determine phytoplankton motion at each time step:

$$z_{n+1} = z_n + w_p dt + 2R(2k_z dt)^{\frac{1}{2}} \qquad \text{Eq. 4}$$

where z_n (m) is the vertical position after n iterations, w_p (m/h) is the vertical rise (+) or sink (-) rate, dt (h) is the time step, R is a uniformly distributed random value with a mean of 0 and a range

of -1 to 1, and k_z (m^2/h) is the vertical diffusivity. Diffusivity was held constant for Mix and NoMix treatments at 3.6 or 0.135 m^2/h respectively, as measured in previous WCR tracer tests (Mangot, 2018).

2.2.4 Phytoplankton Growth and Division

The change in biomass of agents depends on their photosynthetic and respiration rates, as well as its biomass from the previous time step (Hellweger et al., 2008) :

$$\frac{dm}{dt} = (u_p - u_R)m \qquad \text{Eq. 5}$$

where μ_p (1/h) is photosynthetic rate, μ_R (1/h) is respiration rate, and m (mol C/cell) is biomass. For all ABM simulations, μ_R is assumed constant at 0.00208 1/h for all simulated phytoplankton as previous ABM models have assumed (Hellweger et al., 2008). The photosynthetic rate (μ_p), which also impacts growth, was calculated at each time step based on known limitation coefficients that was calculated in the model. The photosynthetic rate depends on temperature, light, and phosphorus limitation levels:

$$u_p = u_{P,max} L_T L_L L_P \qquad \text{Eq. 6}$$

where $\mu_{p,max}$ (h^{-1}) is the maximum photosynthetic rate, L_T (unitless) describes the dependence of cyanobacteria specific growth rate on temperature (Prokopkin et al., 2006), L_L (unitless) is the light limitation term, and L_P (unitless) is the phosphorus limitation term. Since the WCR experiments had a constant temperature of 25° C throughout the experiment, and was replete with nutrients, L_T and L_P were assumed to be 1 (have a negligible imact on population growth), thereby making photosynthetic rate only dependent on light availability.

Light limitation kinetics can be calculated using the Monod formulation (i.e. $\Phi_L = \frac{I}{I+h}$) (Han, 2020), however, prior phytoplankton ABMs (Hellweger et al., 2008) have used the light formulation from Prokopkin (2006) called the photoinhibition model. The photoinhibition model began taking form when Steele (1962) developed a theoretical equation for the photosynthesis-light relation that includes effects of inhibition in intense light (Steele, 1962). Inhibition is further described by Crill (1977), who considered inhibition when developing an analog model called the photosynthesis-light curve. The analog model defines each parameter as an analog of a hypothetical photosynthetic system. The model consists of 2 parameters: photosynthetic factories (PSF) and hit probability. Crill (1977) explains that a PSF is the center for trapping light and conducting reactions to produce a photoproduct. A PSF is activated by a certain amount of light (i.e. a unit of light), and it doesn't process any more light until the completion of a reaction. Steele's equation could ultimately be derived from the analog model (Crill, 1977). Eilers and Peeters (1988) took Crill's formulation but modified it to allow different probabilities of the PSF being in one of 3 states: rest (x_1; before light has hit it), activated (x_2; after light has hit it), and inactivated / inhibited (x_3; if hit by another unit of light while it's still processing the first). Their formulation for production rate, p, is $p = \frac{I}{aI^2+bI+c}$, where a, b, and c include the probability that the PSF is in 1 of 3 states. Lastly, Prokopkin (2006) took the previous ideas to create new algal light limitation formulation. The term for light limitation (i.e. dependence of growth rate upon irradiance) is written on the basis of Bouger-Lambert law ($F(E) = \frac{E_h}{uE_h^2+E_h+h}$) where E_h (W/m^2) is the average irradiance on the water layer, h (W/m^2) is the half saturation constant on light, and μ is the coefficient of growth rate inhibition by light (m^2/W). Then the specific growth rate (μ_{ns}) is dependent on limiting factors for nutrients (S), temperature (T), and light (E) and is calculated

by: $\mu_{ns} = \mu_{xmax}\mathrm{F(S)F(T)F(E)}$. Current phytoplankton ABMs have been using Prokopkin's (2006) inhibition model to calculate light limitation (Hellweger et al., 2008).

Following an exploration of the ABM sensitivity to light limitation model (Section 3.2.1) it was determined that the Monod model yielded a RMSE of only 1% less than using the light inhibition model equation. We opted to use a model that featured photoproduction (in light) and photoinhibition (after some time, at higher intensities) as we believed it better reflects the natural behavior of phytoplankton (Eilers & Peeters, 1988). For the purpose of our model therefore we used (Prokopkin et al., 2006):

$$L_L = \frac{I}{I + h + (uI^2)} \qquad \text{Eq. 7}$$

where I (W/m^2) is the available light (irradiance), h (W/m^2) is the light half saturation constant, and u (m^2/W) is the inhibition constant. Since L_L is proportional to I, and I is directly proportional to k_e and turbidity, L_L is directly impacted by turbidity.

For future exploration of nutrient dynamics in the ABM, nutrient limitation was simulated using Droop kinetics (Droop, 1973) which represents growth as a function of internal nutrients and allows for luxury uptake (storage) of nutrients as done in prior phytoplankton ABM studies (Hellweger et al., 2008):

$$L_P = 1 - \frac{q_{0,P}}{q_P} \qquad \text{Eq. 8}$$

where $q_{0,P}$ (molP/molC) is the minimum internal phosphorus (P) concentration and qP (molP/molC) is the internal phosphorus concentration.

The change in internal P over time is calculated using intracellular nutrient mass balance (Hellweger & Kianirad, 2007):

$$\frac{dq_P}{dt} = V_{DIP} - (\mu_P - \mu_R)q_P \qquad \text{Eq. 9}$$

where V_{DIP} (molP/molC·d) is the dissolved inorganic P uptake rate and $(u_P - u_R)q_P$ is the dilution of q_P from increased biomass. Uptake is calculated using the Michaelis-Menten model with a modification term (Thingstad, 1987) in order to prevent unreasonably high P quotas (i.e. under high nutrient and low growth conditions) (Hellweger et al., 2008):

$$V_{DIP} = V_{max,DIP}\frac{DIP}{(31K_{m,DIP})+DIP}\frac{(q_{max,P}-q_P)}{q_{max,P}-q_{0,P}} \qquad \text{Eq. 10}$$

where $V_{max,DIP}$ (molP/molC·d) is the maximum uptake rate, $K_{m,DIP}$ (molP/L) is the half saturation constant of algal phosphatase (enzyme to create organic P) (Ou et al., 2008), DIP (g P/L) is the concentration of dissolved inorganic P in the water column, $q_{max,P}$ (molP/molC) is the maximum P quota.

For future exploration of temperature dynamics in the ABM, temperature dependence was simulated using the formulation shown in Prokopkin (2006) and as used in prior phytoplankton ABM studies (Hellweger et al., 2008):

$$L_T = \exp\left(-\left(\frac{T-T^0}{q}\right)^2\right) \qquad \text{Eq. 11}$$

Where T (°C) is the temperature, T^0 (°C) is the optimum temperature, and q (°C) is the thermal dispersion parameter. The general optimum temperature range of phytoplankton encompassed the constant temperature of the laboratory, therefore the impact of temperature on population growth was considered negligible (Hellweger et al., 2008).

Cell division is based on biomass (m) and the minimum biomass threshold (m_o). When the agent grows to $2m_o$, it creates 2 daughter cells. A randomly generated split factor ranging from

0.05 to 0.095 determines the new m of each daughter cell. All other properties, including S_R and chlorophyll-a, remains the same. For ABMs simulating 1 general breed of phytoplankton, m_o is initialized and held constant at a value of 8.4E-13 mol C/cell. To add stochasticity, initialized m values of each phytoplankton varies from 3.45E-13 to 1.19E-12 mol C/cell (Hellweger et al., 2008). For ABMs simulating 2 breeds—cyanobacteria (cyanos) and non-cyanobacteria (noncyanos)— m_o is initialized and held constant at a value of 6.85E-13 and 9.95E-13 for cyanos and noncyanos respectively (Hellweger et al., 2008). To add stochasticity, initialized m values of cyanos and noncyanos vary from 1.95E-13 to 5.85E-13 mol C/cell and 4.95E-13 and 1.49E-12 mol C/cell respectively (Hellweger et al., 2008).

2.2.5 Cell mortality

Agents can die based on a death rate (μ_D), biomass, or their representative number (S_R; cell count/agent; explained in 2.2.6). If a randomly generated number (between 0 and 1) is less than agent's probability of dying ($\mu_D dt$) then the agent dies. Alternatively, if an agent's biomass is less than or equal to zero, or its S_R is less than 1, then the agent dies.

2.2.6 Agent collectives

Billions of phytoplankton in the WCRs must be modeled, but modeling each individual cell would take a single simulation years to run (Fredrick et al., 2013). Therefore in this study we use individual agents, called super-agents, to represent a number of cells as determined by its representative value, S_R (cells/agent). For an ABM simulating 1 breed, the initial S_R is calculated by dividing the number of cells measured in the WCR at time zero by 600 agents. For a 2-breed simulation, the measured number of cyano and noncyano counts are divided by 300 agents each. The total number of allowable agents is maintained between 1 and 1700 in order to best capture

growth patterns while maintaining practical simulation run times (approximately 60 seconds per run and 4 hours for calibration).

To keep the number of agents within these constraints, agents will split or combine during simulations. If there is only a single agent left, the model will split the agent to form 2 agents, each with half the S_R of the original agent, maintaining its other variables (e.g. m) the same. In a 1-breed ABM, if the total number of breeds reaches 1700, the model will combine the 2 agents with the lowest S_R. The new agent's S_R will be the sum of the original two, and its biomass is determined by a weighted average of the two original agents. In a 2-breed simulation, the same occurs except agents combine if the total counts of cyano or noncyano exceed 850 agents each. This method to constrain the number of agents was implemented in prior studies (Fredrick et al., 2013).

2.2.7 Scheduling

A flow chart of the actions taken at each time step is shown in Appendix Figure D.1. At the beginning of each time step, the water patches will calculate the algal shading that occurs at its respective depth, then it will use this value and non-algal turbidity to calculate the light available in the patch. Each phytoplankton agent will then calculate the distance it will travel and move to a certain depth. Individual agents will take the light data at its new patch location to determine how much it will grow in biomass (m). If its biomass exceeds two times the minimum biomass threshold, it has a 50% chance to split into 2 agents. The model checks if an agent's biomass gets to a value of zero, or if a random number selected is less than the probability of the death rate multiplied by the time step, then the agent will die. If applicable, the agents will combine or split to remain within the allowable agent number range. Lastly the chl-a, cell count, and error measurements from the model are taken and stored in a list to be displayed at the end of the simulation.

2.2.8 Phytoplankton property value ranges

The same four phytoplankton property values are calibrated per breed in each simulation. These properties are important factors that help determine the growth of phytoplankton, and can tell a lot about the environment in which they live. At certain values, these properties can give the phytoplankton an advantage over others to survive certain turbidities or vertical mixing (diffusion) levels. The properties and their allowable ranges are shown in Table 2-1 for 1-Breed, 2-Breed-A1, and 2-Breed-A ABMs. For the 2-breed-A1 and 2-Breed-A ABMs, 2 the constraints of each breed encompassed both cyano and noncyanos ranges as delineated in Table 2-1. In 2-Breed-B, the constraints of each breed were strictly for cyanos and noncyanos as determined by literature and delineated in Table 2-2.

Table 2-1: 1-Breed, 2-Breed-A1, and 2-Breed-A phytoplankton property ranges.

Variable	Description	Minimum Value	Maximum value	Units
h	Light half saturation rate	5 [A,C]	35 [A,C]	W/m^2
w_p	Rise/sink rate	-0.0208 [B]	0.2 [C]	m/h
$\mu_{p,max}$	Max photosynthetic rate	0.02 [A]	0.10 [A]	1/h
μ_D	Death rate	4.2E-4 [C]	8.3E-3 [C]	1/h

[A]: (Hellweger et al., 2008)
[B]: (Grover, 2017)
[C]: (Han, 2020)

Table 2-2: 2-Breed-B phytoplankton property ranges.

Variable	Description	Value				Units
		Cyano		NonCyano		
		Min	Max	Min	Max	
h	Light half saturation rate	18 [A]	35 [A,C]	5 [A,C]	17 [A]	W/m^2
w_p	Rise/sink rate	0 [C]	0.2 [C]	-0.021 [B]	0 [C]	m/h
$\mu_{p,max}$	Max photosynthetic rate	0.02 [A]	0.05 [A]	0.06 [A]	0.10 [A]	1/h
μ_D	Death rate	4.2E-4 [C]	8.3E-3 [C]	4.2E-4 [C]	8.3E-3 [C]	1/h

[A]: (Hellweger et al., 2008)
[B]: (Grover, 2017)
[C]: (Han, 2020)

2.2.9 Experimental Data/ Initialization

The ABMs simulate the WCR experiments conducted in the spring and summer of 2019 (SP19 and SU19). The ABMs also simulate WCR experiments run in a past WCR study from the summer and fall of 2017 (SU17 and FA17) (Mangot, 2018). The ABM uses the light, diffusion, and initial added turbidity measurements taken from the experiments as inputs. During simulation, the model outputs chl-a concentration to compare with the experiments for calibration purposes and performance assessment. It also outputs total phytoplankton counts for more insight on how the phytoplankton are behaving in simulations.

For 1-Breed ABMs, total experimental cell counts (varies by treatment) are divided into 600 initial agents to initialize the representative value, S_R. For 2-Breed versions, experimental counts for cyanos and noncyanos are divided among 300 agents each, so a different S_R is initialized per breed.Therefore, the 1-Breed ABM represents the total experimental counts using agents belonging to 1 breed. Meanwhile the 2-Breed-A1, 2-Breed-A, and 2-Breed-B ABMs have each breed initialized to cyano counts (Breed 1) and noncyano counts (Breed 2).

To initialize the internal chl-a per mol of carbon (Internal_chla_perC), the experimental chl-a concentration at day 1 was multiplied by the total volume and divided by the sum of moles of carbon within each agent. With this value, the amount of chl-a within each agent (Internal_chla; units μg chla/agent) was initialized. Other initialized variables are found in Appendix Table D-3.

2.2.10 Simulations performed

An ABM was created to simulate experiment SP19, which includes low turbidity (LT) and high turbidity (HT) treatments, and SU19, which includes intermittently mixed (IntMix) and mixed (Mix) treatments summarized in Table 2-3 and Table 2-4. An initial run of time steps 0.5 h, and 2 h were tested to determine the best time step (dt). The RMSE of dt = 0.5 h was 1% higher and of

2 h was 1% lower than that of dt = 1 h With reasonable run time and higher resolution of data, a dt of 1 h was selected.

Calibrations using both chl-a and relative abundance (using 2 WCR data points) were initially performed but showed low performance, likely due to limited available experimental count data from the SP19 and SU19 experiments to calibrate the ABM. Therefore it was decided to calibrate each ABM to chl-a since the WCRs have the most data points for that parameter.

Simulations were conducted using 1-Breed and 2-Breeds (2-Breed-A1, 2-Breed-A, and 2-Breed-B) versions to assess the best performing version. Version 2-Breed-A1 uses the calibrated values of 1-Breed for both its agents to confirm that 2 breeds each with the same property values as 1-Breed should give similar chl-a results.

Table 2-3: Summary of ABM simulations run for WCR experiments SP19 and SU19.

	SP19		**SU19**	
Simulation	LT	HT	IntMix	Mix
1 Breed	✓	✓	✓	✓
2-Breed-A1	✓	✓	✓	✓
2-Breed-A	✓	✓	✓	✓
2-Breed-B	✓	✓	✓	✓

Additionally, 1-Breed and 2-breed simulations were conducted and its performance measured for WCR experiments of SU17, which includes Mix and non-mixed (NoMix) treatments, and FA17 which includes Mix, NoMix, and IntMix treatments.

Table 2-4: Summary of ABM simulations run for WCR experiments SU17 and FA17.

	SU17		FA17		
Simulation	Mix	NoMix	Mix	IntMix	NoMix
1 Breed	✓	✓	✓	✓	✓
2 Breed-A					
2 Breed-B	✓	✓			

For further model exploration, the ABM's capabilities were explored and other features were turned on to observe how phytoplankton population simulations were impacted. The ABM's capabilities that were explored included the ability to create vertical profiles of light availability, chl-a, and cell counts. This was created using the calibrated, 1-Breed HT ABM. Features that were turned on and explored included limiting nutrients, changing temperatures, and fully mixing under HT treatment. These features were explored using the 1-Breed HT calibrated ABM, but the model was not calibrated with these features turned on. Turning on these features only served as a way to observe how populations were simulated when changing other environmental parameters in a way that was not tested using the WCRs.

2.2.11 Optimization and Calibration

Netlogo's BehaviorSearch (Stonedahl & Wilensky, 2010) program was used to select the four phytoplankton parameters, given their ranges in Table 2-1 and Table 2-2, to minimize the root mean squared error (RMSE) between the chl-a concentrations measured in the ABM and those of the WCR it simulated. The RMSE is in the same units as the metric it is measuring, which in this case is chl-a concentration (μg Chl-a/L). RMSE gives larger errors more weight, and therefore was used in calibrating the ABMs give the best fit and reduce the chances of large errors (Chai & Draxler, 2014). However, a combination of metrics are often recommended to assess model

performance, therefore the mean absolute error (MAE), which gives equal weight to all errors, is also reported for each ABM simulation result (Chai & Draxler, 2014).

The calibration search algorithm used by BehaviorSearch was the standard genetic algorithm (StandardGA), which is best used for populations (Stonedahl & Wilensky, 2010). Also, the search encoding representation used was grey binary chromosome, which has been found to give better performance for search representations (Stonedahl & Wilensky, 2010). The evaluation limit was set to 300 model runs, which is the limit of the number of model runs a single search process should perform. The number of searches done for each model was 3, meaning that the entire process of 300 model runs to minimize RMSE was repeated a total of 3 times to improve confidence (Stonedahl & Wilensky, 2010).

Calibrated 1-Breed and 2-Breed-B model were run 3 times to obtain 3 RMSE values each. The standard deviation (amount of variation in the set of values) of the RMSE's was used to quantify the stochasticity of the ABMs.

3.0 Results

In the upcoming sections describing the WCR results, chlorophyll-a concentrations and phytoplankton community structure details will be discussed for experiments SP19 and SU19 separately. The results were averaged across duplicate WCRs.

3.1 WCR

3.1.1 WCR SP19 & SU19– Light

Experiment SP19 WCRs' vertical light profiles for day 5 is shown in Appendix Figure A.1 (Appendix A). From 20 to 100 cm in depth, the high turbidity (HT) WCRs available light was less

than the low turbidity (LT) WCRs in light, as expected from a higher turbid environment. However, the values remained within an average of 3% of each other throughout the water column.

For this study, the upper layer of the WCR is defined as 0 to 50 cm in depth, and the lower layer is 95 to 170 cm in depth. On day 5 the LT reactors on average had 12% more available light than the HT reactors. However, in the lower layers the LT reactors had an average of 6% less available light than the HT reactors on day 5. By day 18, LT reactors had an average of 9% more available light than the HT reactors in the upper layers, and 16% more available light in the lower layers, as shown in Figure 3.1.

From day 5 to day 18, the average available light just under the water's surface in both treatments of SP19 decreased from approximately 50 W/m^2 to 40 W/m^2. By day 18 the bottommost measured data point (155 cm) in both treatments was effectively indistinguishable and decreased in available light by approximately 77% compared to day 5.

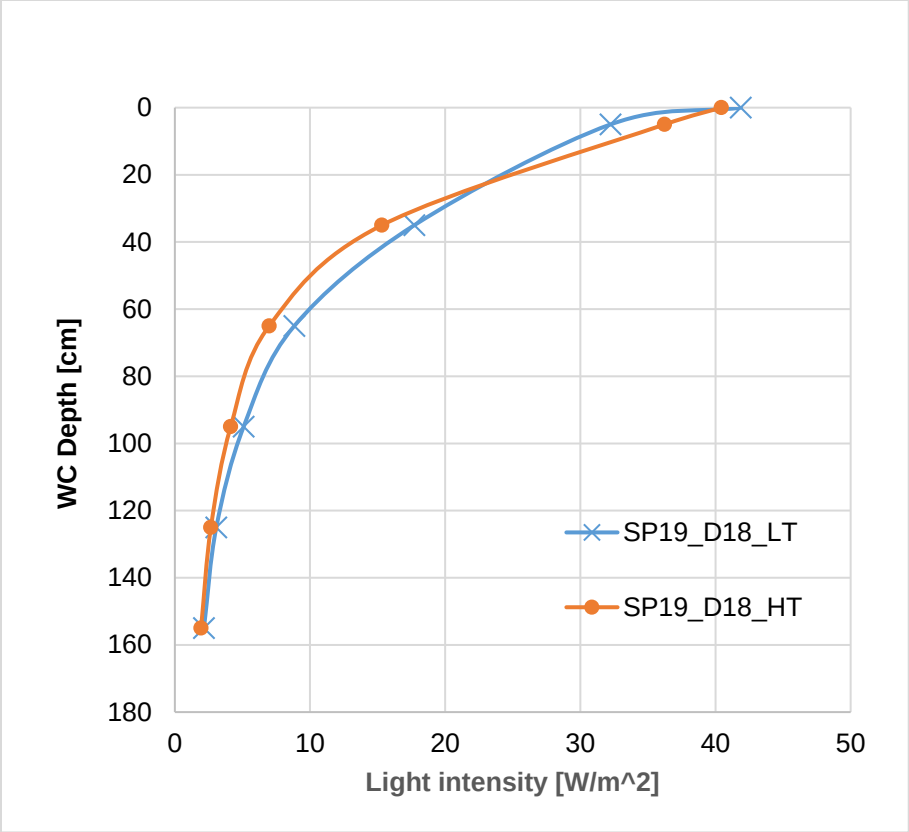

Figure 3.1: Light intensity down the WCRs for experiment SP19 measured on day 18 (D18).

The SU19 WCR experiment vertical light profiles for day 4 and 15 are shown Appendix Figure A.2 (Appendix A). On day 4, the differences in light down the column were nearly indistinguishable, in the upper layer. The intermittently-mixed (IntMix) reactors had an average of 0.2% more available light than the Mix reactors in the upper layer. However, the IntMix reactors showed 37% more available light in the lower layer.

In experiment SU19, by day 15 the differences in light availability between the treatments is noticeable down to 35 cm in depth. After that, the differences are hardly distinguishable. The IntMix reactors had an average of 6% more available light than the mix reactors in the upper layer, and only 1% more available light in the lower layer.

For all SU19 experiments and the SP19 HT experiment an average of less than 5% of the surface light remained below 100 cm. For SP19 LT WCRs approximately less than 20% of surface light remained below 100 cm.

3.1.2 WCR SP19 and SU19 – Nutrients

Nutrient measurements throughout the course of the experiments are shown in Figure 3.2.

SP19

Despite initially adding the same nutrient concentrations to both reactors, the preliminary concentration of $NO_2^- + NO_3^-$ for LT and HT treatments were 213 and 263 μg/L respectively. Initial PO_4^{3-} concentrations for LT and HT treatments were 81 and 82 μg/L. Measurements show that the bentonite clay adds 6.6 μg/L and 62.8 μg/L of PO_4^{3-} and $NO_2^- + NO_3^-$ respectively for a sample of turbidity at 20 mg/L of bentonite. Therefore, the amount of turbidity used for LT adds 5 μg/L and 47 μg/L of PO_4^{3-} and $NO_2^- + NO_3^-$ respectively for the entire WCR. While the amount of turbidity used for HT adds 10 μg/L and 93 μg/L of PO_4^{3-} and $NO_2^- + NO_3^-$ respectively for the entire WCR. Therefore, it is expected that the HT reactors would have a slightly higher PO_4^{3-} and $NO_2^- + NO_3^-$ concentration than the LT reactors.

As expected, PO_4^{3-} and $NO_2^- + NO_3^-$ decreased over time and their amount of decrease appeared to be similar. For SP19, PO_4^{3-} decreased by 47% and 40% in LT and HT respectively from day 1 to day 20. $NO_2^- + NO_3^-$ decreased by 50% in both the LT and HT from day 1 to 20.

SU19

Initial $NO_2^- + NO_3^-$ levels for Mix and IntMix treatments were 206 and 261 μg/L, similar to the SP19 starting conditions. Initial PO_4^{3-} concentrations for Mix and IntMix treatments were 85 and 111 μg/L, making IntMix starting concentration of both nutrients higher than the Mix.

As expected, the general trend of both PO_4^{3-} and $NO_2^- + NO_3^-$ was a decrease over time. For SU19, PO_4^{3-} decreased by 57% and 68% in Mix and IntMix respectively from day 1 to day 20. $NO_2^- + NO_3^-$ decreased by 84% and 72% in the Mix and IntMix from day 1 to 20.

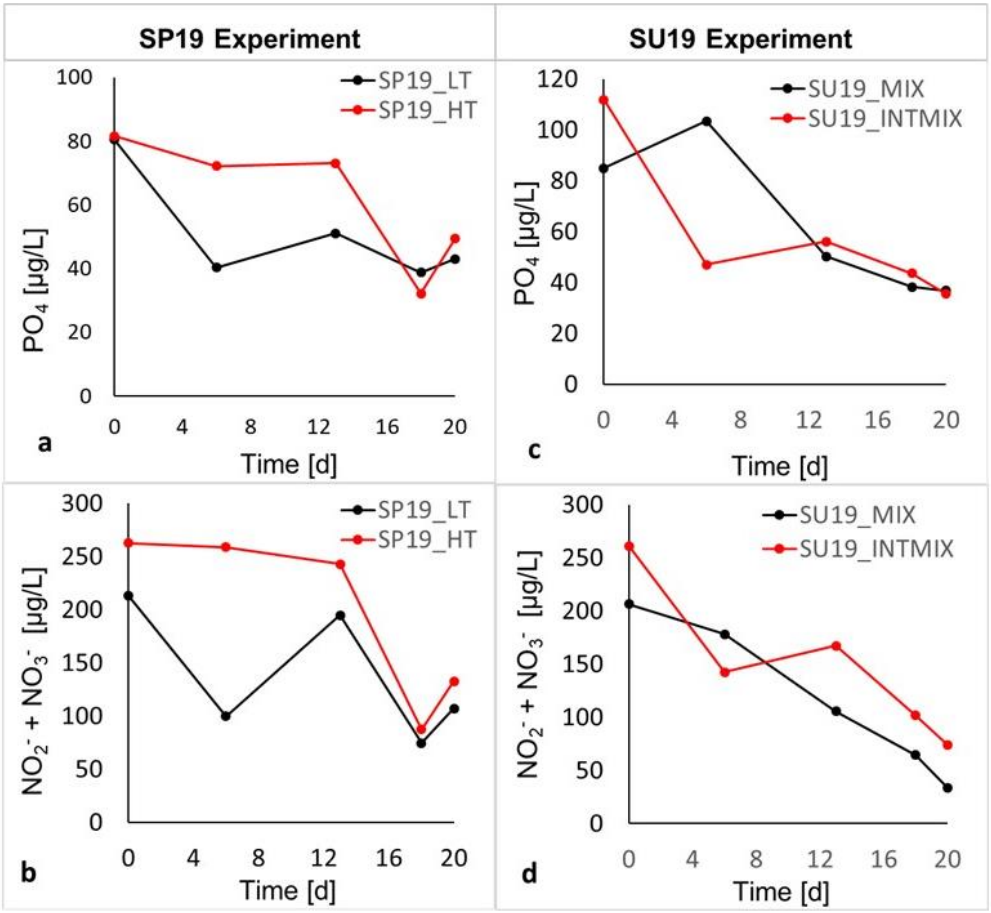

Figure 3.2: Concentrations of PO_4^{3-} (a, c) and $NO_2^- + NO_3^-$ (b, d) for both treatments in each SP19 and SU19 experiment.

Comparing experiments SP19 and SU19, there was higher percentage decrease of nutrients for the Mix and IntMix treatments (SU19) than the turbidity WCRs (SP19). Despite minor differences in initial nutrients and their trends over time, both SP19 and SU19 experiments were replete with nutrients through the majority of the experiment. The nutrients added were meant to be over 5 times the half-saturation constant of nitrogen (half-saturation is 20 µg N L^{-1}) and phosphorus (half-saturation is 5 µg N L^{-1}) (Chapra, 2008; Han, 2020). The results show that PO_4^{3-}

remained above 25 µg/L for both SP19 and SU19 experiments. In experiment SP19 NO_2^- + NO_3^- fell below 100 only on day 18, and in experiment SU19 it fell and remained below 100 after day 13 and day 18 for Mix and IntMix respectively. Therefore, the nutrients were never fully depleted for the duration of the experiment.

3.1.3 WCR SP19 – Chl-a and Counts

SP19- Chlorophyll-a

SP19 Chl-a results (Figure 3.3) showed that the LT WCR had a lag phase until day 5, the population grew until day 17, reaching a maximum of 25 µg/L, and then declined until the end of the experiment on day 20. The HT WCR entered the exponential growth phase at day 8, reached its peak Chl-a concentration at day 14 of 25 µg/L, and declined. Following day 13 the HT reactor appears to enter a stagnation/decline phase until the conclusion of the experiment at day 20.

Comparing the 2 treatments, HT reached its peak 3 days before LT, and both treatments reached the same maximum Chl-a level. HT had an average of 18% higher Chl-a concentration than LT throughout the experiment.

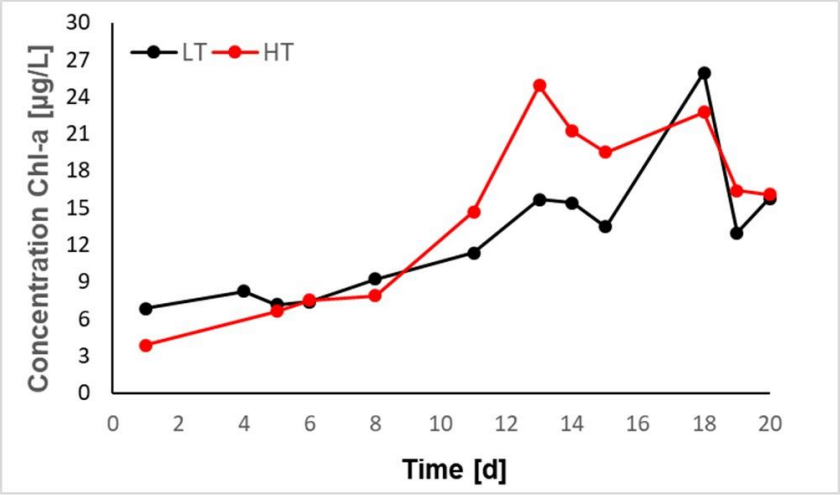

Figure 3.3: SP19 chlorophyll levels over time per WCR treatment. An outlier data point was removed for HT day 2.

SP19 - phytoplankton counts

In addition to Chl-a, counts of individual organisms was also measured for the WCRs as shown in Table 3-1 and Table 3-2 for LT and HT respectively. The raw data for counts is shown in Appendix Table A-3 and Appendix Table A-4. In the LT treatment of experiment SP19, from day 0 to day 18 the total count of only cyanos increased by 127% while the total counts of only non-cyanos decreased by 25%. Furthermore, the relative abundance of cyanos (total count of cyanos versus total counts of all phytoplankton) increased from 77% on day 1 to 91% on day 18. In contrast, the relative abundance of non-cyanos (total counts of non-cyanos versus total counts of all phytoplankton) decreased from 23% on day 1 to 9% on day 18.

Table 3-1: Experiment SP19 Cyano and non-cyano counts and percent changes in counts for LT treatment for days 0 and 18.

Counts for LT Treatment					
Day	**Total Cyano Counts**	**Total Non-Cyano Counts**	**Total Population Counts**	**Percent Cyanos [%]**	**Percent Non-Cyanos [%]**
1	6.22E7[A]	1.88E7	8.10E7	77	23
18	1.41E8	1.41E7	1.55E8	91	9
Percent Change [%] =	127	-25	92		

[A]Previous value of 6.22E6 was very different from 1.41E8. This could've been an error in count measurement using FlowCAM. Therefore for ABM simulations, the value of 6.22E7 is used.

In the HT treatment, from day 0 to day 18 the total count of only cyanos decreased by 28% while the total count of non-cyanos increased by 175%. Furthermore, the relative abundance of cyanos to the total population decreased from 93% on day 1 to 77% on day 18. In contrast, the relative abundance of non-cyanos to the total population increased from 7% on day 1 to 23% on day 18.

The results show clear dominance of the WCR's dominant cyanobacteria species in the algal bloom under low turbidity conditions.

Table 3-2: Experiment SP19 cyano and noncyano cell counts and percent changes in cell counts for HT treatment for days 0 and 18. These values were averaged across duplicate WCRs.

Counts for HT Treatment					
Day	**Total Cyano Counts**	**Total Non-Cyano Counts**	**Total Population Counts**	**Percent Cyanos [%]**	**Percent Non-Cyanos [%]**
1	2.89E8	2.30E7	3.12E8	93	7
18	2.08E8	6.33E7	2.71E8	77	23
Percent Change [%] =	-28	175	-13		

3.1.4 WCR SU19 - Chl-a and Counts

SU19- Chlorophyll-a

The Mix WCR began with a 23% higher Chl-a concentration, but both treatments paralleled each other in concentration patterns until day 14 when IntMix surpassed mixed and peaked on day 18 at a Chl-a concentration of 16 μg/L, until declining to the same values as Mix until the experiment stopped at day 21.

The Mix treatment peaked on day 11, 7 days before IntMix, reaching a maximum Chl-a concentration of 14 μg/L, and then declined. After day 13 the Chl-a concentration rises slightly but doesn't recover to the value of IntMix until IntMix crashes on day 20.

Comparing the two treatments, Mix reached its peak before IntMix and its peak was 17% less than IntMix. However, Mix had an average of 16% higher Chl-a concentration than IntMix throughout the experiment.

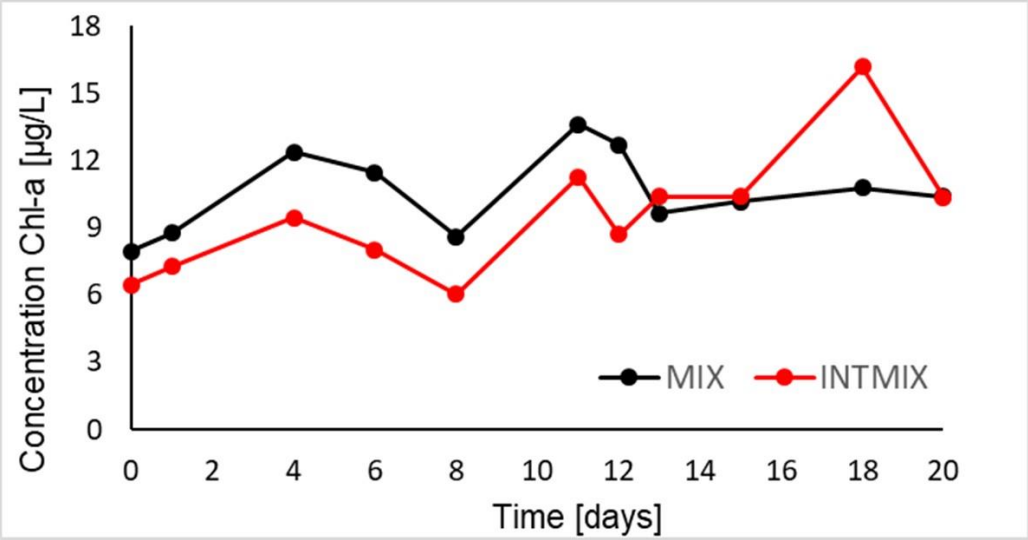

Figure 3.4: SU19 Chl-a levels over time per WCR treatment.

SU19 - phytoplankton counts

Phytoplankton count results from experiment SU19 Mix are shown in Table 3-3. The raw data for counts is shown in Appendix Table A-5 and Appendix Table A-6. In the Mix treatment, from day 0 to day 18 the total count of only cyanos increased by 61% while the total count of non-cyanos increased by 53%. Furthermore, the relative abundance of cyanos (total cyano count versus total population) slightly increased from 76% on day 1 to 77% on day 18. The relative abundance of non-cyanos (total non-cyano count versus total population) slightly decreased from 24% on day 1 to 23% on day 18. Overall, the total counts of cyanos and non-cyanos grew at a comparable rate in the Mix WCRs.

Table 3-3: SU19 Cyano and Non-Cyano counts and percent changes in counts for MIX treatment for days 0 and 18 of the experiment

Counts for Mix Treatment					
Day	**Total Cyano Counts**	**Total Non-Cyano Counts**	**Total Population Counts**	**Percent Cyanos [%]**	**Percent Non-Cyanos [%]**
1	4.88E+07	1.50E+07	6.38E+07	76	24
18	7.87E+07	2.30E+07	1.02E+08	77	23
Percent Change [%] =	61	53	59		

Phytoplankton count results from SU19, IntMix treatment are shown in Table 3-4. In the IntMix WCR, from day 0 to day 18 the total count of only cyanos increased by 393% while the total count of non-cyanos increased by 49%. Furthermore, the relative abundance of cyanos (total cyano count versus total population) increased from 81% on day 1 to 93% on day 18. The relative abundance of non-cyanos (total non-cyano count versus total population) decreased from 19% on day 1 to 7% on day 18.

Comparing the two treatments, the population of cyanos grew at a faster rate than non-cyanos in the IntMix resulting in cyano population dominating the algal bloom.

Table 3-4 : SU19 Cyano and Non-Cyano counts and percent changes in counts for INT-MIX treatment for days 0 and 18 of the experiment

Counts for IntMix Treatment					
Day	**Total Cyano Counts**	**Total Non-Cyano Counts**	**Total Population Counts**	**Percent Cyanos [%]**	**Percent Non-Cyanos [%]**
1	7.08E+07	1.70E+07	8.78E+07	81	19
18	3.49E+08	2.52E+07	3.74E+08	93	7
Percent Change [%] =	393	49	326		

3.1.5 SP19 and SU19 - Phytoplankton community structure

SP19-Cyanos

The dominating cyano species for both LT and HT was *Aphanocapsa*—a spherically shaped, colonial species. For the LT treatment, *Aphanocapsa's* relative abundance (*Aphanocapsa* count versus total cyano count) decreased from 99% to 88% of total cyano counts from day 0 to

18. For the HT treatment, *Aphanocapsa's* relative abundance decreased more than the LT, going from 95% to 51% of total cyano counts from day 0 to 18. The second most abundant cyanobacteria for both treatments on day 0 and 18 was Chroococcus and unknown filamentous cyanobacteria respectively. Therefore, the unknown filamentous cyanobacteria was starting to increase and compete with the *Aphanocapsas* by the last day of the experiment. Raw data describing the community structure and counts is shown in Appendix Table A-3.

SP19-Non-cyanos

The dominating non-cyano species on day 0 for both LT and HT treatments was Diatoms (*Aulacoseira*), at 92% and 72% of total non-cyano counts respectively. By day 18, the dominating non-cyano species for LT and HT treatments changed to dinoflagelletes (round), making up 69% and 68% of the total non-cyano counts respectively. The second most abundant noncyano for both treatments on day 0 and 18 was dinoflagelletes (round) and Diatoms (*Aulacoseira*) respectively. Raw data describing the community structure and counts is shown in Appendix Table A-4.

SU19-Cyanos

Similar to the SP19 experiment, the dominating cyano species for both the Mix and IntMix treatments on day 0 was *Aphanocapsa* at 64% and 75% of the total cyano counts respectively, though there was less dominance in SU19. This species remained the dominating species and increased in relative abundance (compared to total cyano counts) by day 18 where it made up 80% and 88% of the total cyano counts for the Mix and IntMix treatments respectively. The second most abundant identifiable cyano for both treatments on day 0 and 18 was Anabaena S. and Raphidiopsis respectively Raw data describing the community structure and counts is shown in Appendix Table A-5.

SU19-Non-cyanos

The dominating non-cyano species for both the Mix and IntMix treatments on day 0 was dinoflagellates at 90% and 86% of the total non-cyano counts respectively. This species remained the dominating species by day 18 in both treatments. However, its relative abundance in the Mix treatment decreased to 77% while in the IntMix it increased slightly to make up 90% of the total non-cyano counts. The second most abundant non-cyano for both treatments on both day 0 and day 18 was diatoms. Raw data describing the community structure and counts is shown in Appendix Table A-6.

3.1.6 Limitations of findings

For experiment SP19, one of the LT WCRs unknowingly at the time had an impeller shaft made of a different material that rusted off its coating. This zinc coating leached into the water, which may have impacted results. Also in experiment SU19, WCR #1 (Mix) got its impellers tangled with a SPATT bag line, shutting off mixing for at most 2 days out of the 3-week experiment. However, cell counts and chlorophyll data did not significantly differ among the results of the duplicates.

3.2 ABM Results

3.2.1 Optimization Results

As described in section 2.2.11, simulations were run in BehaviorSearch to determine the optimal parameter values to minimize the RMSE between experimental and simulated chl-a. Table 3-5 summarizes the simulations performed and the RMSE and MAE results. RMSE results from calibrating to 2017 WCR experiments is shown in

Appendix Table B-1.

Table 3-5: Summary comparing the RMSE and MAE results of each model type used per experiment for calibration.

Experiment	Model	RMSE (µg chl-a/L)	MAE (µg chl-a/L)
SP19 LT	1-Breed	3.33	2.2
	2-Breed-A1	4.0	3.0
	2-Breed-A	3.5	2.5
	2-Breed-B	30.2	23.9
SP19 HT	1-Breed	5.7	4.1
	2-Breed-A1	6.3	4.8
	2-Breed-A	5.8	4.5
	2-Breed-B	6.0	4.5
SU19 IntMix	1-Breed	2.0	1.6
	2-Breed-A1	2.0	1.6
	2-Breed-A	11.0	7.9
	2-Breed-B	8.5	5.3
SU19 Mix	1-Breed	2.1	1.4
	2-Breed-A1	2.9	2.5
	2-Breed-A	3.2	2.6
	2-Breed-B	8.9	6.3

The version that produced lowest errors was the 1-Breed model with an average RMSE across all experiments of 3.3 µg chl-a/L. The 2-Breed-A1 model, which had the same initial starting variables and used the same property values that were calibrated for 1-Breed but instead simulated 2 breeds, had the next lowest average RMSE of 3.8 µg chl-a/L. The 2-Breed-A model produced lower errors in experiments SP19 HT and SU19 Mix, but higher errors in experiment SU19 IntMix than the 2-Breed-B model. The average RMSE across all experiments for 2-Breed-A and 2-Breed-B is 5.9 µg chl-a/L and 13.4 µg chl-a/L respectively.

To quantify each calibrated ABM's stochasticity among simulations, the RMSE standard deviation was used as displayed in *Table 3-6.* The average standard deviation of 1-Breed and 2-Breed-B was 0.16 and 1.69 µg chla/L respectively.

Table 3-6: Quantifying stochasticity of ABMs using standard deviation.

	Standard Deviation of RMSE values [µg chla/L]	
	1-Breed	2-Breed-B
LT	0.3	2.3
HT	0.16	0.16
IM	0.03	4.15
M	0.13	0.15

SP19 LT was calibrated to explore different features such as different time steps and using the Monod light equation. Results of its calibration RMSE is shown in Table 3-7.

Table 3-7: Summary comparing RMSE of different versions of SP19 LT.

Experiment	Model version	RMSE (µg chl-a/L)
SP19 LT	dt = 0.5 h	3.32
	dt = 2 h	3.37
	Monod light limitation eqn	3.28

3.2.2 Model-data comparison chl-a

The following explains a visual inspection of how well the ABMs simulated each WCR experiment. The chl-a concentrations simulated by the 1-Breed ABMs is compared to WCR measured concentrations in Figure 3.5.Chl-a results of 1-Breed ABMs calibrated to 2017 WCR data is shown in Appendix Figure B.1.The 1-Breed was not only the best performing model type regarding error values, but visually its chl-a simulations tend to closely follow the trend of the measurements. However, there are some sharp rises and falls in data points that the 1-Breed ABM does not capture. Otherwise, it tends to follow the average of the data points well.

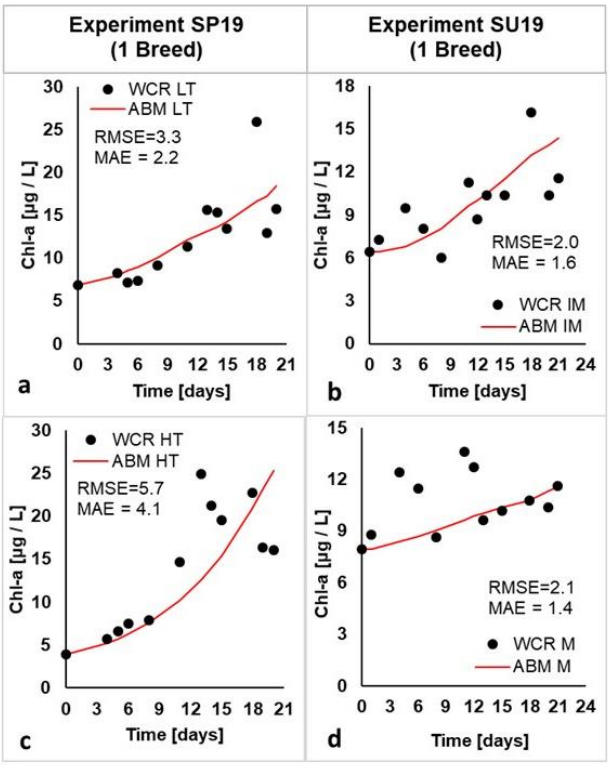

Figure 3.5: Calibrated 1-Breed RMSE results, MAE results, and simulated versus measured chl-a comparison for experiments SP19 LT (a), SU19 IntMix (b), SP19 HT (c) and SU19 Mix (d).

The chl-a concentrations simulated by the 2-Breed-A ABMs is compared to WCR measured concentrations in Figure 3.6. Visually, it does follow the chl-a measured trend for the LT and HT treatment. However, there's a discrepancy where the ABM predicts an exponential increase in chl-a in the IntMix treatment, over-shooting the WCR measured data. In contrast, the ABM tends to under predict the measured data in the Mix treatment.

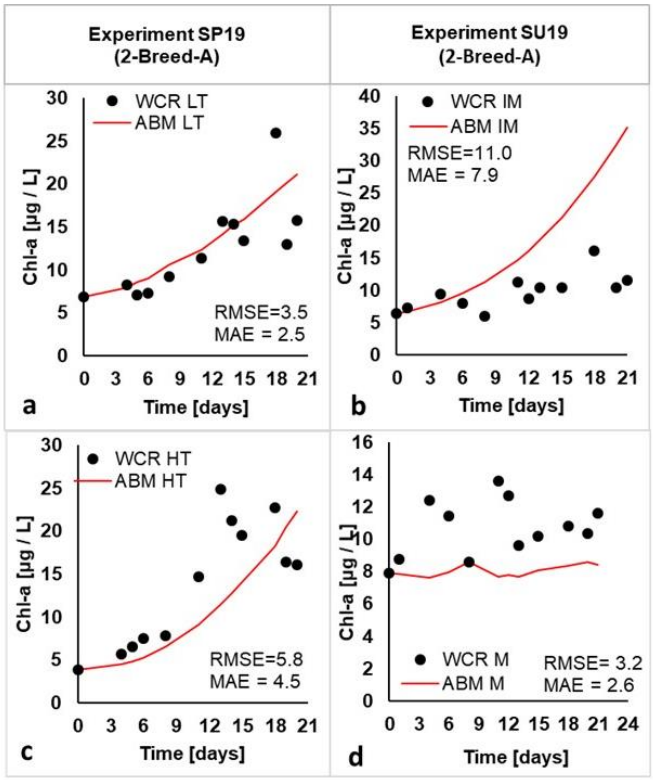

Figure 3.6: Calibrated RMSE results, MAE results, and simulated versus measured chl-a comparison for experiments SP19 LT (a), SU19 IntMix (b), SP19 HT (c) and SU19 Mix (d) for 2-Breed-A.

The chl-a concentrations simulated by the 2-Breed-A1 ABMs is shown in Figure 3.7. Upon visual inspection, the chl-a trends are similar between 2-Breed-A1 and 1-Breed ABMs, but they slightly differ in the LT and Mix. The 2-Breed-A1 dips then increases in the LT (following counts trend of breed 1 dying off in the first 7 days), it also increases at a slightly faster rate in the Mix treatment when compared to 1-Breed.

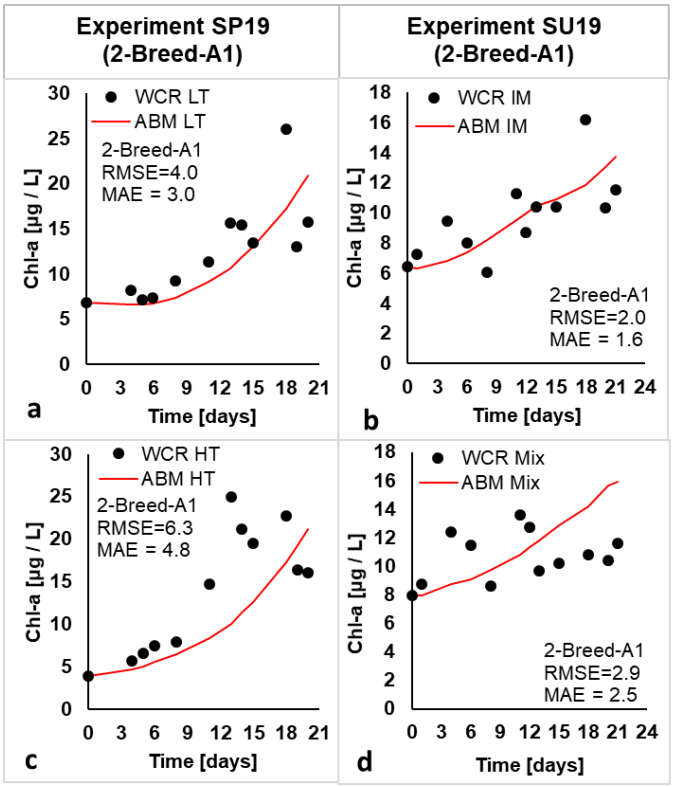

Figure 3.7: RMSE, MAE, and simulated versus measured chl-a comparison for experiments SP19 LT (a), SU19 IntMix (b), SP19 HT (c) and SU19 Mix (d) for 2-Breed-A1.

The chl-a concentrations simulated by the 2-Breed-B ABMs is compared to WCR measured concentrations in Appendix Figure B.2. Visual inspection showed that this type of model did follow the measure chl-a trend for the HT treatment. However, it assumed a similar general shape of the chl-a decreasing and then exponentially increasing for both mixing scenarios. For the IntMix, the ABM assumed an increase after day 13 that overshot the measured data. For the Mix, the simulation fell below the measured data up to day 9 and then by day 12 it overshot the data up to the end of the experiment. The simulation for LT assumed an immediate exponential growth that overshot the measured data throughout the experiment.

3.2.3 Calibrated property values

BehaviorSearch chose phytoplankton property values that resulted in the minimum RMSE between simulated and measured chl-a. The parameter values that favor growth are a low h and μ_d, and a high w_p and μ_{pmax}. These chosen parameters are explained further below for 1-Breed, 2-

Breed-A, and 2-Breed-B ABMs. The green cells with bolded numbers are meant to highlight the advantageous characteristics regarding light given to either breed.

The calibration-selected phytoplankton property values for 1-Breed models and the percentage of their maximum threshold is displayed in Table 3-8. For the LT treatment, calibration selected for a very high half-saturation constant and death rate, while selecting a very low rise rate and an average maximum photosynthetic rate. For HT treatment, calibration selected for a low half-saturation constant and rise rate, and comparable maximum photosynthetic and death rates. For IntMix treatment, a similarly low half-saturation constant and maximum photosynthetic rate was selected, along with an average rise and death rate. The Mix treatment selected for high half-saturation constant and rise rate, along with comparable low maximum photosynthetic and death rates.

Table 3-8: Selected calibrated property values of 1-breed ABMs compared to their set maximum threshold value.

Experiments SP19 and SU19 (1 Breed)								
	LT		HT		IntMix		Mix	
Symbol	Value	% of max threshold	Value	% of max threshold	Value	% of max threshold	Value	% of max threshold
h	32.0	**91.4**	10.4	**29.7**	10.1	**28.9**	24.8	**70.9**
w_p	-0.0053	**2.4**	0.0367	**18.3**	0.0853	**42.6**	0.129	**64.7**
μ_{pmax}	0.0604	**58.0**	0.0411	**39.6**	0.0298	**28.6**	0.0307	**29.5**
μ_d	0.0068	**82.0**	0.00301	**36.3**	0.00451	**54.4**	0.00246	**29.6**

The calibration-selected phytoplankton property values for the 2-Breed-A ABMs and the percentage of their maximum threshold is displayed in Table 3-9.

The turbidity experiments showed faster growth for Breed-1. For the LT treatment, a more advantageous half-saturation constant and death rate was selected for Breed-2, however the more advantageous rise rate and maximum photosynthetic rate chosen for Breed-1 allowed it to have a faster growth rate and dominate over Breed-2. For the HT treatment, the lower light half-saturation constant selected for Breed-1 gave it the most advantage to grow faster.

The SU19 experiments showed one of each breed having more growth over the other depending on the treatment. For the IntMix scenario, although Breed-2 had the most parameters chosen as advantageous, Breed-1 had a more advantageous μ_{pmax} and ultimately had the faster growth causing it to dominate the simulation. Lastly, the lower light half-saturation and higher rise rate selected for Breed-2 in the Mix treatment allowed for Breed-2 to have the after growth rate.

Table 3-9: Selected calibrated property values of 1-breed ABMs compared to their set maximum threshold value.

		Experiments SP19 and SU19 (2 Breed with 1-Breed range)							
		LT		HT		IntMix		Mix	
	Symbol	Value	% of max threshold	Value	% of max threshold	Value	% of max threshold	Value	% of max threshold
Breed-1	h	35	100	25.1	**72**	29.3	84	23.0	66
	w_p	0.160	**80**	0.046	23	0.132	66	0.012	6
	μ_{pmax}	0.0598	**58**	0.0722	69	0.0431	**41**	0.0501	**48**
	μ_d	0.0080	97	0.0064	77	0.0059	71	0.0054	**65**
Breed-2	h	26.3	**75**	32.3	92	15.5	**44**	8.3	**24**
	w_p	0.11	55	0.107	**54**	0.191	**96**	0.129	**65**
	μ_{pmax}	0.023	22	0.0761	73	0.0217	21	0.0349	34
	μ_d	0.0022	**27**	0.0060	73	0.0017	**20**	0.0070	84
Dominant after 20 days		Breed-1		Breed-1		Breed-1		Breed-2	

The calibration-selected phytoplankton property values for the 2-Breed-B ABMs and the percentage of their maximum threshold is displayed in Table 3-10Figure 3.11. For the LT, a more advantageous light half-saturation constant and maximum photosynthetic rate was selected for noncyanos, and they experienced faster growth than cyanos throughout the experiment. For the HT, a more advantageous rise rate and death rate was chosen for cyanos, allowing them to have faster growth and dominating the population during the simulation. In the IntMix treatment, a more advantageous light half-saturation constant and maximum photosynthetic rate was selected for noncyanos, allowing them to grow faster than cyanos and dominate the population. Similarly for the Mix treatment, a more advantageous light half-saturation constant and maximum

photosynthetic rate was selected for noncyanos, along with a lower death rate, allowing noncyanos to grow faster than cyanos and dominate the population.

Table 3-10: Selected calibrated property values of 1-breed ABMs compared to their set maximum threshold value.

		Experiments SP19 and SU19 (2-Breed-B)							
		LT		HT		IntMix		Mix	
	Symbol	Value	% of max threshold	Value	% of max threshold	Value	% of max threshold	Value	% of max threshold
Cyanos	h	21.4	61	26.16	75	34.49	99	29.56	**84**
	w_p	**0.188**	94	**0.122**	61	**0.02**	10	**0.068**	**34**
	μ_{pmax}	0.0470	87	0.0393	72	0.0213	39	0.0183	**34**
	μ_d	**0.0060**	73	**0.0013**	16	**0.0045**	54	0.0083	**99**
Noncyanos	h	**10.4**	61	**13.52**	80	**17**	100	**15.32**	**90**
	w_p	-0.0193	7	-0.0158	24	-0.0092	56	-0.012	**44**
	μ_{pmax}	**0.0651**	63	**0.0707**	68	**0.0763**	73	**0.0667**	**64**
	μ_d	0.0081	97	0.0080	96	0.0081	97	**0.0060**	**73**
Dominant after 20 days		Noncyanos		Cyanos		Noncyanos		Noncyanos	

3.2.4 Model-data comparison counts

Although not calibrated to counts, the ABMs total counts for each breed (for 2-Breed) were compared with measured counts.

The 2-Breed-A1 model's breed counts over time is illustrated in Figure 3.8. The LT treatment shows Breed-1 population decreasing from the beginning. The rest of the treatments have breed 1 starting off with higher counts and continuing its population trend upward to have a final population greater than breed 2.

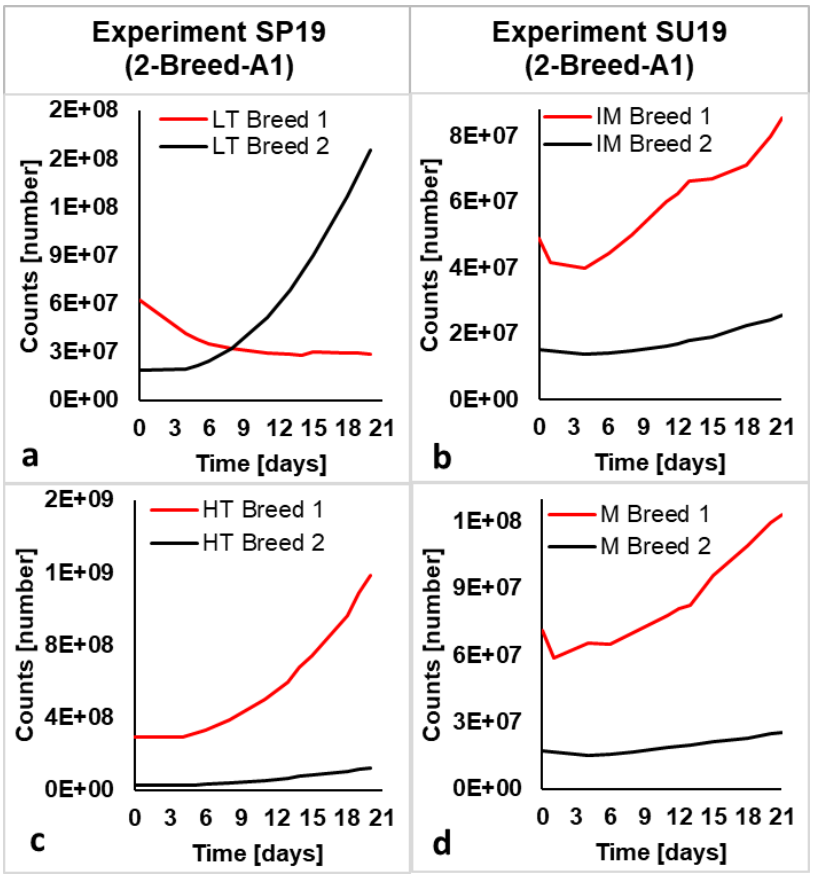

Figure 3.8: 2-Breed-A1 total counts of experiments SP19 LT (a), SU19 IntMix (b), SP19 HT (c) and SU19 Mix (d) using same calibrated phytoplankton property values from 1-Breed for both breeds.

The 2-Breed-A model's breed counts over time is illustrated in *Figure 3.9*. In the Mix treatment, Breed-1 decreased over time. In the LT, HT, and IntMix treatments, both breeds increased, but Breed-1 grew faster, dominating over Breed-2 in these three scenarios. Phytoplankton population behavior from the IntMix ABM is the only simulation that reflects WCR counts where both breed populations increased, but Breed-1 increased faster and dominated the environment.

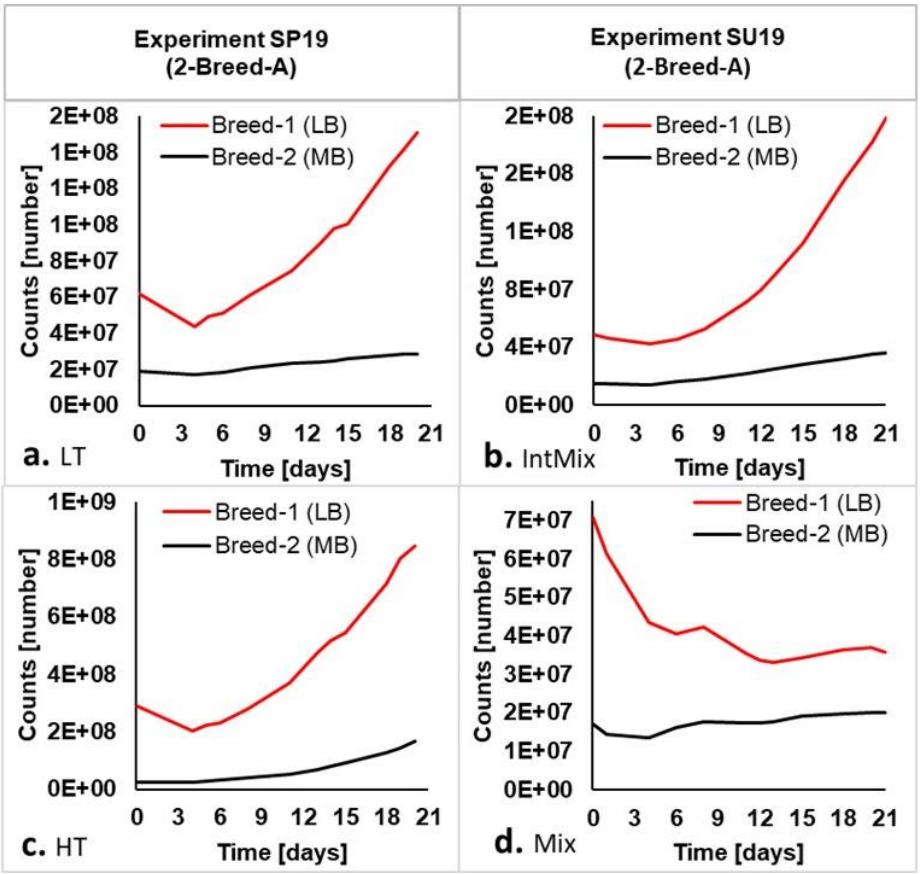

Figure 3.9: 2-Breed-A total counts (after calibration to chl-a) of experiments SP19 LT (a), SU19 IntMix (b), SP19 HT (c) and SU19 Mix (d) for 2-Breed-A ABMs.

The 2-Breed-B model's breed counts over time is illustrated in *Figure 3.10*. In the LT and HT treatment, both breeds increased over time. However, in the LT, noncyanos increased quickly to exceed the cyanos population. In the HT treatment, cyanos increased much faster than the noncyanos, dominating the overall population. In the IntMix treatment, the cyanos initially increased, but then decreased over time, while noncyanos exponentially increased, dominating the total population in the end. In the Mix treatment, cyanos strictly decrease while noncyanos exponentially increase and dominate the population.

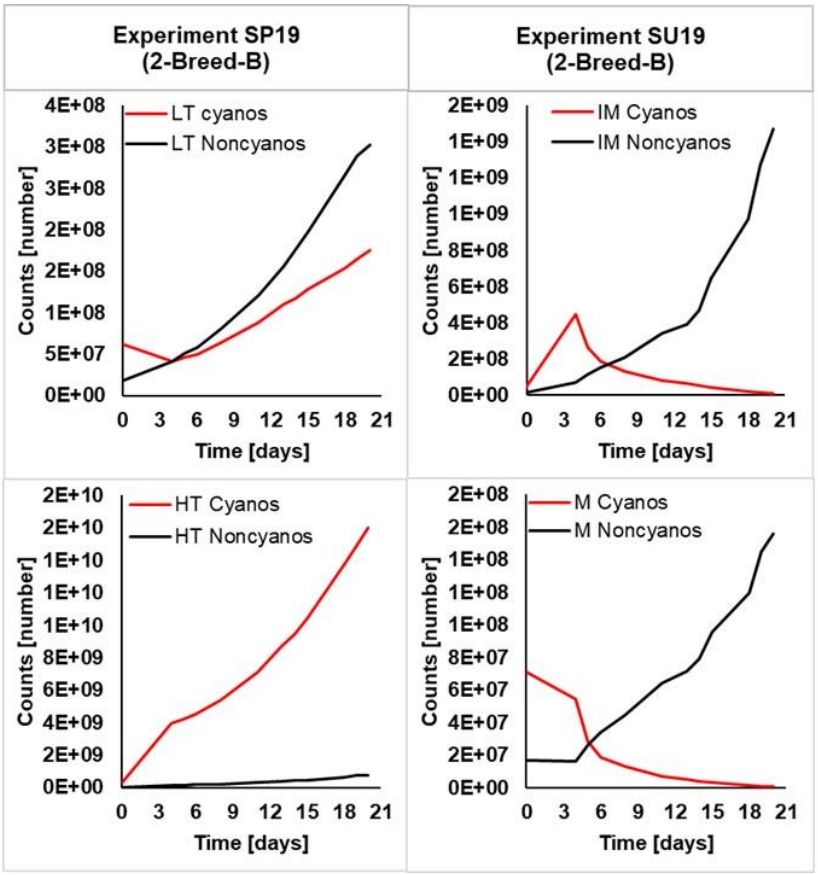

Figure 3.10: 2-Breed-B total counts (after calibration to chl-a) of experiments SP19 LT (a), SU19 IntMix (b), SP19 HT (c) and SU19 Mix (d) for 2-Breed-B ABMs.

3.2.5 Cross Validation

Calibrated 1-Breed ABMs were cross validated (CV) with their respective SP19 and SU19 counterpart treatment. The RMSE of these CVs are compared within each experiment, along with their calibration (C) RMSE results, and displayed in Figure 3.11.

The ABMs had lower errors in simulating different mixing scenarios than they did in simulating different turbidity scenarios. C and CVs produced a total average RMSE of 16.0 µg chl-a/L for experiment SP19 and 2.2 µg chl-a/L for experiment SU19. The average CV RMSEs in particular were 27.5 µg chl-a/L and 2.4 µg chl-a/L for SP19 and SU19 respectively. The ABM performs better in predicting WCR chl-a concentrations under various mixing conditions.

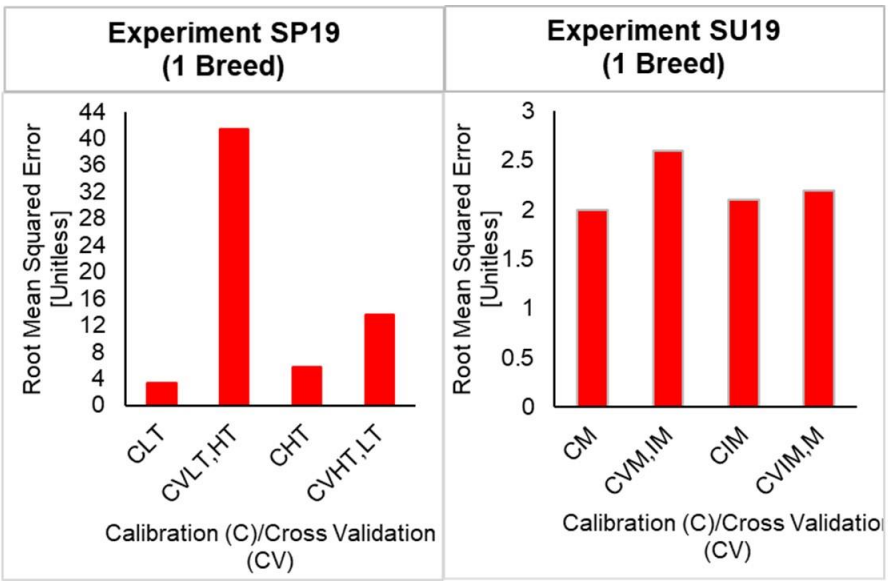

Figure 3.11: RMSE results of 1-breed calibration (C) compared to cross validation (CV) with the opposite treatment within the same experiment. For example, SP19 shows the results of calibrating the LT treatment (CLT) and cross validating it using property values selected for the HT treatment (CVLT,HT).

3.2.6 Model Explorations

In order to explore the capabilities of this ABM, we present a series of WCR profiles for light, cell counts, and chl-a concentrations for the calibrated 1-Breed HT in Figure 3.12. The ABM can provide higher resolution of results for the entire WCR profile, such as cell counts every 0.08 m in depth instead of just at 35 cm of depth as with the experimental data.

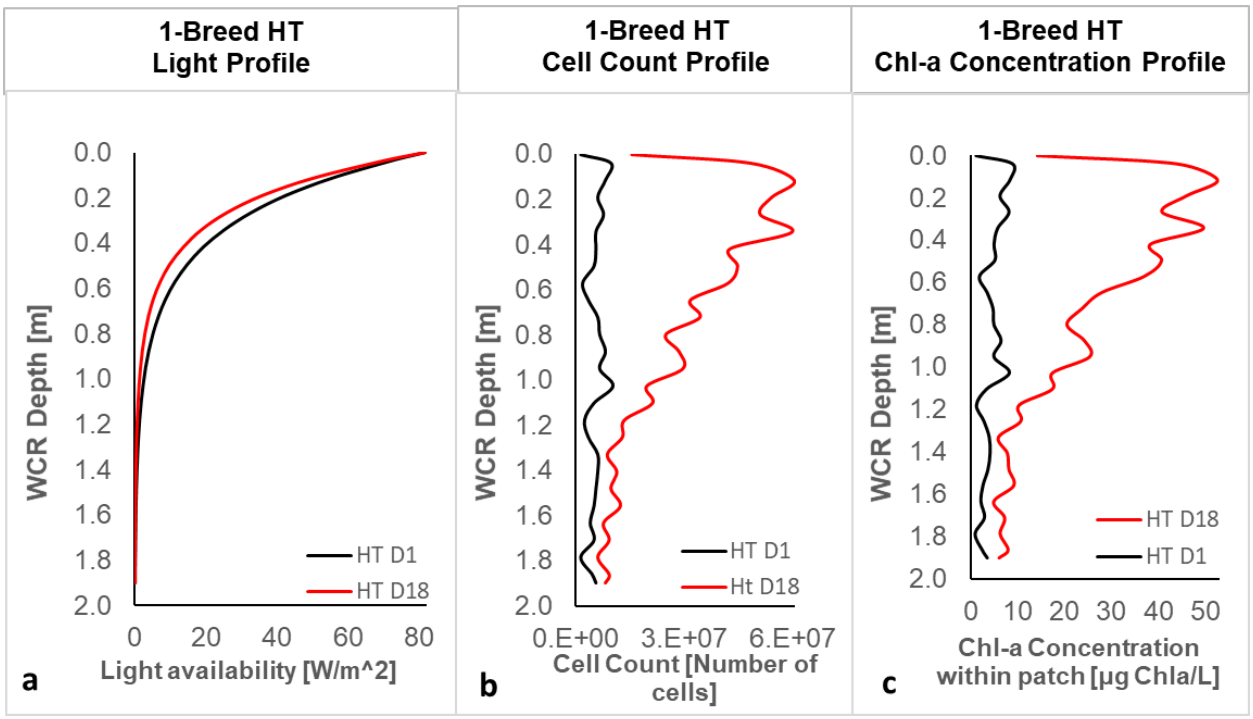

Figure 3.12: 1-Breed HT profile of light intensity (a), total cell count (b), and chl-a concentration (c). The simulation measured each value every 0.08 m in depth.

Another model exploration conducted was using Monod (Mon) instead of inhibition (Inh) light limitation formulation using 1-Breed HT. Table 3-11 compares the average values and Figure 3.13 compares light intensities down the WCR when using each formulation. Results showed that using Monod decreased average light intensity slightly by day 18 by about 3%, however, using the Monod formulation, by day 18 there was about 16% more total cell counts and average chl-a concentration than when using the inhibition formulation.

Table 3-11: Comparing average population results using inhibition versus Monod light limitation formulation for 1-Breed HT.

	Avg light intensity (W/m^2)		Avg cell counts (No. cells)		Avg chl-a conc (µg Chla/L)	
	D1	D18	D1	D18	D1	D18
Inhibition	14.55	12.33	5.6E+06	2.7E+07	4.45	22.40
Monod	14.43	12	5.6E+06	3.1E+07	4.38	25.87
% difference	-0.83	-2.65	0.00	16.12	-1.61	15.51

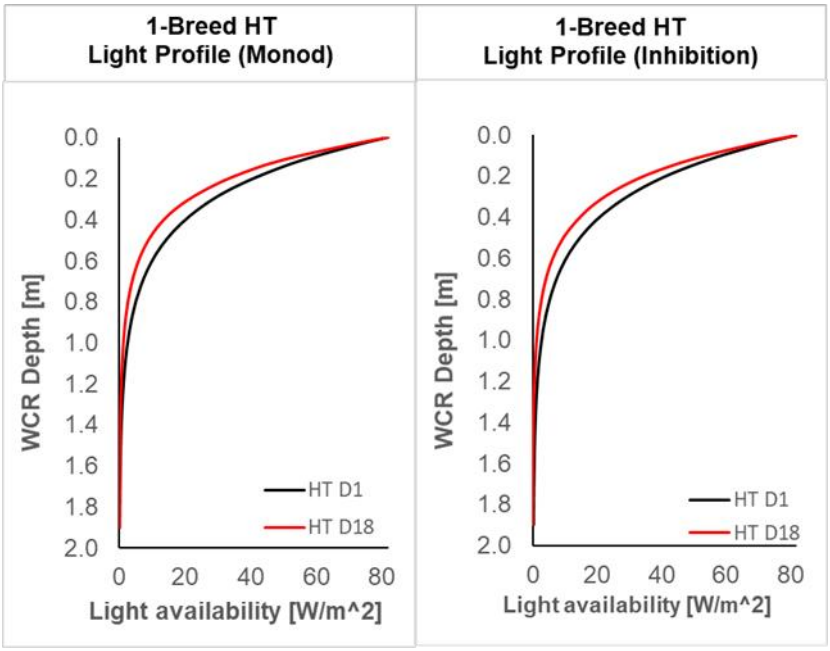

Figure 3.13: Comparing light profile using Monod versus inhibition light limitation formulation for 1-Breed HT

The 1-Breed HT model with a buoyant breed was used to explore different features that were not used during calibration. For example, nutrient limitation was turned on which resulted in less cell counts and chl-a concentration than a nutrient replete environment as shown in Figure 3.14.

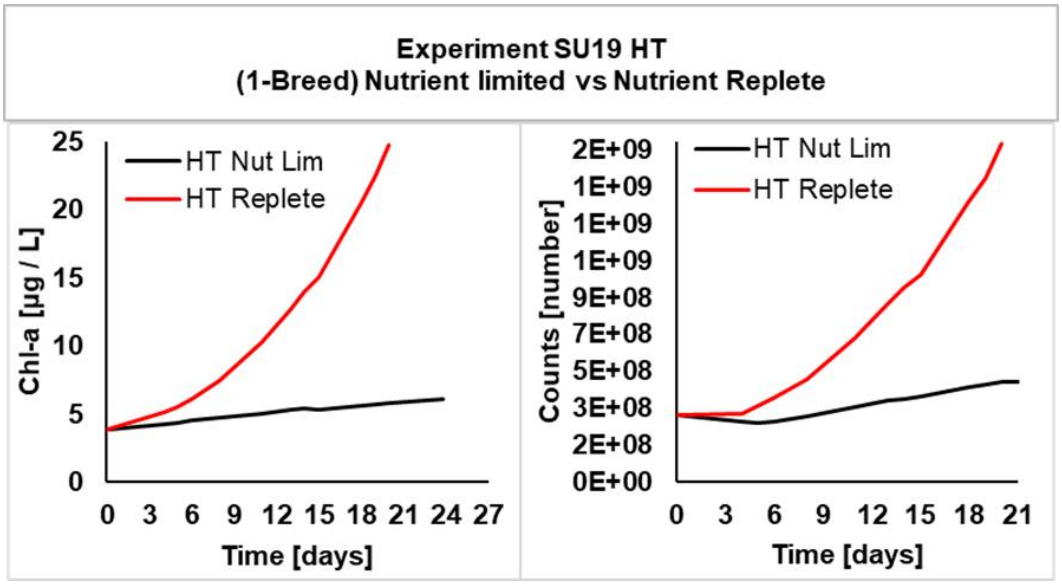

Figure 3.14: Chl-a concentration and cell count results compared in nutrient limited and replete scenarios.

Also, temperature was shifted 5 degrees colder and warmer and the population grew more in the warmer temperature as shown in Figure 3.15.

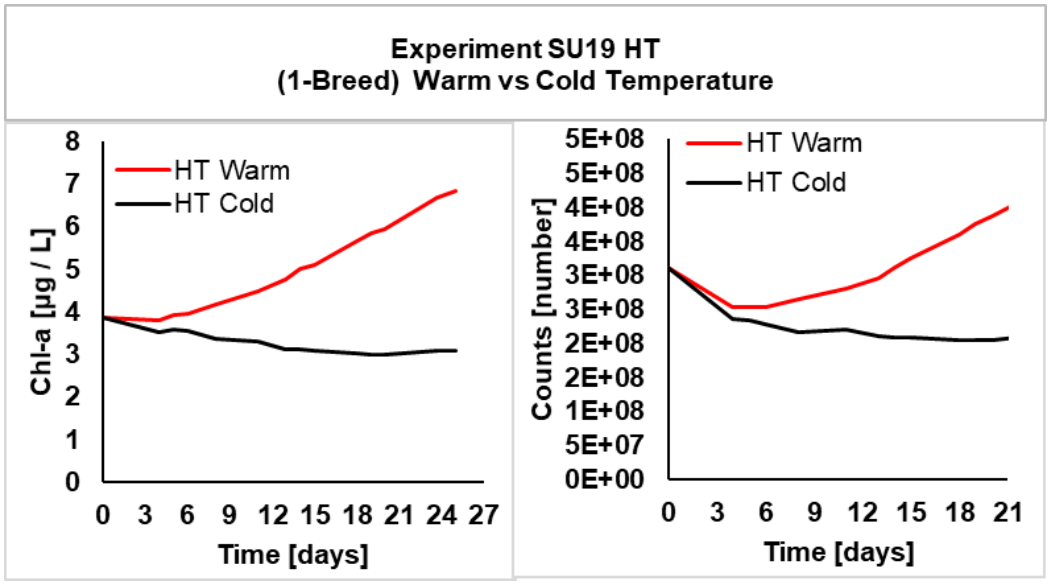

Figure 3.15: Chl-a concentration and cell count results compared in warm and cold scenarios.

Lastly, the HT received constant mixing and with more mixing, the buoyant population didn't grow as much as when there was no mixing as shown in Figure 3.16.

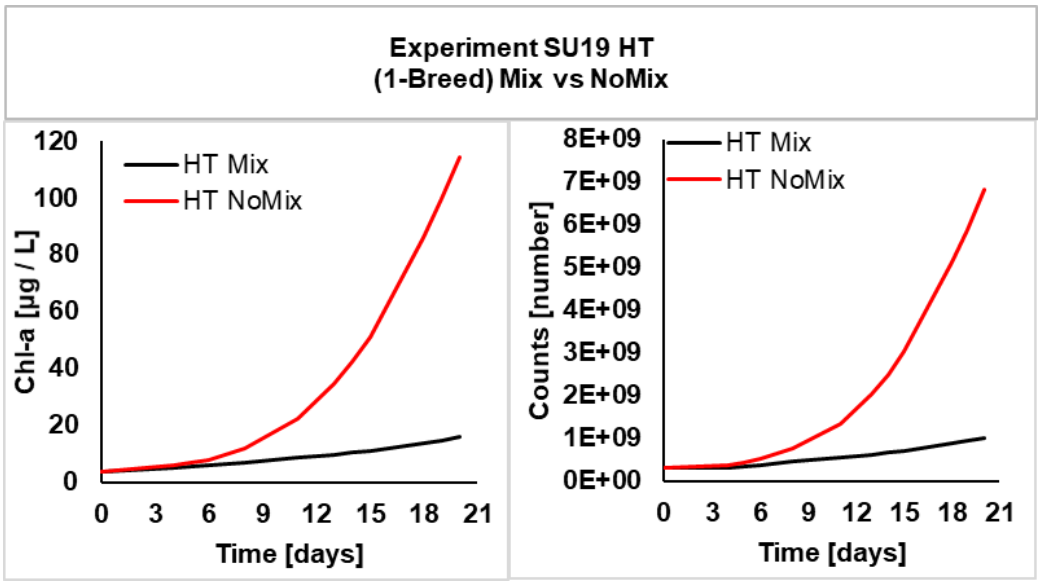

Figure 3.16: Chl-a concentration and cell count results compared in mix and nomix scenarios.

4.0 Discussion

4.1 WCR

4.1.1 SP19 & SU19 Nutrients

NO_3^-, NO_2^- and PO_4^{3-} were measured during the experiment since nitrogen and phosphorus as nutrients have the largest impact on phytoplankton growth in many aquatic systems (Paerl et al., 2016). In this experiment, WCRs began with similar initial PO_4^{3-} concentrations as the previous WCR experiments of Mangot (2018), which was approximately 100 µg/L. However, initial NO_3^- + NO_2^- concentrations of this experiment were 75% less than the previous WCR experiment of (Mangot, 2018): 250 µg/L compared to 1000 µg/L. This difference was likely attributed to the added nutrients in the 2017 experiments coming from a pre-made F/20 media, whereas a nutrient cocktail was developed in-lab for the 2019 experiment as described in the methods section. These differences could have resulted in less NO_3^- + NO_2^- nutrients being added to the WCRs of this study compared to SU17. Although there was less initial NO_3^- + NO_2^- nutrients, the nutrient levels

never completely depleted throughout the experiment and remained at least five times the half-saturation for the majority of the experiments.

In experiment SP19, the difference in turbidity levels may also contribute to the difference in initial nutrient concentrations, since turbidity adds nutrients to the WCR. In experiment SU19, the differences in initial nutrient values is likely attributed to differences in source water since all 4 WCRs had the same amount of artificial turbidity added. Moreover, it is expected that the HT reactors would have a slightly higher PO_4^{3-} and $NO_2^- + NO_3^-$ concentration than the LT reactors. However, we believe the additional nutrient differences observed in either experiment to be attributed to measurement error.

4.1.2 SP19 & SU19 Light

Results suggest that we did achieve a different light environment with LT and HT, and the light environments of Mix and IntMix were indeed similar. With replete nutrients, light was the primary factor limiting growth. The percent available light that remained below 1 m was the similar to the light environment of previous WCR studies (Mangot, 2018). The exception was the SP19 LT WCRs since there was less turbidity to hinder light from reaching the lower depths of the WCR. Reductions in light availability over the course of a given experiment was due to phytoplankton biomass growth and vertical distribution (Mangot, 2018). The decrease in light intensity in the bottommost layers may also be attributed to turbidity (both algal and non-algal) settling towards the bottom of the WCRs.

In the SU19 experiment, the Mix treatment having less available light in the upper layer on day 15 is likely due to the fact that the constant mixing from the impellors, which are located towards the top of the WCRs. Therefore, in the Mix reactors the impellers can keep turbidity suspended, shading light in the upper layer (Mangot, 2018).

4.1.3 Turbidity impact on phytoplankton community structure and total counts

Overall, the HT treatment hindered the growth of cyanos, reducing their total counts over the course of the experiment. Studies show that in some places, including North Carolina, phytoplankton—cyanobacteria especially—dominate in reservoirs during time of low turbidity and increased light availability (Smith, 1990). Turbidity hindering cyanobacteria growth can likely be attributed to suspended solids reducing phosphorus bioavailability. Phosphorus availability can be reduced by formation of salts with minerals such as calcium and iron, both of which can be found in bentonite clay (Douglas et al., 2016; Green & Logan, 1978). Suspended solids can reduce phosphorus bio-availability through solid-phase adsorption (changes its phase from dissolved to unusable solid substrate) or flocculation (Douglas et al., 2016). The presence of inorganic, suspended solids reduces light quality and availability, and can reduce phosphorus availability, thereby reducing the dominance of cyanobacteria as studied in four North Carolina reservoirs (Smith, 1990).

The majority of cyanobacteria present throughout the WCR experiment were *Aphanocapsa*, a spherical, colonial cyanobacteria (Albrecht et al., 2017). At higher turbidity, suspended solids can remove cyanobacteria from the mixed layer through co-flocculation and sedimentation. Colonial cyanobacteria tend to colonize, creating a larger surface area that is more vulnerable to being weighed down by sinking suspended solids than a filamentous green algae (Smith, 1990). This could be the reason why cyanobacteria experienced higher total count growth rates in the LT treatment than in the HT, and why non-cyanos were able to grow in HT treatment. This is further supported by previous research which observed a shift in dominance from cyanobacteria (in the 1970s) to flagellated chlorophytes (non-cyanos) (in the 1990s) when light attenuation increased from elevated suspended sediments (or higher turbidity) (Holz, 1997).

Some cyanobacteria are adapted to grow and thrive in low-light conditions. Typically the predominant cyanobacteria in Jordan Lake are members of the *Oscillatoriales* and *Chroococcales* (Touchette et al., 2007). These types of phytoplankton have remarkable low light adaptation likely as a results from their high surface area to volume ratio (Reynolds & Alex Elliott, 2012). However, the cyanobacteria that dominated the WCRs in this study were of a different type and results show that they were not well-adapted to low-light conditions.

4.1.4 Vertical mixing impact on phytoplankton community structure and total counts

In experiment SU19, the total count of cyanos did not increase as much in the Mix condition as it did in the IntMix, confirming that constant vertical mixing appeared to suppress cyanobacteria population growth relative to night-time mixing alone. This agrees with previous results when testing mixing in the WCRs (Mangot, 2018). Cyanobacteria can regulate their buoyancy and thus control their position in the water column to outcompete non-motile phytoplankton for light. Therefore, more vertical mixing impedes with cyanobacteria's ability to move to their optimal position, and gives non-motile phytoplankton a chance to achieve a higher, more optimal position in the water column (Huisman et al., 2004).

Furthermore, cyanos and noncyanos maintaining similar relative abundances at day 1 as they did on day 18 of being in the Mix treatment shows that this environment is likely closest to the source water environment. We obtained the source water from a marina where boat traffic likely helps to keep the water column well mixed, just like in the WCR Mix treatment.

4.1.5 SP19 & SU19 Chl-a

Since the bentonite clay used for artificial turbidity naturally contains nutrients, the HT WCR of experiment SP19 started with slightly more nutrients, possibly stimulating a faster initial increase of chl-a in HT compared to LT. Furthermore, throughout the experiment the HT

population had a higher average chl-a level than the LT. This could potentially be because a high chl-a to biovolume ratio is one property that helps phytoplankton have more efficient light-harvesting capability, along with more accessory pigments (Havens et al., 2003; Schwaderer et al., 2011). Therefore, having more chl-a in lower light environments, such as in a HT environment, can greatly benefit phytoplankton that need light to survive and grow. Although HT may hinder cyano counts, it perhaps encourages higher Chl-a in these phytoplankton.

4.1.6 WCR Research Contribution and future work

The WCR is novel way to test impacts of environmental changes on phytoplankton community structure and behaviors in a controlled manner, including how light, nutrients, mixing, turbidity, and temperature drive population dynamics. Gaining more data on how these factors impact phytoplankton growth and community structures can help to better calibrate and validate future ABM models, making them more robust in predicting blooms under various environmental conditions.

To date, WCRs have been used to test the effects of vertical mixing and turbidity on phytoplankton population dynamics in a controlled setting. In addition to those features, water temperature has a direct impact on both phytoplankton growth and nutrient cycling via mineralization, and has been identified as an important driver of algal blooms (Paerl, 2008). Therefore in future experiments, different temperatures can be tested in duplicates to observe its impacts on phytoplankton blooms. In these future experiments, more phytoplankton count data could be collected to better calibrate ABMs not just to chl-a, but also to counts. Thus far WCRs replete with nutrients have been tested, however experimenting with different limiting levels of initial nutrients could allow ABMs to calibrate to nutrient levels using Droop kinetics. This could

give insight on P movement from external to internal forms. Furthermore, nitrogen (N) and P could be tested as limiting separately to see their impacts on community structure.

4.2 ABM

4.2.1 Performance of chlorophyll-a simulations

The ABMs were able to capture the general measured chl-a trends, however they did not capture the sharp rises and falls of the data. In the model, since chl-a is directly proportional to biomass, chl-a directly follows the trend of biomass (i.e. counts). In our simulations, there are no events that make drastic changes to the biomass. For example, in the simulation there is no pulse of nutrients to make biomass quickly spike (Visser et al., 2016). Also, previous studies show that virus abundance have a significant correlation to chl-a (Tijdens et al., 2007), however no virus was included in the ABM that would make the population die and cause a dip in biomass. Therefore, the chl-a concentration maintained a steady trend proportional to the total biomass in the system.

Holding a constant Chl-a/molC ratio could have also reduced chl-a dynamics within our models. Although previous ABM studies have assumed constant Chl-a/molC (Hellweger et al., 2008), studies involving the population averaged model CE-QUAL-W2 (2-D laterally averaged water quality model) have shown the importance of implementing a variable chl-a/algal biomass ratio for improved performance and prediction capabilities of a model (Sadeghian et al., 2018). One study found that using variable Chl-a:C ratios reduced model simulation errors (RMSE) by about 50% (Sadeghian et al., 2018).

Although hypothesized to have lower error due to more degrees of freedom, the calibrated 2-Breed ABM versions produced higher RMSE than 1-Breed. To explore the difference between 1-Breed and 2-Breed further, the 2-breed-A1version was used to simulate 2 breeds with equal parameter values as the calibrated 1-Breed. This resulted in 3.6% lower RMSE than the 1-Breed

for the LT treatment, but a 2.6% higher RMSE for the HT treatment. Upon closer inspection, the only difference between 1-Breed and 2-Breed-A1 ABMs is that 1-Breed represents the total population cell counts (cyanos and noncyanos), so the initial S_R (total number of cells/600 agents) is equal per agent. As a result, when agents grow and divide into 2 agents, the S_R of each daughter cell is equal to the original cell, thereby doubling the total number of cells represented by the parent agent. As agents divide, they each add to the total number of cells (and biomass) at a constant rate that is similar to one another. In contrast, 2-Breed-A1 is initialized with one breed of agents representing total cyano cell counts ($S_{R,C}$), and one breed representing noncyano counts ($S_{R,NC}$). Therefore initial $S_{R,C}$ (cyano cell counts / 300 agents) and $S_{R,NC}$ (noncyano cell counts/300 agents) are different. This difference leads to different growth rates per breed. The test using 2-Breed-A1 showed that simulating breeds of 2 different growth rates impact chl-a. Even if modeling 2 breeds each with the same properties as 1-Breed, the simulated total counts, and therefore chl-a, trends will be different.

A potential reason that calibrated 2-Breed versions experience higher RMSE could be attributed to the fact that the difference in growth rates and calibrating two times more parameters are adding complexity that is difficult for BehaviorSearch to calibrate to. Furthermore, a prior study that used BehaviorSearch as an optimization tool found that in many problems, the genetic algorithms (such as the one chosen for calibration in this study) may have a tendency to converge towards local optimum or even arbitrary points rather than the global optimum of the problem (Massobrio, 2013). In future ABM calibrations, a deeper investigation in the best algorithms to use, and perhaps increasing the number of searches, could better ensure a global optimum to be reached, especially for the 2-Breed ABM versions.

4.2.2 Calibration-selected property values

The parameter values that favor growth are a low h and μ_d, and a high w_p and $\mu_{pmax.}$ For the 1-Breed LT treatment, optimization selected for a high light half-saturation constant (h) and a very low rise rate (i.e. sinking rate), which makes sense since there is enough light that there is no need for the phytoplankton to have a low h to better maximize available light or a faster rise rate to get to the top of the WCR if light reaches the lower depths. However, the HT treatment selects for a lower and more advantageous h to better maximize any available light in a darker system. The low h must compensate for a low, but still positive rise rate. The maximum photosynthetic rate and death rates are similar for HT and therefore likely doesn't play as big a role as light half saturation and rise rate in determining community structure. The high death rate in the LT treatment is likely attributed to the fact that population must stay low in order to meet the low chl-a measurements.

For IntMix, optimization selected a more favorable, lower h than in the Mix, which is reasonable since Mix increases the chances of each individual making it to the top WCR layer to obtain sufficient light (Huisman et al., 2004). For Mix, calibration selected for a higher, more favorable rise rate. This is likely because diffusion provides an equal boost upwards as it does downwards in the water column, therefore a higher rise rate ensures that the phytoplankton can better compete with any downward push of the mixing for better chances of survival. The death rate was selected to be higher for the IntMix, which is likely a way to control population to not get too high since chl-a only reaches a maximum of about 11 μg Chl-a/L, and keeping population down helps to maintain a low chl-a concentration to better match the experimental data points.

For 2-Breed-A results, the LT column shows that the advantageous rise rate and maximum photosynthetic rate allow Breed-1 to grow faster. However, the HT treatment shows that the light

half-saturation property was deemed most important in providing Breed-1 the advantage to grow faster and dominate the population.

For the 2-Breed-A IntMix scenario, although Breed-2 had the most parameters chosen as advantageous, the higher photosynthetic rate chosen for the Breed-1 ultimately allowed them to best maximize the light available and dominate the population. Lastly, the lower light half-saturation and higher rise rate proved most important in the Mix treatment to make Breed-2 grow while Breed-1 decreased in counts. There wasn't any one specific advantageous property to determine which 1 breed dominated. These varying properties illustrate the complexities of how organisms can adapt and use internal characteristics to compensate for other areas that are lacking. For instance, phytoplankton can have a beneficial light half-saturation to obtain an advantage regardless of position in the WCR, such as how noncyanos are known to do in the environment (Visser et al., 2016). In contrast, phytoplankton can also use their buoyancy in order to achieve a higher position in the water column that has more light, such as how cyanos do (Huisman et al., 2004).

For the 2-Breed-B ABMs, the calibration was forced to select parameters within a certain generic range for cyanos and noncyanos (Hellweger et al., 2008). Adhering to literature values, the light half-saturation constant and maximum photosynthetic ranges of the noncyanos are naturally more advantageous than cyanos (Hellweger et al., 2008). Therefore the calibration was forced to always pick more advantageous values for these properties for noncyanos. This could be a reason why noncyanos dominated all treatments except for HT. Although noncyanos had a disadvantage with a settling (instead of a rising) velocity in all treatments, the sinking rate's negative impact to the population was more pronounced in the HT scenario.

Although the parameter ranges for vertical velocity strictly resembled either a generic buoyant (assumed cyano) or generic sinking (assumed noncyano) breed, it is understood that these groupings are generic, and may not be an accurate representation for all noncyanos. For example, dinoflagellates, which fall under the grouping of noncyano, are known to be a buoyant species with the potential to have a rise rate (Rivkin et al., 1982). Results showed that in the SP19 and SU19 WCR experiments, dinoflagellates always dominated the noncyanos population by the end of the experiment. Therefore it may improve future ABM calibrations to alter the vertical velocity parameters to incorporate typical characteristics of the dominating group of phytoplankton in the experiment. However in the development of the ABM in this study, the focus was to use rising cyano's and sinking noncyano's typical characteristic values found in literature (Hellweger et al., 2008) to calibrate to the experiments.

4.2.3 Simulated cell counts

In 2-Breed-A, the Mix treatment showed 1 breed increasing and the other decreasing. Furthermore, in 2-Breed-B IntMix and Mix treatments, noncyanos dominated over the cyanos while in the HT, cyanos dominated over noncyanos. The tendency of 1 breed typically dominating the other in the 2-breed models could be attributed to an ecological theory called the intermediate disturbance hypothesis (IDH) which describes a link between diversity and disturbance. IDH states that diversity comes from constant and varied perturbations (Reynolds et al., 1993). This implies that when a natural community experiences constant, unchanged external conditions, community structure progresses towards uniformity, a single species, or a single set of advantageous characteristics (Reynolds et al., 1993). Therefore, undisturbed successions, such as the ABMs simulating a single treatment over many generations of phytoplankton, should eventually approach competitive exclusion (i.e. 1 species) (Reynolds et al., 1993).

The behavior of the 2-Breed-A IntMix counts agreed with WCR measurements, while that of the Mix treatment agreed with observations of prior research studies such as (Huisman et al., 2004). Phytoplankton population behavior from the IntMix ABM is the only simulation of the 2-Breed-A method that reflects what was seen in the WCR experiments, which was a large increase in cyanos that ultimately dominated the environment. Although Mix WCR measurements showed an increase in both breeds, the Mix ABM phytoplankton population behavior of Breed-1 increasing and Breed-2 decreasing supports observations from previous studies where intensified mixing has led to complete species replacement from cyanos to green algae and diatoms (noncyanos) (Huisman et al., 2004). Another explanation for Breed-2 overtaking Breed-1 in the Mix ABM could be that Breed-2 had a more advantageous light half-saturation constant selected for it. Mixing greatly randomizes the vertical position and therefore light availability for all phytoplankton. Studies have shown that eukaryotic algae such as green algae and diatoms (noncyanos) are better adapted to larger fluctuations in photo irradiances, while cyanos are more sensitive, and therefore one breed can overtake the other in well-mixed conditions (Visser et al., 2016).

Although 2-Breed-A HT ABM didn't cause a decrease in 1 breed's counts as observed in WCR experiments regarding cyanos, the behavior of Breed-1 supports previous studies that state some cyanobacteria HABs thrive under high nutrient, and low light conditions caused by turbidity via adaptations (Paerl, 2008). Table 3-9 confirms that in the HT scenario, Breed-1 was given a better light half saturation constant than Breed-2, making them better adapted to low light conditions and thereby faster growers in that turbid condition. This is further supported in the results of 2-Breed-B where cyanos dominated in the HT treatment.

In 2-Breed-B scenarios, noncyanos dominated the population in the LT treatment. The LT gives the noncyano sinking species more opportunity for available light (Paerl, 2008). Combine that with a more advantageous selected properties of half saturation constant and maximum photosynthetic rate to further maximize light and growth and this allows noncyanos to easily dominate the system (Paerl, 2008). In 2-Breed-B IntMix and Mix scenarios, cyano populations decreased. Although they have positive rise rates, these rates were selected to be low, thereby reducing their chances to grow and dominate.

4.2.4 Cross Validations

The 1-Breed ABM overall better predicts WCR chl-a concentrations under various mixing conditions and is therefore more robust at predicting under different mixed scenarios since its cross validations (CV) yielded a lower average RMSE of 1.8 μg chl-a/L.

A reason for its poor CV performance for different turbidity levels may be because its chl-a levels are too sensitive, or too dependent, on turbidity. Biomass growth (i.e. chl-a) depends solely on light limitation, which is directly impacted by turbidity as shown in Eq. 1, Eq. 2, Eq. 3, and Eq. 7. Also, studies have shown that turbidity largely impacts algal biomass in natural reservoirs (Smith, 1990). The property values selected by calibration is determined for phytoplankton that experience only one type of turbidity for generations, which doesn't allow them to gain any properties to adapt to an environment with changing turbidity. As a result, the model's chl-a concentration results are very sensitive to changing turbidity levels. In contrast, mixing only impacts the position of phytoplankton, which could easily be overcome by their vertical velocities.

4.2.5 Model Explorations

Results from exploring the profiles of chl-a and total counts of the calibrated 1-Breed HT ABM showed expected trends. The chl-a and total counts tended to be highest in the upper

layers, maximizing around 0.3 m. Below 0.3 m the values decreased, hitting their minimum level soon after 1 m deep. This follows the trend seen in prior WCR studies of higher chl-a level in the upper layers of the water column (Mangot, 2018). This also agrees with observations of other studies that state how placement the upper layers provide more light availability which is beneficial for phytoplankton growth (Huisman et al., 2004; Visser et al., 2016).

Results from exploring other features (i.e. temperature, nutrients, and mixing) in the 1-Breed HT revealed population patterns that we would expect. The ABM was using a buoyant species, like cyanos, and its population grew best in warm, no-mix, nutrient-replete environments as we would expect based on literature and prior field studies (Huisman et al., 2004; Liu et al., 2011; Paerl et al., 2011).

5.0 Conclusion

This study confirmed the ability to develop and calibrate ABMs to WCR experimental data. Results of the WCR experiments suggest that HT and Mix treatments suppress the growth of cyanobacteria. HT and Mix treatments also encourage higher total chlorophyll-a levels in the phytoplankton population.

Results of the ABM simulations suggest that the 1-Breed version follows the chl-a measured tends in each treatment well, yielding the lowest average total RMSE of 3.3 μg chl-a/L. Also the 1-Breed version proved to be robust in simulating various mixing scenarios while producing similar RMSEs. Our optimization program showed difficulty in optimizing the 2-Breed versions compared to the 1-Breed, which can be looked into further in future ABM experiments. In summary, this study showed that an ABM can be calibrated to reproduce measured chlorophyll-a trends of WCRs.This ABM is the first step to exploring the experimental WCRs. Phytoplankton growth depends on light, nutrients, and temperature. This study focused on the light aspect,

however field study measurements have confirmed that algae adjust their chl-a:C ratios based on P availability (Sadeghian et al., 2018), therefore nutrients (i.e. phosphorus) can be further explored with this ABM to improve future calibrations to WCR chl-a data. Furthermore, the proportion of nutrients (e.g. N:P) are known to impact community composition, along with productivity and toxin production (Glibert, 2017). Therefore the impact of nitrogen and phosphorus ratios on community structure and chlorophyll-a could be explored in future simulations and WCR experiments. Temperature can also be studied using the WCRs and implemented in the ABM. Considering nutrients and temperature along with light can reduce the model's sensitivity to turbidity, improving its robustness to replicate WCRs under various turbidity scenarios.

In addition to growth parameters, the morphology of phytoplankton can also be considered, such as the impact of having colonial species, like *Aphanocapsa*, be modeled against filamentous phytoplankton.

Three time steps were explored in this study, however it would be beneficial to do a more extensive search on the best time step for this model. Also, a more extensive test to find the best algorithms to use on BehaviorSearch can potentially improve the optimum value.

Seeing how IDH could have played a role in reducing coexistence between breeds in the ABMs, a way to overcome this in the future could be by adding perturbations such as random virus spread to attack a population at random. If nutrients are added as a feature, perturbations can also include sudden pulses or reductions in nutrients.

Furthermore, it seems more difficult for BehaviorSearch to find an optimal solution for 2-Breed ABM. This was unexpected and suggests a complexity in optimization that we didn't account for and will need to be considered in future research.

The ABMs of this study was only calibrated to measured chl-a. However, future studies with the WCR should have more count data points to improve ABM calibration to not just chl-a, but also counts, since one way to make calibration more robust in ABMs is by assessing model output against multiple criteria (Badham et al., 2017). Also having 8 parameters allows the opportunity to calibrate to more data within a single WCR experiment. More data can be found in model exploration shown in 3.2.6, which includes WCR profiles that give insight to vertical variability, allowing exploration of other phytoplankton behaviors like vertical distribution of chl-a or cell counts. Therefore, 8 parameters can be used to fit to not just overall chl-a concentration, but chl-a concentrations in the upper versus lower layers, or at more depths. Also, 2017 experiments have more count data available for different days and depths, which can provide more data for a better calibration. Lastly, multiple experiments could be calibrated at one time which can yield a lower RMSE, especially when using the 8 parameters of the 2-Breed.

Overall, the 1-breed ABM, when calibrated to the WCR's chl-a, performs well in producing the general trend for that WCR. A calibrated ABM able to reproduce WCR results under both various mixing and turbidity conditions will allow for month-long WCR experiments to be run in-silico in a matter of minutes. This will help us to better understand how environmental parameters impact bloom formation, giving us another alternative modeling tool to help determine better water management techniques. This tool could help improve the water quality in our shallow, eutrophic reservoirs and allow us to make more informed decisions for engineered reservoir solutions. Considering these factors would elevate the ABM and in the future can even allow it to explore phytoplankton communities and populations even under unforeseen conditions, including increased temperatures expected from climate change.

6.0 References

Albrecht, M., Pröschold, T., & Schumann, R. (2017). Identification of Cyanobacteria in a eutrophic coastal lagoon on the Southern Baltic Coast. *Frontiers in Microbiology*, *8*(MAY), 923. https://doi.org/10.3389/fmicb.2017.00923

Badham, J., Jansen, C., Shardlow, N., & French, T. (2017). Calibrating with multiple criteria: A demonstration of dominance. *JASSS*, *20*(2). https://doi.org/10.18564/jasss.3212

Berglund, E. Z., & Asce, M. (2015). *Using Agent-Based Modeling for Water Resources Planning and Management*. https://doi.org/10.1061/(ASCE)WR.1943-5452.0000544

Bucci, V., Nunez-Milland, D., Twining, B. S., & Hellweger, F. L. (2012). Microscale patchiness leads to large and important intraspecific internal nutrient heterogeneity in phytoplankton. *Aquatic Ecology*, *46*(1), 101–118. https://doi.org/10.1007/s10452-011-9384-6

Cael, B. B., Heathcote, A. J., & Seekell, D. A. (2017). The volume and mean depth of Earth's lakes. *Geophysical Research Letters*, *44*(1), 209–218. https://doi.org/10.1002/2016GL071378

Chai, T., & Draxler, R. R. (2014). Root mean square error (RMSE) or mean absolute error (MAE)?-Arguments against avoiding RMSE in the literature. *Geosci. Model Dev*, *7*, 1247–1250. https://doi.org/10.5194/gmd-7-1247-2014

Chapra, S. (1997). *Surface Water Quality Modeling*. WCB McGraw Hill.

Chapra, S. (2008). *Surface water-quality modeling*. Waveland press.

Crill, P. A. (1977). The photosynthesis-light curve: A simple analog model. *Journal of Theoretical Biology*, *64*(3), 503–516. https://doi.org/10.1016/0022-5193(77)90284-3

Di Toro, D. M. (1978). Optics of turbid estuarine waters: Approximations and applications. *Water Research*, *12*(12), 1059–1068. https://doi.org/10.1016/0043-1354(78)90051-9

Douglas, Hamilton, Robb, Pan, Spears, & Lurling. (2016). Guiding principles for the development and application of solid-phase phosphorus adsorbents for freshwater ecosystems. *Aquatic Ecology*, *50*. https://doi.org/10.1007/s10452-016-9575-2

Downing, J. A., Prairie, Y. T., Cole, J. J., Duarte, C. M., Tranvik, L. J., Striegl, R. G., McDowell, W. H., Kortelainen, P., Caraco, N. F., Melack, J. M., & Middelburg, J. J. (2006). The global abundance and size distribution of lakes, ponds, and impoundments. *Limnology and Oceanography*, *51*(5), 2388–2397. https://doi.org/10.4319/lo.2006.51.5.2388

Droop, M. R. (1973). SOME THOUGHTS ON NUTRIENT LIMITATION IN ALGAE [1]. *Journal of Phycology*, *9*(3), 264–272. https://doi.org/10.1111/j.1529-8817.1973.tb04092.x

Eilers, P. H. C., & Peeters, J. C. H. (1988). A model for the relationship between light intensity and the rate of photosynthesis in phytoplankton. *Ecological Modelling*, *42*(3–4), 199–215. https://doi.org/10.1016/0304-3800(88)90057-9

Fredrick, N. D., Berges, J. A., Twining, B. S., Nuñez-Milland, D., & Hellweger, F. L. (2013). Use of agent-based modeling to explore the mechanisms of intracellular phosphorus heterogeneity in cultured phytoplankton. *Applied and Environmental Microbiology*, *79*(14), 4359–4368. https://doi.org/10.1128/AEM.00487-13

Glibert, P. M. (2017). Eutrophication, harmful algae and biodiversity — Challenging paradigms in a world of complex nutrient changes. *Marine Pollution Bulletin*, *124*(2), 591–606. https://doi.org/10.1016/j.marpolbul.2017.04.027

Green, & Logan. (1978). Phosphate Adsorption-Desorption Characteristics of Suspended Sediments in the Maumee River Basin of Ohio. *Journal of Environmental Quality*, *7*(2). https://acsess-onlinelibrary-wiley-

com.prox.lib.ncsu.edu/action/doSearch?AllField=Phosphate+Adsorption-Desorption+Characteristics+of+Suspended+Sediments+in+the+Maumee+River+Basin+of+Ohio&SeriesKey=15372537

Grover, J. P. (2017). Sink or swim? Vertical movement and nutrient storage in phytoplankton. *Journal of Theoretical Biology*, *432*, 38–48. https://doi.org/10.1016/j.jtbi.2017.08.012

Han, Y. (North C. S. U. (2020). Evaluating the Roles of Light, Mixing, and Nutrients on Algal Production and Cyanobacteria Dominance in a Shallow Reservoir through Computational Modeling. *Unpublished*.

Havens, K. E., James, R. T., East, T. L., & Smith, V. H. (2003). N:P ratios, light limitation, and cyanobacterial dominance in a subtropical lake impacted by non-point source nutrient pollution. *Environmental Pollution*, *122*(3), 379–390. https://doi.org/10.1016/S0269-7491(02)00304-4

Hawkins, P. R., & Griffiths, D. J. (1993). Artificial destratification of a small tropical reservoir: effects upon the phytoplankton. In *Hydrobiologia* (Vol. 254).

Hellweger. (2017). 75 years since Monod: It is time to increase the complexity of our predictive ecosystem models (opinion). *Ecological Modelling*, *346*(Supplement C), 77–87. https://doi.org/10.1016/j.ecolmodel.2016.12.001

Hellweger, & Bucci, V. (2009). A bunch of tiny individuals-Individual-based modeling for microbes. *Ecological Modelling*, *220*(1), 8–22. https://doi.org/10.1016/j.ecolmodel.2008.09.004

Hellweger, F., & Kianirad, E. (2007). *Accounting for Intrapopulation Variability in Biogeochemical Models Using Agent-Based Methods*. https://doi.org/10.1021/es062046j

Hellweger, & Kianirad. (2007). *Accounting for Intrapopulation Variability in Biogeochemical*

Models Using Agent-Based Methods. https://doi.org/10.1021/ES062046J

Hellweger, Kravchuk, E. S., Novotny, V., & Gladyshev, M. I. (2008). Agent-based modeling of the complex life cycle of a cyanobacterium (Anabaena) in a shallow reservoir. *Limnology and Oceanography*, *53*(4), 1227–1241. https://doi.org/10.4319/lo.2008.53.4.1227

Holz, J. . (1997). Phytoplankton community response to reservoir aging, 1968–92. *Hydrobiologia*, *346*, 183–192. https://doi-org.prox.lib.ncsu.edu/10.1023/A:1002978302479

Huang, J., Xu, Q., Wang, X., Xi, B., Jia, K., Huo, S., Liu, H., Li, C., & Xu, B. (2015). *Evaluation of a Modified Monod Model for Predicting Algal Dynamics in Lake Tai*. *7*, 3626–3642. https://doi.org/10.3390/w7073626

Huisman, J., Sharples, J., Stroom, J. M., Visser, P. M., Kardinaal, W. E. A., Verspagen, J. M. H., & Sommeijer, B. (2004). CHANGES IN TURBULENT MIXING SHIFT COMPETITION FOR LIGHT BETWEEN PHYTOPLANKTON SPECIES. *Ecology*, *85*(11), 2960–2970. https://doi.org/10.1890/03-0763

Ke, Z., Xie, P., Guo, L., Liu, Y., & Yang, H. (2007). In situ study on the control of toxic Microcystis blooms using phytoplanktivorous fish in the subtropical Lake Taihu of China: A large fish pen experiment. *Aquaculture*, *265*(1–4), 127–138. https://doi.org/10.1016/j.aquaculture.2007.01.049

Lewis, D. M., Elliott, J. A., Lambert, M. F., & Reynolds, C. S. (2002). The simulation of an Australian reservoir using a phytoplankton community model: PROTECH. In *Ecological Modelling* (Vol. 150). www.elsevier.com/locate/ecolmodel

Liu, X., Lu, X., & Chen, Y. (2011). The effects of temperature and nutrient ratios on Microcystis blooms in Lake Taihu, China: An 11-year investigation. *Harmful Algae*, *10*(3), 337–343. https://doi.org/10.1016/J.HAL.2010.12.002

Mangot, A. (2018). *Effects of Vertical Mixing on Phytoplankton Communities in a Shallow , Turbid Water Column Experiment*.

Massobrio, G. (2013). *Optimizing the behavior of trading agents using genetic algorithms in a stock exchange simulation framework with real data* [University of Turin]. https://terna.to.it/tesi/massobrio.pdf

Ou, L., Wang, D., Huang, B., Hong, H., Qi, Y., & Lu, S. (2008). *Comparative study of phosphorus strategies of three typical harmful algae in Chinese coastal waters*. https://doi.org/10.1093/plankt/fbn058

Paerl, H. (2008). Nutrient and other environmental controls of harmful cyanobacterial blooms along the freshwater-marine continuum. *Advances in Experimental Medicine and Biology*, *619*, 217–237. https://doi.org/10.1007/978-0-387-75865-7_10

Paerl, H., Thad Scott, J., McCarthy, M. J., Newell, S. E., Gardner, W. S., Havens, K. E., Hoffman, D. K., Wilhelm, S. W., & Wurtsbaugh, W. A. (2016). It Takes Two to Tango: When and Where Dual Nutrient (N & P) Reductions Are Needed to Protect Lakes and Downstream Ecosystems. *Environ. Sci. Technol*, *17*, 44. https://doi.org/10.1021/acs.est.6b02575

Paerl, Xu, H., McCarthy, M. J., Zhu, G., Qin, B., Li, Y., & Gardner, W. S. (2011). Controlling harmful cyanobacterial blooms in a hyper-eutrophic lake (Lake Taihu, China): The need for a dual nutrient (N & P) management strategy. *Water Research*, *45*(5), 1973–1983. https://doi.org/10.1016/J.WATRES.2010.09.018

Prokopkin, I. G., Gubanov, V. G., & Gladyshev, M. I. (2006). Modelling the effect of planktivorous fish removal in a reservoir on the biomass of cyanobacteria. *Ecological Modelling*, *190*(3–4), 419–431. https://doi.org/10.1016/j.ecolmodel.2005.05.011

Reynolds, C. S., & Alex Elliott, J. (2012). Complexity and emergent properties in aquatic ecosystems: predictability of ecosystem responses. *Freshwater Biology*, *57*(SUPPL. 1), 74–90. https://doi.org/10.1111/j.1365-2427.2010.02526.x

Reynolds, Padisak2, J., & Sommer3, U. (1993). Intermediate disturbance in the ecology of phytoplankton and the maintenance of species diversity: a synthesis. In *Hydrobiologia* (Vol. 249).

Reynolds, Wiseman, S. W., Godfrey, B. M., & Butterwick, C. (1983). Some effects of artificial mixing on the dynamics of phytoplankton populations in large limnetic enclosures. In *Journal of Plankton Research* (Vol. 5). https://academic.oup.com/plankt/article/5/2/203/1488209

Riley, G. (1956). Oceanography of Long Island Sound. In *New Haven: Bingham Oceanographic Laboratory*.

Rivkin, R. B., Seliger, H. H., Swift, E., & Biggley, W. H. (1982). *MARINE BIOLOGY Light-Shade Adaptation by the Oceanic Dinoflagellates Pyrocystis noctiluca and P. fusiformis ** (Vol. 181).

Rowe, M. D., Anderson, E. J., Wynne, T. T., Stumpf, R. P., Fanslow, D. L., Kijanka, K., Vanderploeg, H. A., Strickler, J. R., & Davis, T. W. (2016). Vertical distribution of buoyant *Microcystis* blooms in a Lagrangian particle tracking model for short-term forecasts in Lake Erie. *Journal of Geophysical Research: Oceans*, *121*(7), 5296–5314. https://doi.org/10.1002/2016JC011720

Sadeghian, A., Chapra, S. C., Hudson, J., Wheater, H., & Lindenschmidt, K.-E. (2018). *Improving in-lake water quality modeling using variable chlorophyll a/algal biomass ratios*. https://doi.org/10.1016/j.envsoft.2017.12.009

Schwaderer, A. S., Yoshiyama, K., de Tezanos Pinto, P., Swenson, N. G., Klausmeier, C. A., & Litchman, E. (2011). Eco-evolutionary differences in light utilization traits and distributions of freshwater phytoplankton. *Limnology and Oceanography*, *56*(2), 589–598. https://doi.org/10.4319/lo.2011.56.2.0589

Smith, V. H. (1990). *Effects of Nutrients and Non-algal Turbidity on Blue-green Algal Biomass in Four North Carolina Reservoirs, Lake and Reservoir Management*. *6*(2), 125–131. https://doi.org/10.1080/07438149009354702

Steele, J. H. (1962). *Environmental Control of Photosynthesis in the Sea* (Vol. 7, Issue 2).

Stonedahl, F., & Wilensky, U. (2010). *BehaviorSearch*. Center for Connected Learning and Computer Based Modeling, Northwestern University.

Thingstad, T. F. (1987). *Utilization of NI P, and organic C by heterotrophic bacteria. I. Outline of a chemostat theory with a consistent concept of "maintenance" metabolism* (Vol. 35).

Tijdens, M., Hoogveld, H. L., Kamst-Van Agterveld, M. P., Simis, S. G. H., Baudoux, A.-C., Laanbroek, H. J., & Gons, H. J. (2007). *Population Dynamics and Diversity of Viruses, Bacteria and Phytoplankton in a Shallow Eutrophic Lake*. https://doi.org/10.1007/s00248-007-9321-3

Touchette, B. W., Burkholder, J. M., Allen, E. H., Alexander, J. L., Kinder, C. A., Brownie, C., James, J., & Britton, C. H. (2007). *Eutrophication and cyanobacteria blooms in run-of-river impoundments in North Carolina*. *23*(2), 179–192. https://doi.org/10.1080/07438140709353921

Trolle, D., Skovgaard, H., & Jeppesen, E. (2008). *The Water Framework Directive: Setting the phosphorus loading target for a deep lake in Denmark using the 1D lake ecosystem model DYRESM-CAEDYM*. https://doi.org/10.1016/j.ecolmodel.2008.08.005

Verhamme, E. M., Redder, T. M., Schlea, D. A., Grush, J., Bratton, J. F., & DePinto, J. V. (2016). Development of the Western Lake Erie Ecosystem Model (WLEEM): Application to connect phosphorus loads to cyanobacteria biomass. *Journal of Great Lakes Research, 42*(6), 1193–1205. https://doi.org/10.1016/j.jglr.2016.09.006

Visser, P. M., Ibelings, B. W., Bormans, M., & Huisman, J. (2016). Artificial mixing to control cyanobacterial blooms: a review. *Aquatic Ecology*, *50*(3), 423–441. https://doi.org/10.1007/s10452-015-9537-0

Weiskerger, C. J., Rowe, M. D., Stow, C. A., Stuart, D., & Johengen, T. (2018). Application of the Beer–Lambert Model to Attenuation of Photosynthetically Active Radiation in a Shallow, Eutrophic Lake. *Water Resources Research*, *54*(11), 8952–8962. https://doi.org/10.1029/2018WR023024

Wilensky, U. (1999). *NetLogo* (6.1.0). Center for Connected Learning and Computer-Based Modeling, Northwestern University. http://ccl.northwestern.edu/netlogo/

7.0 Appendices

Appendix A: WCR Additional Information

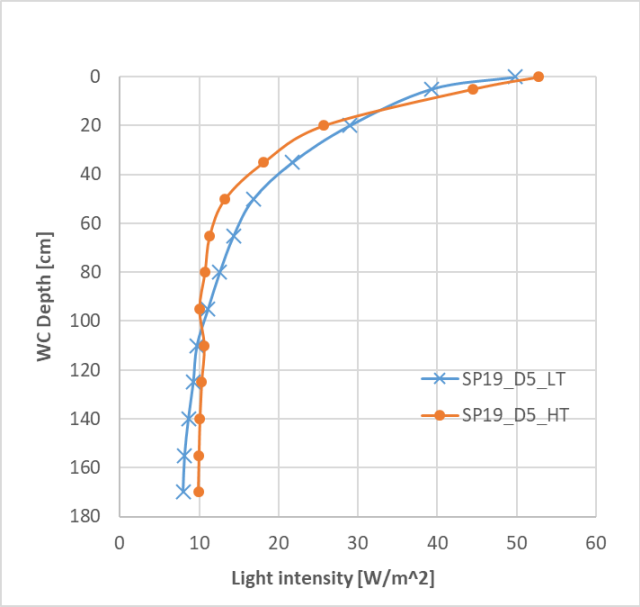

Appendix Figure A.1: Light profile for SP19 WCRs on day 5.

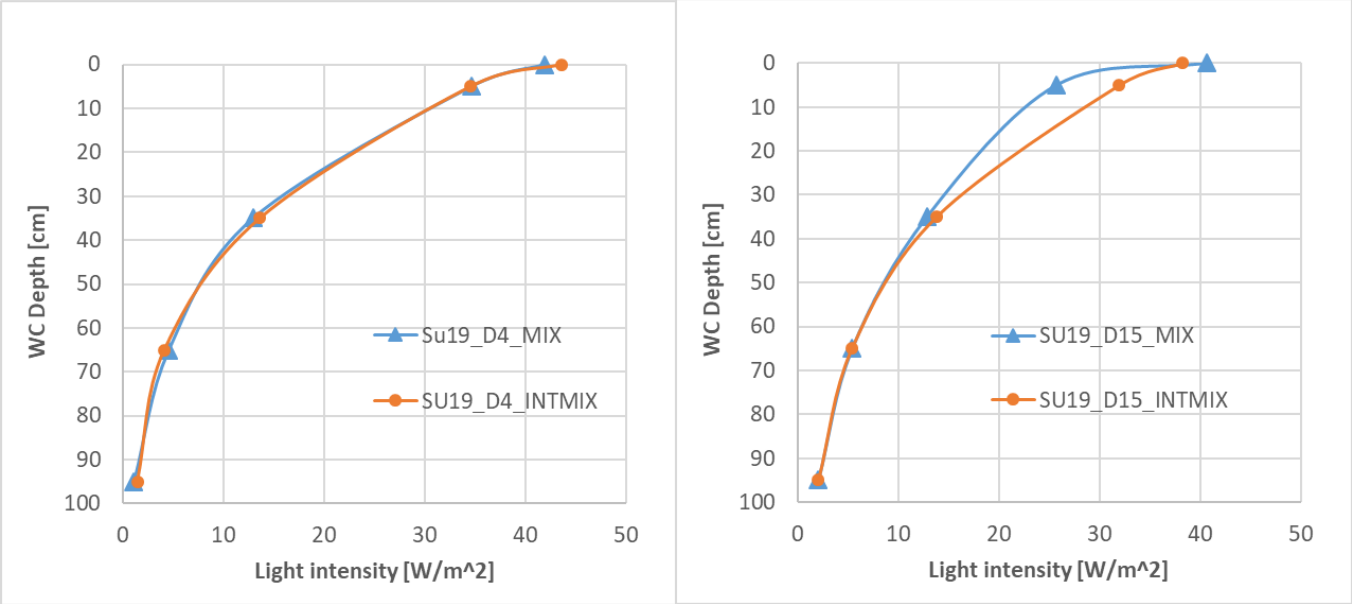

Appendix Figure A.2: Light profile for SU19 WCRs on day 4 (D4) and 15 (D15).

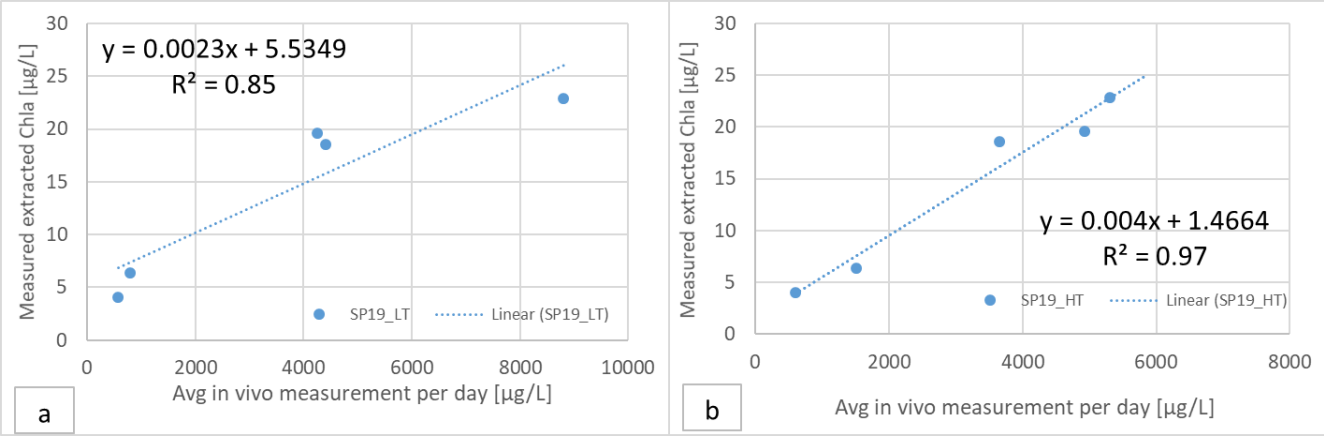

Appendix Figure A.3: SP19 Measured extracted chl-a vs in vivo for LT (a) and HT (b) treatment. The equation displayed on each graph is the regression line used to estimate the actual chl-a values.

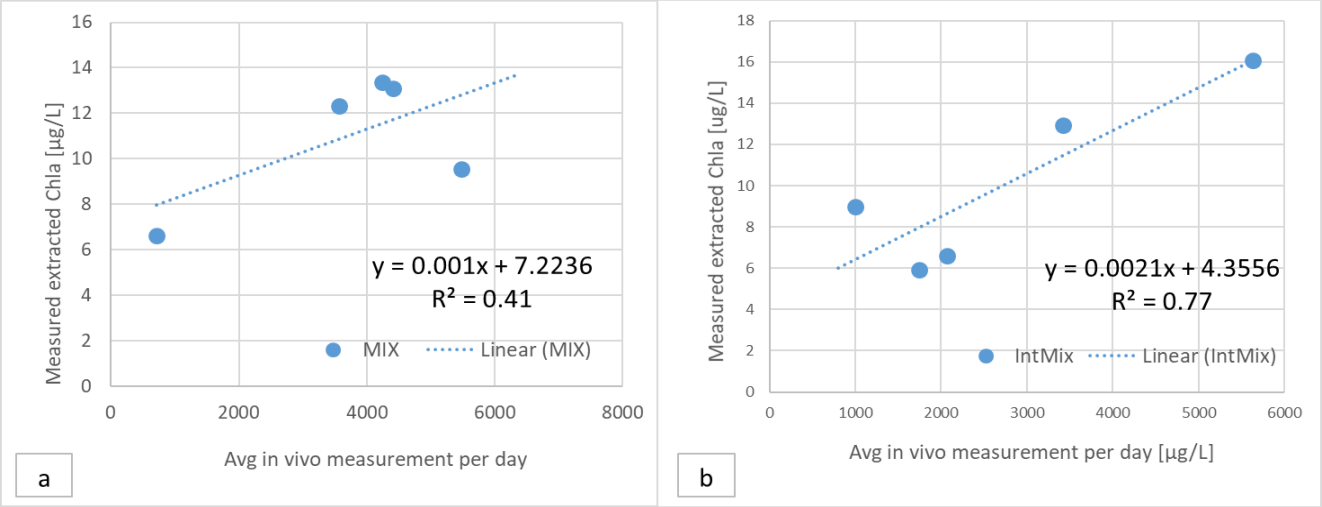

Appendix Figure A.4: SU19 Measured extracted chl-a vs in vivo for Mix (a) and IntMix (b) treatment. The equation displayed on each graph is the regression line used to estimate the actual chl-a values.

A.1 Experimental Setup Procedure.

For both experiments, each WCR was initially filled with 40 L DIW and 10 L of artificial turbidity one day before collecting lake-water. After brining the lake-water into the lab, a long, flexible tube with a funnel at the top end of it was used to gently transfer equal volumes of lake-water into each WCR to prevent shearing of the organisms. For only experiment SP19, the phytoplankton tow was evenly divided and distributed among each WCR. For both experiments, the nutrients were evenly divided and distributed among each WCR. Lastly, DIW was used to fill the remaining volumes of the WCRs in each experiment to reach a final water height of 1.9 m,

representing a total volume of 134.4L. Total water height/volume of each WCR was maintained throughout the course of both experiments by periodic addition of DIW to compensate for any evaporation and sample volume removal.

Appendix Table A-1: Details of sample volumes and tests involved in a grab sample.

Tests for Grab Samples

Test	Volume Sample (mL)	Test Details
Extracted chlorophyll	20	• Tested in Plankton Ecology Lab, NCSU • Tested following EPA 445.0 method using 45 mm GF/F Whatmann filters, sonication, and 6 mL of 100% Acetone.
FlowCAM	15	• Tested in Plankton Ecology Lab, NCSU • Water sample preserved using acid lugol solution (5%)
dissolved inorganic nutrients	75	• Measured for TP, TN, Ammonia, Phosphate, and nitrite+nitrate • Sample came from chl-a extraction filtrate that was kept at -20°C
Community characterization	15	• Measured using light microscopy by North Carolina State University Center for Applied Aquatic Ecology (CAAE, NCSU)

A.2 Phytoplankton community structure

Cell counts of phytoplankton species of cyanos and noncyanos were counted using FlowCAM and displayed in the following tables.

Appendix Table A-2: Legend for WCR treatments given WCR number.

WC	Treatment	
	SP19	SU19
1 & 2	low	mix
3 & 4	high	intmix

Appendix Table A-3: SP19 Community structure for cyanos.

			Total Cyano Count (no. cells)							
WC Number_Day_Depth	V sample (ml)	Tot V WCR samples (ml)	Anabaena S	Aphanocapsa	Chroococcus	Unknown filamentous *	Total count cyanos	Cyano density (count/ml)	Avg cyano density (count/ml)	Tot cyano in 134.3 L (no. cells)
Lake	2.3	1.0			1		1	1	1	1.40E+05
WCR1_D1_5cm	3.2	5.9		80			80	25		1.67E+06
WCR1_D1_110cm	2.7						0	0	12	
WCR2_D1_5cm	2.4	4.2		216		2	218	91		1.08E+07
WCR2_D1_110cm	1.8			124		2	126	69	80	
WCR3_D1_5cm	3.4	6.3	2.0	23783	29	4	23818	7032		5.23E+08
WCR3_D1_110cm	2.9		1.0	2212		6	2219	754	3893	
WCR4_D1_5cm	2.5	5.4		1114	87	9	1210	477		5.55E+07
WCR4_D1_110cm	2.8		1.0	863	125		989	349	413	
WCR1_D18_5cm_2	2.3	4.5		265			265	116		1.43E+07
WCR1_D18_110cm	2.2			217			217	98	107	
WCR2_D18_5cm	1.6	3.9	10.0	2722	10	908	3650	2217		2.68E+08
WCR2_D18_110cm	2.2		6.0	3054	4	870	3934	1777	1997	
WCR3_D18_5cm	1.0	1.6	2.0	428		1203	1633	1644		1.78E+08
WCR3_D18_110cm	0.6		1.0	281		308	590	1013	1328	
WCR4_D18_5cm	0.7	1.4		1130.96	2	313	1446	1997		2.37E+08
WCR4_D18_110cm	0.6		4.0	588.5	110	288	991	1537	1767	

Appendix Table A-4: SP19 Community structure for noncyanos.

			Total Noncyano Count (no. cells)								
WC Number_Day_Depth	V sample (ml)	tot V (ml)	Diatoms-Aulacoseira	Diatoms-Asterionella	Diatoms - Synedra	Diatoms - Nitzschia	Dinos - round	Total count non-cyanos	non-cyanos density (count/ml)	Avg non-cyanos density (count/ml)	Tot non-cyanos in 134.3 L (cells/L)
Lake	2.3	1.0	1500	10				1510	1578	1578	2.12E+08
WCR1_D1_5cm	3.2	5.9	232					232	72		8.66E+06
WCR1_D1_110cm	2.7		151		2			153	57	64	
WCR2_D1_5cm	2.4	4.2	435				88	523	219		2.90E+07
WCR2_D1_110cm	1.8		344				45	389	213	216	
WCR3_D1_5cm	3.4	6.3	466		1		45	512	151		2.29E+07
WCR3_D1_110cm	2.9		464		4		92	560	190	171	
WCR4_D1_5cm	2.5	5.4	323	1		154	89	567	224		2.32E+07
WCR4_D1_110cm	2.8		206	1			137	344	121	173	
WCR1_D18_5cm_2	2.3	4.5	20				119	139	61		9.81E+06
WCR1_D18_110cm	2.2		127		3		59	189	85	73	
WCR2_D18_5cm	1.6	3.9	31		1		297	329	200		1.84E+07
WCR2_D18_110cm	2.2		44		1		120	165	75	137	
WCR3_D18_5cm	1.0	1.6	20		1	409	186	616	620		8.08E+07
WCR3_D18_110cm	0.6		55	1	1	5	278	340	584	602	
WCR4_D18_5cm	0.7	1.4	11	4	2	8	149	174	240		4.58E+07
WCR4_D18_110cm	0.6		33	1	2		249	285	442	341	

Appendix Table A-5: SU19 community structure for cyanos.

			Total Cyano Count (no. cells)									
WC Number_Day_Depth	V sample (ml)	tot V (ml)	Anabaena F.	Anabaena S	Raphidiopsis	Aphanocapsa	Chroococcus	Unknown filamentous*	Total count cyanos	Cyano density (count/ml)	Avg cyano density (count/ml)	Tot non-cyanos in 134.3 L (cells/L)
Lake	1.0	0.96	8	330		2722	10	908	3978	4158	4158	5.58E+08
WCR1_D1_5cm	2.0	5.6	7	65		456	2	84	614	309	290	3.89E+07
WCR1_D1_110cm	3.6		20	116		571	21	247	975	271		
WCR2_D1_5cm	2.4	5.0	44	121		1137	18	468	1788	748	437	5.87E+07
WCR2_D1_110cm	2.6		9	48		207		66	330	125		
WCR3_D1_5cm	1.8	7.1	12	109		661	10	478	1270	716	491	6.60E+07
WCR3_D1_110cm	5.4		1	114		1079	6	226.25	1426	266		
WCR4_D1_5cm	5.4	9.5	8	115		3576	18	152	3869	722	564	7.57E+07
WCR4_D1_110cm	4.2		23	151		1200	20	298.5	1693	406		
WCR1_D18_5cm_2	4.4	9.7	1			844		192	1037	238	227	3.05E+07
WCR1_D18_110cm	5.3					681		464	1145	216		
WCR2_D18_5cm	2.3	5.8	1	3		3960	6	57.6	4028	1767	944	1.27E+08
WCR2_D18_110cm	3.5			2		62	4	359	427	122		
WCR3_D18_5cm	3.2	4.3			15	7276.5		223.2	7515	2328	2448	3.29E+08
WCR3_D18_110cm	1.1					2639		80	2719	2568		
WCR4_D18_5cm	1.1	2.4	1	3		4488		753	5245	4832	2749	3.69E+08
WCR4_D18_110cm	1.3		0	3	8	311		521	843	667		

Appendix Table A-6: SU19 Community structure for noncyanos.

			Total Noncyano Count (no. cells)											
WC Number_Day_ Depth	V sample (ml)	tot V (ml)	Diatoms-Aulacoseira	Diatoms-Asterionella	Diatoms-Synedra	Diatoms-Nitzschia	Dinos-round	Greens-Scenedesmus	Greens-Staurastrum	Greens	Total count non-cyanos	non-cyanos density (count/ml)	Avg non-cyanos density (count/ml)	Tot non-cyanos in 134.3 L (cells/L)
Lake	1.0	1.0	3		151		297				451	471	471	6.33E+07
WCR1_D1_5cm	2.0	5.6	2		26		178				206	104	112	1.50E+07
WCR1_D1_110cm	3.6		2		31		396		2		431	120		
WCR2_D1_5cm	2.4	5.0			34		343				377	158	112	1.50E+07
WCR2_D1_110cm	2.6				22		151				173	66		
WCR3_D1_5cm	1.8	7.1			22		372		2		396	223	135	1.82E+07
WCR3_D1_110cm	5.4				40		214		1		255	48		
WCR4_D1_5cm	5.4	9.5			56		348				404	75	117	1.58E+07
WCR4_D1_110cm	4.2		5	2	109		538		10.5		665	159		
WCR1_D18_5cm_2	4.4	9.7	9		13		147	2			171	39	27	3.67E+06
WCR1_D18_110cm	5.3				16		59	7			82	15		
WCR2_D18_5cm	2.3	5.8	48		210	10	663	7		10	948	416	315	4.23E+07
WCR2_D18_110cm	3.5		27		134	12	555	4		18	750	215		
WCR3_D18_5cm	3.2	4.3	1	2	18	1	232	1		3	258	80	106	1.42E+07
WCR3_D18_110cm	1.1		1	3	9		124	1		2	140	132		
WCR4_D18_5cm	1.1	2.4	14	1	1	2	428	1		2	449	414	270	3.62E+07
WCR4_D18_110cm	1.3		14		8	4	117	1		15	159	126		

Appendix B: ABM Additional Information

Appendix Table B-1: Summary of the RMSE results of each model type when calibrated to 2017 WCR experiment treatments.

Experiment	Model	RMSE (µg chl-a/L)
FA17 Mix	1-Breed	7.2
	2-Breed-A	
	2-Breed-B	
FA17 IntMix	1-Breed	8.0
	2-Breed-A	
	2-Breed-B	
FA17 NoMix	1-Breed	7.2
	2-Breed-A	
	2-Breed-B	
SU17 Mix	1-Breed	3.5
	2-Breed-A	
	2-Breed-B	5.9
SU17 NoMix	1-Breed	7.4
	2-Breed-A	
	2-Breed-B	10.1

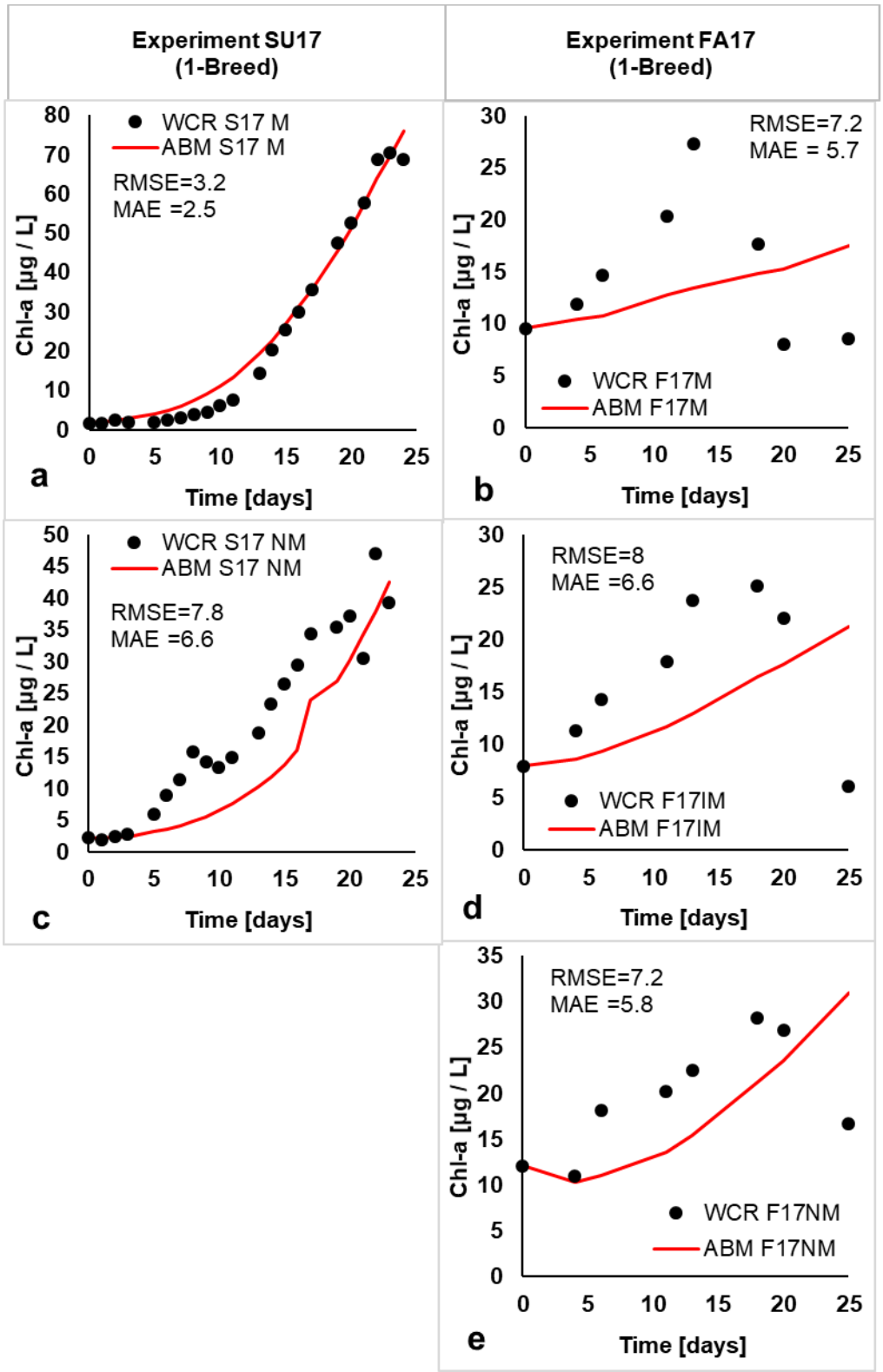

Appendix Figure B.1: Calibrated 1-Breed ABMs to WCR experiments SU17 Mix (a), FA17 Mix (b), SU17 NoMix (c), FA17 IntMix (d), and FA17 NoMix (e).

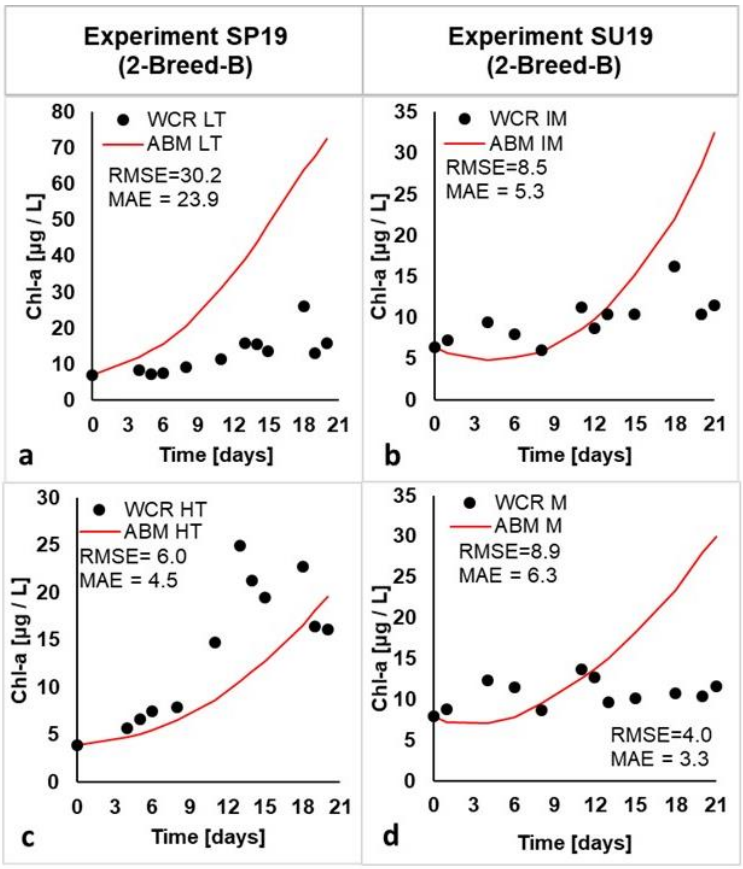

Appendix Figure B.2: 2-Breed-B calibration RMSE results, MAE results, and ABM versus WCR data comparison for experiments SP19 LT (a), SU19 IntMix (b), SP19 HT (c) and SU19 Mix (d).

Appendix C: ABM Code

C.1 Attached is the ABM code for 2-Breed-B for IntMix

```
;When setting up model, items to hardcode before running:
 ;1) WCR Chla
 ;2) initial breed counts
 ;3) time points chla data was taken
 ;4) Turbidity
 ;5) Diffusion



;;set environment parts
globals [
  water
  day?
  day-length
  dt
  k_ew        ;light extinction for particle-free water, units [1/m]
  z_tot       ; total depth [m]
  unit_area   ;surface unit area to get volume [m^2]
  tot_V       ;total volume [m^3]
  number-dead ;number_dead = no. dead agents
  dead_P      ;amount of P released from dead agents
  total_P
  q_P_dead_gP
  run-time_sec;keeps sum of run-time [s]
  number-of-cyanos
  number-of-noncyanos
  diffusion   ;units [m/h^2]
  Turbidity   ;units [mg/L]
  Total_chla  ;chla units [ug chla/L]
  T           ;water temperature (deg C)
  I_o         ;Light intensity at surface
  biomass_initial_molC
  K

;;Agent accounting
  n-start-phytos
  n-min-phytos
  n-max-phytos

 ;;agent fixed properties
   u_repro_cyanos
   m_o_cyano
   u_repro_noncyanos
```

```
  m_o_noncyano


;;calculated values
  S_R_min
  m_min
  q_P_min
  q_P_gP_min
  Internal_chla_min
 Internal_chla_perC ;[ug chla / mol C ]

;;Residual lists
 chla-time-list
 chla-ABM-list
 chla-WCR-list
 chla-Error         ;residual = error
 chla-SE            ;SE = squared error
 chla-SE-normalized
 chla-SSE           ;sum of SE normalized
 total-SSE
 chla-RMSE
 Total-RMSE
 chla-Error-MAE
 abs-chla-SE
 chla-MAE
 Total-MAE

;;Cyano-count
 cyano-count-time-list
 cyano-count-time-list-RA
 cyano-count-WCR-list
 cyano-count-ABM-list
 cyano-count-ABM-list-RA
 cyano-count-Error
 cyano-count-SE
 cyano-count-SE-normalized
 cyano-count-SSE

;;Noncyano-count
 noncyano-count-time-list
 noncyano-count-time-list-RA
 noncyano-count-WCR-list
 noncyano-count-ABM-list
 noncyano-count-ABM-list-RA
 noncyano-count-Error
 noncyano-count-SE
```

```
  noncyano-count-SE-normalized
  noncyano-count-SSE

 ;;Relative abundance
  cyano-noncyano-RelAbundance-time-list
  cyano-noncyano-RelAbundance-WCR-list
  cyano-noncyano-RelAbundance-ABM-list
  cyano-noncyano-RelAbundance-Error
  cyano-noncyano-RelAbundance-SE
  cyano-noncyano-RelAbundance-SE-normalized
  cyano-noncyano-RelAbundance-SSE

  abc
]

;;2 breeds of phytoplankton
breed [ phytos a-phyto ]
breed [cyanos a-cyano]
breed [noncyanos a-noncyano]


turtles-own [
  Internal_Chla      ;[ug chla / agent]

  m                ;m = biomass, units [ mol C / cell]  <<< multiply by S_R to get total Carbon per
agent
  q_P              ;actual P quota (conc in cell) [mol P / mol C]
  q_P_gP             ;amount of P in entire agent [gP]
  dq_P/dt
  u_p              ;photosyntetic rate. initialize u_p and u_r in set-up phytos
  u_R              ;respiration rate
  W_PO4              ;excretion rate [molP/molC*d]
  q_P_used_gP        ;P usedfrom storage [g P], -(u_p-u_R)*q_P
  S_R
  dmdt
  molC_per_agent
]


patches-own [
  I             ;light intensity [W/m^2]
  k_e             ;light Extinction coefficient [1/m]
  a             ;conc chla above patch [ug chla / L ]
  DIP_actual     ;[g/L] , only water patches
  DIP_actual_gP  ;[g]
  V_patch        ;[L]
```

```
]

;;set-up and restart model
to setup
  clear-all
  setup-scales    ;setup day length, time, and spatial intervals
  setup-globals   ;setup unchanging environment
  setup-resources ;setup light, nutrients
  setup-phytos    ;create phytoplankton
  setup-chla-perC
  ask turtles [calculate-internal_chla]
  reset-ticks
end

to setup-scales
  set-patch-size 28 ;sets size of patches, and phytoplankton will change accordingly
end

to setup-globals
  set water patches with [ pycor <= max-pycor ] ;assuming all patches are water, and at pycor=0
is surface of water
  ;;****SET dt in unit hours
  set dt 1
  ;;****SET number of hours of daylight
  set day-length 12 / dt                ;hours light, *can add slider to adjust

  set k_ew 0                          ;light extinction for particle-free water, units [1/m]
  ask water [
  ;;total depth modeling
  set z_tot 1.9                       ;[m] when move z amount, include fd (z_tot * pycor)/(abs min-
pycor)

  ;;unit surface area modeling
  set unit_area 0.07069               ;sets surface unit area of WCR [m^2]; we mainly focus on
depth. Diameter =
  set tot_V z_tot * unit_area * (10 ^ 3) ;units [L]; Helps later calculating conc chla since need
total volume. *Checked math and it works!
                                      ;tot_V = 134.3 L

  ;;patch Volume [L]
  set V_patch tot_V / count water       ;V_patch units [L].  no. water patches = 51, so V_patch =
2.6333 L


  set DIP_actual_gP DIP_actual * V_patch
  ]
```

```
  ;;Water temperature
  set T 25                        ;Water Temp [deg C]. Used WCR value

  ;;Light at surface
  set I_o 81.77                    ;Alex Exp B, MIX ; I_o = solar radiation at surface of WCR, units
[W/m^2]

  ;;****SET Turbidity, N
  set Turbidity 300                ;300

  ;;;;Phytoplankton agent count values;;;;
  set n-min-phytos 1               ;units [agent]
  set n-max-phytos 1700              ;units [agent] ;;try 200 for now previously 200
  set n-start-phytos 600             ;(n-min-phytos + n-max-phytos) / 2 ;;should = 105, units
[agent]

   ;;phytoplankton fixed properties
  set u_repro_cyanos 50
  set m_o_cyano 6.85E-13             ;;6.85E-13 = avg  ; 9.8E-13 = max, chose min hellweger =
3.9E-13
  set u_repro_noncyanos 50
  set m_o_noncyano 9.95E-13          ;;new avg = 9.95E-13; 5.5E-12 = old avg; min = 9.9E-13,
chose max hellweger = 1E-12


  ;;****UPDATE NUMBER-OF-... WITH EACH EXPERIMENT RUN;;;
   set number-of-cyanos 48780000       ;SU19 IntMix WCR 1&2
   set number-of-noncyanos 15000000    ;SU19 IntMix WCR 1&2

  ;;Track dead phyto and P
  set number-dead 0

  ;;****SET WCR values before each run
  let chla-time-list-h [ 0 24     96      144     192     264     288     312     360     432     480
          504]    ;units = h ; SU19 IntMix
  set chla-time-list (map [element -> (element) / dt ] chla-time-list-h )
  set chla-ABM-list n-values 12 [0]                          ;creates list of certain number
potential inputs

  set chla-WCR-list [6.45      7.29    9.45    8.01    6.04    11.27   8.70    10.38   10.39   16.19
          10.37   11.54] ;SP19 HT

  set Total_chla 6.45
```

```
  ;;initialize lists
  set cyano-count-ABM-list-RA n-values 12 [0]
  set noncyano-count-ABM-list-RA n-values 12 [0]

  ;;Error initialization
  set chla-Error [6.45   7.29     9.45     8.01     6.04     11.27   8.70     10.38   10.39   16.19   10.37
          11.54] ;SP19 HT
  set chla-SE n-values 12 [100] ;SP19 HT and LT                          ;initialize 12 values as 100.
Yini EXP SP high turbidity
  set cyano-count-Error [586034843 73841743 829237113]                  ;SPRING 2019 WCR
1&2

end

to setup-resources
  ask patches with [pycor = 0] [ set I 81.77 ]
  recolor-environment true
end


to recolor-environment [setting-up?]
  ;;color water at night
  ask water [
    ifelse I > 0 [
      set pcolor yellow - 4 + 1  ] [
      set pcolor blue - 0.1 * distance patch 0 0 ]
  ]
end


to setup-phytos
  create-cyanos round ( n-start-phytos / 2 )
  [
    set shape "circle"
    set size 0.5
    set color red
    set u_p 0.05 * dt                                    ;= 1.2 / 24 to start with half ; u_pmax_cyanos;
initial photosynthetic rate [1/d] converted to 1/dt, assuming maximum u_p to begin to prevent
initial steep biomass drop
    set u_R ( 0.00208 * dt )                             ;0.05 1/d , assuming constant respiration
rate converted to 1/dt
    set m ((random-float 3.9 * 10 ^ (-13 ) ) + ( 1.95 * 10 ^ (-13) ))  ;add min value (m0) to be in
range. initial phyto biomass [mol C/cell];  individual = cell
    setxy [pxcor] of one-of water [pycor] of one-of water
    set S_R ( number-of-cyanos / ( n-start-phytos / 2 ) )          ;units [cells/agent]
    set biomass_initial_molC ( m * S_R ) ; [ molC / agent]
```

```
   set q_P_gP q_P * m * S_R * 31                              ;starting S_R of phytos: same number
of agents each, but different S_R

  ]

  create-noncyanos round ( n-start-phytos / 2 )
  [
    set shape "circle"
    set size 0.5
    set color green
    set u_p ( 0.08 * dt )                                    ;initial photosynthetic rate [1/d] converted to
1/dt
    set u_R (0.00208 * dt )                                    ;assuming constant respiration rate
converted to 1/dt
    set m ((random-float 9.9 * 10 ^ (-13 ) ) + ( 4.95 * 10 ^ (-13) ))   ;add min value (m0) to be in
range. initial phyto biomass [mol C/cell];  individual = cell
    setxy [pxcor] of one-of water [pycor] of one-of water
    set S_R ( number-of-noncyanos / ( n-start-phytos / 2 ) )           ;units [cells/agent]
    set biomass_initial_molC ( m * S_R ) ; [ molC / agent]
    set q_P_gP q_P * m * S_R * 31
  ]

end

to setup-chla-perC
  ask turtles [
    set molC_per_agent (m * S_R)
  ]
    set Internal_chla_perC (Total_chla * tot_V) / (sum [molC_per_agent] of turtles)   ;[ug chla /
mol C]
end

to calculate-internal_chla
 set Internal_chla (Internal_chla_perC * m * S_R)                    ;[ug chla / agent]
end


;;;;;;;;;;;;;;;;;;;
;;;;;;;GO;;;;;;;;;;
;;;;;;;;;;;;;;;;;;;

to go
 reset-timer
  if count turtles = 0 or ticks = ( 601 / dt)  ;run for 25 days = 600 hours
  [
    user-message  "Run finished"
```

```
  write "chla-ABM-list is: "
  show chla-ABM-list
  write "cyano-count-ABM-list-RA is:"
  show   cyano-count-ABM-list-RA
  write "noncyano-count-ABM-list-RA is:"
  show   noncyano-count-ABM-list-RA
  ;;Show ABM errors
  write "Total RMSE is:"
  show Total-RMSE
  write "Total MAE is:"
  show Total-MAE
  stop
]

;;Calculate ABM lists at beginning of time step
if ticks = 0
[ calculate-cyano-count-ABM-list-RA
 calculate-noncyano-count-ABM-list-RA
  calculate-chla-ABM-list
]

;;spread light
ask water [
calculate-shading
update-light
update-Nutrients
]

;;turtle commands: treat each agent as individual, then scale up using S_R
if any? cyanos [
ask cyanos [move-random-walk-cyanos]
]
 if any? noncyanos [
ask noncyanos [move-random-walk-noncyanos]
]

if any? cyanos [
ask cyanos[grow-cyano]
]
if any? noncyanos [
ask noncyanos[grow-noncyano]
]

if any? cyanos [
ask cyanos [cyanos-cell-division]
]
```

```
   if any? noncyanos [
  ask noncyanos [noncyanos-cell-division]
  ]

  if any? cyanos [
  ask cyanos [ check-if-dead-cyanos]
  ]
   if any? noncyanos [
  ask noncyanos [ check-if-dead-noncyanos]
  ]

  ask turtles [update-internal-chla]
  update-total-chla

  if ticks != 0 [
  calculate-chla-ABM-list
  calculate-cyano-count-ABM-list-RA
  calculate-noncyano-count-ABM-list-RA
  ]

    combine-phyto-agents
    split-phyto-agents

 ;;Errors
   calculate-chla-Error
   calculate-chla-RMSE
   calculate-total-RMSE
 ;;print timer
 let c timer           ;create list of time of each tick
                     ;ticks = actual number of ticks, and tick = to advance. wrong because not asking
patch or agent? e.g ask patches [ifelse
 set run-time_sec run-time_sec + c
;print run-time_sec
 tick
;set total-run-time sum
end


to update-internal-chla
  ;set Internal_chla Internal_chla_perC * m     ;+ chla_coeff_I * I
  set Internal_chla Internal_chla_perC * m * S_R  ; [ug Chl-a/agent]
end

to update-total-chla
  set Total_chla ( (sum [Internal_chla] of turtles) / tot_V )
end
```

```
to calculate-shading                    ;all xcor are the same
  ifelse ( sum [V_patch] of patches with [pycor > [pycor] of myself ] <= 0 ) or ( sum
[Internal_chla] of turtles with [ycor > [pycor] of myself and xcor = [pxcor] of myself] <= 0)
  [
    set a 0                             ;if no volume of chla directly above patch, then a = 0, otherwise:
  ]
  [
    set a ((sum [Internal_chla] of turtles with [ycor > [pycor] of myself and xcor = [pxcor] of
myself] ) / (sum [V_patch] of patches with [ pycor > [pycor] of myself ] ))
    ]
                                ;show a: checked and it works fine! (a = sum chla / (number patches
above * (134 L / 51 patches))
                                ;Can change turbidity to equal slider in future calibraton

  let k_e' k_ew + 0.008108 * Turbidity ;Math checked and works!
  set k_e k_e' + 0.0088 * a + ( 0.054 * a ^ ( 2 / 3 ) )
end

to update-light
 let z ( - pycor ) * ( z_tot / abs ( min-pycor ) )  ;depth is pycor = center of patch

 ;;Day and night features
 ifelse day-and-night?
  [                                     ;true = light on
  ifelse ticks mod (24 / dt) < day-length [
   set I I_o * e ^ ( ( - k_e ) * z )              ;I considers shading term (a) via k_e
    ask water
      [set pcolor yellow - 2 + I * 0.02 ]
   ]

   [  ask water                                 ;every other 12 hours (or 24/dt), light turns off
      [
        set I 0
        set pcolor blue - 0.1 * distance patch 0 0
      ]
   ]
  ]

  [                                     ;False = light remains on all day
    set I I_o * e ^ ( ( - k_e ) * z )
    ask water [
      set pcolor yellow - 2 + I * 0.02
    ]
  ]
```

```
end

To update-nutrients
  ask water [ set DIP_actual (sum [DIP_actual] of patches ) / (count patches) ]  ;only water
end


to move-random-walk-cyanos
 set diffusion 3.6 * ( dt ^ 2 )              ;3.6, so that if intermittent mixing False, then fully mixed
all the time
 set K diffusion                          ;can set as slider in future
  If Intermittent-Mixing?
   [Ifelse ticks mod ( 24 / dt) < day-length   ;day time
     [set K 0.135 * ( dt ^ 2 )   ]          ;Day diffusion without mixing
     [set K diffusion ]                   ;Night Diffusion at 100 rpm
  ]
 let R random-float (2) - 1                ;R is random decimal value between -1 and 1, checked!

 let dz ( w_p_cyanos * dt ) + (  2 * R * ( (2 * K * dt ) ^ (1 / 2 ) ) )

 let y_new ycor + ( dz )                    ;thoughts before: since y-axis values are negative, must
subtract dz from current
                                          ;ycor so if dz = +0.2, would actually mean go deeper so ycor + (-
0.2) will go lower
                                          ;down y-axis, since  represent depth as ycor = 0 to +50 as go down
y-axis
                                          ;w_p is sinking velocity, which is positive in the downward
direction
 ( ifelse y_new > 0 [
   set ycor ycor - y_new                   ;Reflective boundary on top
   ]
   y_new < ( -50 ) [
     set ycor -50                         ;solid boundary on bottom
  ]
   [set ycor y_new ] )
end


to move-random-walk-noncyanos
 set diffusion 3.6 * ( dt ^ 2 )              ;3.6, so that if intermittent mixing False, then fully mixed
all the time
 set K diffusion                           ;can set as slider in future

  If Intermittent-Mixing?
   [Ifelse ticks mod (24 / dt ) < day-length    ;day time
     [set K 0.135 * ( dt ^ 2 )]              ;Day diffusion without mixing
```

```
    [set K diffusion ]                    ;Night Diffusion at 100 rpm
  ]

  ; R is random decimal value between -1 and 1, checked!
 let R random-float (2) - 1
 let dz ( w_p_noncyanos * dt ) + (  2 * R * ( (2 * K * dt ) ^ (1 / 2 ) ) ) ;;negative dz means sinking
;ask phytos [
  let y_new ycor + ( dz ) ; thoughts before: since y-axis values are negaive, must subtract dz from
current ycor so if dz = +0.2, would actually mean go deeper so ycor + (-0.2) will go lower down
y-axis, since normally represent depth as ycor = 0 to +50 as go down y-axis

  ;Reflective boundary on top and solid on bottom
 ( ifelse y_new > 0
    [
   set ycor ycor - y_new
   ]
   y_new < ( -50 )
    [
     set ycor -50
  ]
   [set ycor y_new ]
  )
end


To grow-cyano
 ;;Calculate Nutrient Limitation
; let L_p 1 - ( q_op_cyanos / q_p )        ;L_p = P limitation (unitless)
let L_P 1
 ;;Calculate Light Limitation             ;using I [W/m^2] already calculated from patches before
 let u 0.001                             ;light inhibition constant [m^2/W]
;let h 25                                 ;slider h = half saturation constant [W/m^2]. Value for anabaena
(cyanos). e in literature.
 let L_L ( I / ( I + h_cyanos + (u * I ^ ( 2 ) ) ) )
                                  ;checked printed values with excel workbook, seems to use correct I
;let L_L 1

  ;;Temperature Limitation
;  let T 25                               ;Water Temp [deg C]. Used WCR value
;  let T* 22                              ;optimum temp [deg C]. For anabaena (cyano)
;  let q 5                                ;thermal dispersion parameter. For anabaena (cyano)
;  let L_T exp ( - ( ( ( T - T* ) / q ) ^ 2 ) ) ;print L_T works fine

  ;;Calculate Photosynthetic rate, u_p

;  ifelse q_P < q_oP_cyanos ;!!!!taken out here
```

```
;  [set u_p 0]      ;!!!!taken out here                          ;photosynthetic rate = 0 when q_P < q_oP
    ;;else statement:
;  [
    let growth_rate u_pmax_cyanos * L_L * L_P   ;growth-rate = u_p ; not considering L_T since
constant in lab
  (ifelse
    growth_rate >= u_pmax_cyanos
      [set u_p u_pmax_cyanos]                ;if true
      [set u_p growth_rate]                  ;else
  )
;  ]

  ;;Calculate cell change in growth
  set dmdt ( u_p - u_R ) * m                  ;units [molC/cell*dt]
  set m  m + ( ( dmdt ) * dt )                ;can set m precision ( m + (dm/dt) * dt ) 20
                                  ;can set label precision (m) 4
end

To grow-noncyano
  ;;Calculate Nutrient Limitation
  ;let L_p 1 - ( q_op_noncyanos / q_p ) ;; L_p = P limitation (unitless)
   let L_P 1                              ;assuming replete with nutrients

  ;;Calculate Light Limitation -- use I [W/m^2]
  let u 0.001                             ;inhibition constant [m^2/W]
 ; let h 15                               ;half saturation constant [W/m^2]. Value for anabaena (cyanos)
  let L_L ( I / ( I + h_noncyanos + (u * I ^ ( 2 ) ) ) )  ;checked printed values with excel
workbook, seems to use correct I

  ;;Temperature Limitation
 ;let T 25 ;; Water Temp [deg C]. Used WCR value
;  let T* 17 ;;optimum temp [deg C]. For anabaena (cyano)
;  let q 10 ;; thermal dispersion parameter. For anabaena (cyano)
;  let L_T exp ( - ( ( ( T - T* ) / q ) ^ 2 ) ) ;; print L_T works fine

  ;;;Photosynthetic rate u_p
 ; let u_pmax 1.8 / 24 ;; [1/h] ; For noncyanos
;    ifelse q_P < q_oP_noncyanos
;  [set u_p 0]
    ;else statement:
;  [
    let growth_rate u_pmax_noncyanos * L_L * L_P
  (ifelse
    growth_rate >= u_pmax_noncyanos
      [set u_p u_pmax_noncyanos]              ;if true
      [set u_p growth_rate]                   ;else
```

```
  )

  ;;calculate cell change in growth
  set dmdt ( u_p - u_R ) * m                    ;converting [1/d]*1/24 = [1/h]
  set m m + ( ( dmdt ) * dt )                   ;CHANGE PRECISION
end


to cyanos-cell-division
  If m >= ( 2 * m_o_cyano ) and random 100 < u_Repro_cyanos
  [
    let Mm m
;    let Mqm q_P * m                          ; [molP/cell]
    let SF ( random-float 0.95 + 0.05 )        ;SF = abs (random-normal 0.5 1), mean = 0.5, sd = 2,
use abs because value must be > 0, not = 0
                                  ;1-1.07 for instance would give a negative m value
    set m Mm * SF                             ;SF = split fraction, so m of daughter cell 1 = SF and 2 is 1
- SF ;;!!!check if decimals cause trunction error from such small numbers
;    set q_P Mqm * (SF / Mm )                  ; [ molP/molC ]
;   set q_P q_P
   hatch 1
    [
    set m Mm * (1 - SF)
;    set q_P q_P                              ;molP/molC
;    set q_P Mqm * ( (1 - SF) / Mm )
    ]
  ]
end

to noncyanos-cell-division
  ;;Can be changed in "Setting-up" too ??why m_o not taken from "setting-up
  ;; procedure?
;  let m_o 0.9 * 10 ^ (-12)
  If m >= ( 2 * m_o_noncyano ) and random 100 < u_Repro_noncyanos
  [
    let Mm m
;   let Mqm q_P * m                           ; [molP/cell]
    let SF ( random-float 0.95 + 0.05 )          ;SF = abs (random-normal 0.5 1), mean = 0.5, sd = 2,
use abs because value must be > 0, not = 0
                                  ;1-1.07 for instance would give a negative m value
    set m Mm * SF                             ;SF = split fraction, so m of daughter cell 1 = SF and 2 is 1
- SF ;;!!!check if decimals cause trunction error from such small numbers
;   set q_P Mqm * (SF / Mm )                  ; [ molP/molC ]
;   set q_P q_P
   hatch 1
    [
```

```
    set m Mm * (1 - SF)
;    set q_P q_P                          ;molP/molC
;    set q_P Mqm * ( (1 - SF) / Mm )
    ]
  ]
end

to update-internal-P
  set q_P_gP  q_P * m * S_R * 31    ;Calculate q_P_gP [gP]

  ;;Calculate q_P_used [molP/molC*h]
  let q_P_used 0
  if (u_p - u_R) * q_P > 0
  [set q_P_used (u_p - u_R) * q_P]          ;using q_P from previous time step!!!!!!!!!

  ;;Calculate q_P_used_gP [gP] per entire agent
  set q_P_used_gP q_P_used * m * S_R * 31 * dt
end


to check-if-dead-cyanos
 ;if random-float 0.25 < ( (0.00042 + (random-float 0.0792)) * dt ) or m < 0 or S_R < 1 ;;makes
cyanos u_D range 0.00042 1/h (Yue) to 0.0025 1/h (hellweger)
  if random-float 1 < ( u_D_cyanos * dt ) or m < 0 or S_R < 1    ;q_P < q_oP . probability of
death rate = u_D * dt
 [
    set number-dead number-dead + 1                          ;can calculate dead_P which has 1 value
per time step or add each time step???
    ;set DIP_actual DIP_actual + ( q_p_gP / V_patch)            ;P recycling, units [gP/L]
;    set q_P_dead_gP q_P_dead_gP + (q_p_gP)                    ;amount of P released from dead
agents [g] , q_p = molP/molC
;    set q_P_gP 0
;    set q_P 0
    die
  ]
end



to check-if-dead-noncyanos
  ;let m_o 0.9 * 10 ^ (-12)
  if random-float 1 < ( u_D_noncyanos * dt ) or m < 0 or S_R < 1  ;; instead of comared to 1,
compared to 1/24= 0.042 q_P < q_oP;probability of death rate = u_D * dt
 [
    set number-dead number-dead + 1
    ;;calculate dead_P which has 1 value per time step or add each time step???
```

```
    ;set DIP_actual DIP_actual + ( q_p_gP / V_patch) ;units [gP/L]
    set q_P_dead_gP q_P_dead_gP + (q_p_gP)  ;amount of P released from dead agents [g] , q_p
= molP/molC
    set q_P_gP 0
    set q_P 0
    die
  ]
end


to combine-phyto-agents                  ;Combine agents S_R when count >200
  while [ ( count cyanos + count noncyanos ) > n-max-phytos and count cyanos > 850] [
      if any? cyanos [
  ask min-one-of cyanos [S_R]            ;make least S_R phyto die
    [
      set S_R_min S_R
      set m_min m
;      set q_P_min q_P
;      set q_P_gP_min q_P_gP
      set Internal_chla_min Internal_chla
      die
    ]
    ]

     if any? cyanos [
  ask min-one-of cyanos [S_R]            ;combine least S_R phyto with another low S_R phyto
    [
     set m (m_min * S_R_min + m * S_R) / (S_R_min + S_R)
;     set q_P  (q_P_min * S_R_min + q_P * S_R) / (S_R_min + S_R)
;     set q_P_gP  (q_P_gP_min * S_R_min + q_P_gP * S_R) / (S_R_min + S_R)
;     set  Internal_chla (Internal_chla_min * S_R_min + Internal_chla * S_R) / (S_R_min + S_R)
     set Internal_chla (Internal_chla_min + Internal_chla )
     set S_R S_R + S_R_min
    ]
    ]
  ]

 while [ ( count cyanos + count noncyanos ) > n-max-phytos and count noncyanos > 850] [
  ; while [ ( count cyanos + count noncyanos ) > n-max-phytos]  ;for noncyanos
      if any? noncyanos [
  ask min-one-of noncyanos [S_R]
    [
      set S_R_min S_R
      set m_min m
      set Internal_chla_min Internal_chla
;      set q_P_min q_P
```

```
;      set q_P_gP_min q_P_gP
                                ;can add updated chla here
      die
    ]
    ]
  if any? noncyanos [
    ask min-one-of noncyanos [S_R]
    [
     set m (m_min * S_R_min + m * S_R) / (S_R_min + S_R)
;     set q_P  (q_P_min * S_R_min + q_P * S_R) / (S_R_min + S_R)
;     set q_P_gP  (q_P_gP_min * S_R_min + q_P_gP * S_R) / (S_R_min + S_R)
     set S_R S_R + S_R_min
     set Internal_chla (Internal_chla_min + Internal_chla )
    ]
  ]
 ]
end




;;Split agents when count < 10
to split-phyto-agents
if any? cyanos [
  while [count cyanos <= n-min-phytos]
[
ask max-one-of cyanos [S_R]
[
let S_R1 S_R
let Internal_chla_1 Internal_chla
set S_R ( S_R / 2 )
set Internal_chla ( Internal_chla / 2 )

hatch 1[
       set S_R ( S_R1 / 2 )
       set Internal_chla ( Internal_chla_1 / 2  )
]
 ]
  ]
   ]

if any? noncyanos [
while [count noncyanos <= n-min-phytos]
[
ask max-one-of noncyanos [S_R]
[
```

```
let S_R1 S_R
let Internal_chla_1 Internal_chla
set S_R ( S_R / 2 )
set Internal_chla ( Internal_chla / 2 )
hatch 1 [
        set S_R S_R1 / 2
        set Internal_chla ( Internal_chla_1 / 2  )
]
 ]
  ]
   ]
end


to calculate-chla-ABM-list
 ask turtles [
    set Internal_chla Internal_chla_perC * m * S_R              ;[ug Chl-a/agent]
  ]
 set total_chla ( (sum [Internal_chla] of turtles) / tot_V )      ;units [ug chla / L ]

 (ifelse
    ticks = ( 0 / dt )
 [set chla-ABM-list (replace-item 0 chla-ABM-list total_chla) ]
 ticks = ( 24 / dt )
          [set chla-ABM-list (replace-item 1 chla-ABM-list total_chla) ]
 ticks = ( 96 / dt )
          [set chla-ABM-list (replace-item 2 chla-ABM-list total_chla) ]
 ticks = (144 / dt )
          [set chla-ABM-list (replace-item 3 chla-ABM-list total_chla) ]
 ticks = ( 192 / dt )
          [set chla-ABM-list (replace-item 4 chla-ABM-list total_chla) ]
 ticks = (264 / dt )
          [set chla-ABM-list (replace-item 5 chla-ABM-list total_chla) ]
 ticks = (288 / dt )
  [set chla-ABM-list (replace-item 6 chla-ABM-list total_chla) ]
 ticks = (312 / dt )
          [set chla-ABM-list (replace-item 7 chla-ABM-list total_chla) ]
 ticks = (360 / dt )
          [set chla-ABM-list (replace-item 8 chla-ABM-list total_chla) ]
 ticks = (432 / dt )
  [set chla-ABM-list (replace-item 9 chla-ABM-list total_chla) ]
 ticks = (480 / dt )
          [set chla-ABM-list (replace-item 10 chla-ABM-list total_chla) ]
 ticks = (504 / dt )
  [set chla-ABM-list (replace-item 11 chla-ABM-list total_chla)]
   [])
```

```
end

to calculate-cyano-count-ABM-list-RA

 let total_cyano_count ( sum [S_R] of cyanos )      ;units [ug chla / L ]

 (ifelse
    ticks = ( 0 / dt )
 [set cyano-count-ABM-list-RA (replace-item 0 cyano-count-ABM-list-RA total_cyano_count) ]
 ticks = ( 24 / dt )
          [set cyano-count-ABM-list-RA  (replace-item 1 cyano-count-ABM-list-RA
total_cyano_count) ]
 ticks = ( 96 / dt )
          [set cyano-count-ABM-list-RA  (replace-item 2 cyano-count-ABM-list-RA
total_cyano_count) ]
 ticks = (144 / dt )
          [set cyano-count-ABM-list-RA  (replace-item 3 cyano-count-ABM-list-RA
total_cyano_count) ]
 ticks = ( 192 / dt )
          [set cyano-count-ABM-list-RA  (replace-item 4 cyano-count-ABM-list-RA
total_cyano_count) ]
 ticks = (264 / dt )
          [set cyano-count-ABM-list-RA  (replace-item 5 cyano-count-ABM-list-RA
total_cyano_count) ]
 ticks = (288 / dt )
  [set cyano-count-ABM-list-RA  (replace-item 6 cyano-count-ABM-list-RA  total_cyano_count)
]
 ticks = (312 / dt )
          [set cyano-count-ABM-list-RA  (replace-item 7 cyano-count-ABM-list-RA
total_cyano_count) ]
 ticks = (360 / dt )
          [set cyano-count-ABM-list-RA  (replace-item 8 cyano-count-ABM-list-RA
total_cyano_count) ]
 ticks = (432 / dt )
  [set cyano-count-ABM-list-RA  (replace-item 9 cyano-count-ABM-list-RA  total_cyano_count)
]
 ticks = (480 / dt )
          [set cyano-count-ABM-list-RA (replace-item 10 cyano-count-ABM-list-RA
total_cyano_count) ]
 ticks = (504 / dt )
  [set cyano-count-ABM-list-RA  (replace-item 11 cyano-count-ABM-list-RA
total_cyano_count)]
   [])
end
```

```
to calculate-noncyano-count-ABM-list-RA
 let total_noncyano_count ( sum [S_R] of noncyanos )      ;units [ug chla / L ]


 (ifelse
    ticks = ( 0 / dt )
 [set noncyano-count-ABM-list-RA (replace-item 0 noncyano-count-ABM-list-RA
total_noncyano_count) ]
 ticks = ( 24 / dt )
          [set noncyano-count-ABM-list-RA  (replace-item 1 noncyano-count-ABM-list-RA
total_noncyano_count) ]
 ticks = ( 96 / dt )
          [set noncyano-count-ABM-list-RA  (replace-item 2 noncyano-count-ABM-list-RA
total_noncyano_count) ]
 ticks = (144 / dt )
          [set noncyano-count-ABM-list-RA  (replace-item 3 noncyano-count-ABM-list-RA
total_noncyano_count) ]
 ticks = ( 192 / dt )
          [set noncyano-count-ABM-list-RA  (replace-item 4 noncyano-count-ABM-list-RA
total_noncyano_count) ]
 ticks = (264 / dt )
          [set noncyano-count-ABM-list-RA  (replace-item 5 noncyano-count-ABM-list-RA
total_noncyano_count) ]
 ticks = (288 / dt )
  [set noncyano-count-ABM-list-RA  (replace-item 6 noncyano-count-ABM-list-RA
total_noncyano_count) ]
 ticks = (312 / dt )
          [set noncyano-count-ABM-list-RA  (replace-item 7 noncyano-count-ABM-list-RA
total_noncyano_count) ]
 ticks = (360 / dt )
          [set noncyano-count-ABM-list-RA  (replace-item 8 noncyano-count-ABM-list-RA
total_noncyano_count) ]
 ticks = (432 / dt )
  [set noncyano-count-ABM-list-RA  (replace-item 9 noncyano-count-ABM-list-RA
total_noncyano_count) ]
 ticks = (480 / dt )
          [set noncyano-count-ABM-list-RA (replace-item 10 noncyano-count-ABM-list-RA
total_noncyano_count) ]
 ticks = (504 / dt )
  [set noncyano-count-ABM-list-RA  (replace-item 11 noncyano-count-ABM-list-RA
total_noncyano_count)]
   [])
end
```

```
to calculate-ABM-cyano-count
(ifelse ticks = (0 / dt)
   [set cyano-count-ABM-list (replace-item 0 cyano-count-ABM-list (sum [S_R] of cyanos))
;summing up all cells represented by all agents
    ]
 ticks = (336 / dt)                                                    ;14 days
          [set cyano-count-ABM-list (replace-item 1 cyano-count-ABM-list (sum [S_R] of
cyanos))
  ]
 ticks = (696 / dt)                                                    ;29 days
          [set cyano-count-ABM-list (replace-item 2 cyano-count-ABM-list (sum [S_R] of
cyanos))
  ]
   [] )
end

to calculate-ABM-noncyano-count
(ifelse ticks = (0 / dt)
   [set noncyano-count-ABM-list (replace-item 0 noncyano-count-ABM-list (sum [S_R] of
noncyanos) )
   ]
 ticks = (336 / dt) ; 14 days
          [set noncyano-count-ABM-list (replace-item 1 noncyano-count-ABM-list (sum [S_R] of
noncyanos))
  ]
 ticks = (696 / dt) ; 29 days
          [set noncyano-count-ABM-list (replace-item 2 noncyano-count-ABM-list (sum [S_R] of
noncyanos))
  ]
   [] )
end

to calculate-chla-Error
   set chla-Error (map - chla-WCR-list chla-ABM-list )                ;subtract WCR - ABM
chla values
   set chla-Error-MAE (map - chla-WCR-list chla-ABM-list )
end

to calculate-cyano-count-Error
   set cyano-count-Error (map - cyano-count-WCR-list cyano-count-ABM-list  )
end


to calculate-noncyano-count-Error
   set noncyano-count-Error (map - noncyano-count-WCR-list noncyano-count-ABM-list  )
end
```

```
to calculate-chla-RMSE
  set chla-SE (map [element -> (element) ^ 2 ] chla-Error )      ;cyano-count-SE (residual squared)
  let N length chla-SE
  set chla-RMSE  sqrt ( sum chla-SE / N )

  let b length chla-Error-MAE
  set abs-chla-SE (map [element -> abs (element) ] chla-Error-MAE)
  set chla-MAE (sum abs-chla-SE / b)
end

to calculate-total-RMSE
  set Total-RMSE chla-RMSE
  set Total-MAE chla-MAE
end



to calculate-total-SSE
  set Total-SSE chla-SSE
end
```

Appendix D: ABM ODD

D.1 Overview

D.1.1 Purpose

The purpose of this model is to simulate phytoplankton behaviors and emerging properties in experimental WCRs for various treatments.

D.1.2 State Variables and Scales

The model space is a 1 horizontal by 50 vertical patches that represent the WCR with a unit area of 0.071 m^2, height of 1.9 m, and total volume of 134.3 L. The model runs for 600 ticks (25 days), where each tick is 1 hour.

The entities, or agents modeled are super-agents, meaning that each agent simulates many cells. Entities can belong to the same category, also called a breed. In the 1-Breed there is one type of breed modeled. In the 2-Breed-A1, 2 breeds are modeled each with the same initial condition and property ranges for calibration. In 2-Breed-A, 2 breeds are modeled each with different initial conditions and constants, but same allowable property ranges for calibration. In 2-Breed-B, 2 breeds are modeled with different allowable property ranges for calibration.

A state variable can distinguish agents within different breeds, distinguish agents within the same breed, or trace how the agent changes over time. Some of the agents' state variables differentiate breeds, while others change over time within the same breed. Properties that distinguish agents (entities) between breeds are shown in Appendix Table D-1. Properties that distinguish agents (entities) within the same breed and that trace how agents change over time are shown in Appendix Table D-2. A property that is held constant between breeds and over time is μ_R at 0.00208 1/h. Patch variable includes light intensity (I; units W/m^2)

Appendix Table D-1: State variables that differ between breeds.

Model Variable	Description	Units
w_p	Vertical velocity	m/h
$\mu_{p,max}$	Maximum photosynthetic rate	1/h
μ_D	Death rate	1/h
h	Light half-saturation constant	W/m^2
m_o	Biomass division threshold	Mol C/cell

Appendix Table D-2: State variables that trace how agents change over time.

Model Variable	Description	Units
m	Cell biomass	mol C/cell
μ_p	Photosynthetic rate	1/h
S_R	Representative number	Number of cells/agent

D.1.3 Process overview and scheduling

Appendix Figure D.1 illustrates the events that occur in each time step. First patches consider shading to calculate the light available. Then agents use their vertical velocity and environmental diffusion to calculate and move a certain distance vertically. Agents use the light available to them in that new patch. If the agent's biomass is greater than 2 times its threshold biomass, it has a 50% chance of dividing into 2 daughter cells. If the agent meets certain requirements, it may also die. Agents combine/split to maintain the number of agents within a certain range for optimum ABM performance, and lastly chl-a and total counts are measured.

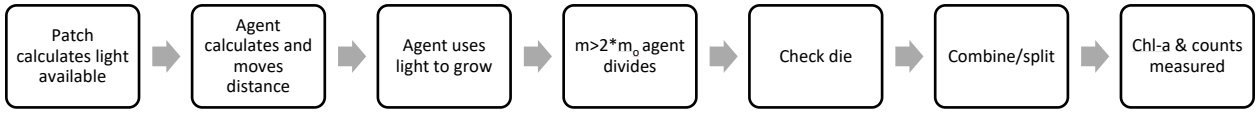

Appendix Figure D.1: Flow chart illustrating scheduling that occurs with each time step.

D.2 Design Concepts

D.2.1 Basic principles

The mechanisms will create differences between agents regarding their parameter values (i.e. m, $\mu_{p,}$ and S_R) and these differences will lead to heterogeneity in chl-a within each cell. This heterogeneity affects the population-level behavior of total chl-a concentration and cell counts.

D.2.2 Emergence

Total chl-a concentration is the key result from the ABM. The models are calibrated to get this result as close to experimental results as possible.

D.2.3 Adaptation, Objectives, Learning, and Prediction

The agents in this model do not have objectives, learning, prediction, or adaptation.

D.2.4 Sensing

Agents sense the light available within patches to calculate their growth. Also, agents consider the global variable diffusion to help determine their movement. Patches sense the agents above them to determine shading in order to calculate light availability.

D.2.5 Interaction

Indirect interaction occurs between agents due to agents in patches above reducing light available to other agents in the patch of interest.

D.2.6 Stochasticity

Randomization occurs in initial biomass (m) value generated, the probability of cell division, the probability when an agent dies, and the generated "R" term in the random walk equation.

D.2.7 Collectives

There are no physical aggregations of agents.

D.3 Details

D.3.1 Initialization

Total initial number of agents is 600 agents. Experimental counts (varies by treatment) are divided into the 600 initial agents to initialize the representative value, S_R. For 2-Breed versions, 300 agents are initialized for each breed. Also, experimental counts for cyanos and noncyanos are used to initialize S_R for agents of each breed.

To initialize the internal chl-a per mol of carbon (Internal_chla_perC), the experimental chl-a concentration at day 1 was multiplied by the total volume and divided by the sum of moles of carbon within each agent. With this value, the amount of chl-a within each agent (Internal_chla; units μg chla/agent) was initialized. Appendix Table D-3 shows other initialized values based on ABM version.

Appendix Table D-3: Initialized values for each ABM breed. Values and ranges came from prior literature.

	1-Breed	2-Breed-A1		2-Breed A/B	
Variable (units)		Breed 1	Breed 2	Breed 1 / cyanos	Breed 2 / noncyanos
μ_p (1/h)	0.065	0.065	0.065	0.05	0.08
m_o (molC/cell)	8.4E-13	8.4E-13	8.4E-13	6.85E-13	9.95E-13
m (molC/cell)	3.45E-13 to 1.49E-12	3.45E-13 to 1.49E-12	3.45E-13 to 1.49E-12	1.95E-13 to 5.85E-13	4.95E-13 to 1.49E-12

D.3.2 Input

Model does not use input from external sources such as data files or other models to represent processes that change over time.

D.3.3 Submodels

Included in section 2.2.